AN ABSTRACT OF THE DISSERTATION OF

Jianyong Wu for the degree of Doctor of Philosophy in Chemistry presented on November 23, 2009.

Title: Tandem Mass Spectrometric Analysis of Protein and Peptide Adducts of Lipid Peroxidation-Derived Aldehydes

Abstract approved:

Dr. Claudia S. Maier

The adduction of proteins and other biomolecules by electrophilic lipid peroxidation products such as 4-hydroxy-2-nonenal (HNE), 4-oxo-2-nonenal (ONE), malondialdehyde (MDA) or acrolein (ACR) is thought to be an initiating and/or propagating factor in the pathophysiology of several diseases such as atherosclerosis, diabetes, Alzheimer's, Parkinson's and other age-related disorders. The identification of protein sites modified by oxylipids is of key relevance for advancing our understanding how oxidative damage affects structure and function of proteins. Here, the use of MALDI tandem mass spectrometry with high energy collision-induced dissociation (CID) on a TOF/TOF instrument for sequencing oxylipid-peptide conjugates was systematically studied. Three synthesized model peptides containing one nucleophilic residue (i.e. Cys, His or Lys) were reacted

with MDA, HNE, ONE and ACR. MALDI-MS analysis and MS/MS analysis were performed to confirm the adduct type and the modification sites. Michael adducts and Schiff bases were the predominant products under pH 7.4 within 2 hours. All MS/MS spectra of Michael adducts show the neutral loss of the oxylipid moiety ions. MS/MS spectra of Cys-containing peptide oxylipid conjugates exhibit additional characteristic neutral loss of HS-oxylipid moiety ions. MS/MS spectra of His-containing peptide oxylipid conjugates show characteristic oxylipid-containing His immonium ions. Spectra of Lys-containing peptide oxylipid conjugates (Schiff base) also show oxylipid-containing Lys immonium ions. However, there is no neutral loss of the oxylipid moiety ion for these Schiff bases.

Determining the extent or relative amounts of the oxidative damage in cells could provide valuable insights into the molecular mechanisms of the diseases caused by oxidative stress. Relative quantitation of oxylipid-modified proteins in biological samples is a challenging problem because of the complexity and extreme dynamic range that characterize these samples. In this study, the reagents, N'-aminooxymethylcarbonylhydrazino-D-biotin (ARP) and iodoacetyl-PEO_2-biotin (IPB), were used to enrich acrolein-modified Cys-containing peptides and the corresponding unmodified ones from subsarcolemmal mitochondria (SSM). The ratios between them were determined by nanoLC-SRM analysis. Model Cys-containing peptides labeled with ARP-acrolein and IPB were employed to

demonstrate this method. Seven acrolein-modifed Cys-containing peptides from five mitochondrial proteins were quantified. The ratios for those seven peptides from the CCl_4-treated rats are higher than the control ones indicating that the ratios of acrolein-modified peptides to unmodified ones are potential markers of oxidative stress *in vivo*.

Age-dependent changes of protein carbonyls were investigated in subsarcolemmal mitochondria by using LC-SRM analysis of distinct ACR-modified Cys-containing peptides. Immunochemical analysis using an anti-ACR monoclonal antibody supported an increase of proteins modified by acrolein with age. However, total protein carbonyls measurement using ARP in Western blot analysis did not conform to this change suggesting that age-related changes in protein carbonyls are complex and would benefit from more specific measurement protocols.

Tandem Mass Spectrometric Analysis of Protein and Peptide Adducts of Lipid Peroxidation-Derived Aldehydes

by
Jianyong Wu

A DISSERTATION

submitted to

Oregon State University

in partial fulfillment of
the requirements for the
degree of

Doctor of Philosophy

Presented November 23, 2009
Commencement June 2010

Doctor of Philosophy dissertation of Jianyong Wu presented on November 23, 2009.

APPROVED:

Major Professor, representing Chemistry

Chair of the Department of Chemistry

Dean of the Graduate School

I understand that my dissertation will become part of the permanent collection of Oregon State University libraries. My signature below authorizes release of my dissertation to any reader upon request.

Jianyong Wu, Author

ACKNOWLEDGEMENTS

The author expresses heartfelt appreciation to his wife, Ping Shi, for her love, support and understanding. The author is very appreciative for his major professor, Dr. Claudia S. Maier for providing guidance, support, encouragement, and trust. In addition, the author is grateful to Juan Chavez and the other members in Dr. Maier's group for support and encouragement. The author is also very thankful for support from his committee members as well as Dr. Max Deinzer and Dr. Staci Simonich. Many thanks are given to Michael Hare, Lilo Barofsky, Brian Arbogast, Jeff Morre and the rest of the mass spectrometry group for their support. Thanks are also given to Blaine R. Roberts for the help with peptide synthesis. This work was supported by National Institutes of Health (NIH).

CONTRIBUTION OF AUTHORS

Dr. Claudia S. Maier provided leadership in all aspects of this dissertation. Juan Chavez and the author wrote the Chapter 1 together as a mini review to be submitted. Dr. Michael Hare provided suggestions in interpreting results and edited chapter 3. Jie Zhang performed quantum calculation in Chapter 3. Kristina Jonsson and Cristobal Miranda helped to perform some Western Blots in Chapter 5. The author helped with sample preparation and data analysis in the study presented as Appendix A and B.

TABLE OF CONTENTS

TABLE OF CONTENTS (Continued)

Page

LIST OF FIGURES

LIST OF FIGURES (Continued)

Figure Page

LIST OF TABLES

LIST OF SCHEMES

Tandem Mass Spectrometric Analysis of Protein and Peptide Adducts of Lipid Peroxidation-Derived Aldehydes

CHAPTER 1. Introduction

Mass Spectrometric Analysis of Oxidative Stress Induced Modifications to the Proteome

Jianyong Wu and Juan Chavez

Introduction

Molecular oxygen (O_2) is essential for the cellular respiration of all aerobic organisms. While its chemical reactivity provides a source of energy to drive the process of life, it also makes O_2 a potentially dangerous toxin. Reactive oxygen species (ROS) are highly reactive byproducts formed as a result of the use of oxygen. A host of ROS including superoxide, hydrogen peroxide, hydroxyl radical, peroxy radical and peroxynitrite are produced endogenously through numerous metabolic pathways, including oxidative phosphorylation, oxidation of xanthine by xanthine oxidase, cytochrome P-450 detoxification reaction and oxidation of NADPH by NADPH oxidase [1-3]. Besides endogenous sources, ROS can also be formed by exogenous agents like ozone, pesticides, photochemical smog and ionizing radiation [3]. Although at high levels ROS are potentially damaging to key cellular components, at lower levels they also play an important role in cell signaling [4, 5]. Additionally they are very important in immune response, where they are generated by neutrophils in lethal quantities to kill pathogens [6]. Conditions of oxidative stress can nonetheless result when cellular homeostasis is disrupted due to excessive production of ROS and/or failure of the biological system's ability to detoxify the reactive intermediates or repair the resulting damage.

Mitochondria and Oxidative Stress

Serving as the primary energy plant for the cell, and consuming approximately 90% of the molecular oxygen taken in during aerobic respiration, mitochondria are central to studies of oxidative stress. The mitochondrial electron transport chain (ETC) complexes serve to reduce molecular oxygen into water, and in turn generate a proton gradient across the inner mitochondrial membrane, which drives the process of ATP production. Although electron transport through the complexes is a highly efficient process, many studies have shown that a small but significant percentage of the molecular oxygen consumed by the mitochondria, is nonetheless converted into reactive oxygen species including the radical anion superoxide ($O^{\cdot}{}_2^-$) and H_2O_2, due to electron "leakage" from the ETC complexes [7, 8]. Mitochondria are therefore a major source of superoxide within the cell [9]. On its own, superoxide is relatively stable and innocuous, however it serves as a precursor for other more reactive and damaging ROS including hydrogen peroxide, peroxynitrite, and the hydroxyl radical [10]. Although there is some debate about the actual mechanism of electron leakage, generally Complex I, and Complex III are regarded as the primary production sites of ROS from the ETC. In addition to the ETC, mitochondria contain a multiplicity of other ROS-producing sources including cytochrome b5 reductase, monoamine oxidases, dihydrooroate dehydrogenase, dehydrogenase of α-glycerophosphate, succinate dehydrogenase, aconitase, and α-ketoglutarate dehydogenase.

However, the contribution to the total mitochondrial ROS production by these seven sources remains unknown [11].

Antioxidant defense system

Under normal physiological conditions a balance of the ROS produced during respiration is maintained by a complex multi-leveled antioxidant defense system [11, 12]. This network of enzymes and non-enzymatic antioxidants serve to protect proteins, DNA and other important biomolecules which are critical to the function of the cell. The mitochondrial superoxide dismutase (Mn-SOD) serves to eliminate superoxide by dismutation to form hydrogen peroxide, which can then be catalytically decomposed into water and O_2 through the action of peroxidases. When the concentration of $O^{\cdot}{}_2^-$ or H_2O_2 gets too high, H_2O_2 can react with superoxide to form the extremely reactive hydroxyl radical ($HO^{\cdot}$). Additionally H_2O_2 can undergo the Fenton reaction with divalent metal cations such as Fe^{2+} and Cu^{2+} also producing $HO^{\cdot}$.

The mitochondrial membrane, being rich in polyunsaturated fatty acids (PUFAs), is particularly susceptible to ROS damage resulting in the lipid peroxidation process. Typically antioxidants such as ubiquinione, ascorbic acid (vitamin C) and the lipid soluble α-tocopherol (vitamin E), serve as radical scavengers thereby protecting the vulnerable PUFAs. Additionally other small molecule antioxidants including pyruvate, flavonoids, and carotenoids help to scavenge ROS [12]. One

of the most important and thoroughly studied mechanisms of antioxidant defense is the glutathione-based detoxification system. Consisting chiefly of thiol containing tripeptide, glutathione (GSH, L-γ-glutamyl-L-cysteinylgylcine), mitochondria utilize this system as both a renewable radical scavenger and as a sacrificial consumable antioxidant [13]. Glutathione exists in a reduced (GSH) and oxidized state (GSSG). In the reduced state, GSH can scavenge unstable ROS including superoxide and hydroxyl radicals by functioning as an electron donor to eliminate the reactive radicals. As a result GSH is converted into its oxidized disulfide form GSSG. The reduced form of GSH can be enzymatically regenerated in the mitochondrial matrix by glutathione reductase. Additionally in conjunction with the enzyme glutathione peroxidase, GSH can serve as an electron donor in the conversion of hydrogen peroxide to water. Acting in a sacrificial manner, the free thiol in GSH can react with electrophilic 2-alkenals derived from the lipid peroxidation process, either non-enzymatically or in a catalyzed reaction with the aid of glutathione-S-transferase. The glutathione-oxylipid conjugate can then be secreted from the mitochondria and the cell [14]. Mitochondrial GSH is consumed in this process and therefore needs to be replenished from the cytosolic GSH pool. Typically mitochondria maintain a relatively high concentration of GSH. If a high enough concentration of GSH cannot be maintained then oxidative stress induced damage will occur.

Under conditions of oxidative stress the antioxidant system becomes

overwhelmed and a host of lipid peroxidation products are formed. Among these, include the α，β -unsaturated aldehydes, such as HNE, ONE, HHE, acrolein etc [15]. These lipid-derived electrophiles are known to be potent cellular toxins, longer lived, and potentially more damaging to the cell than the ROS that generated them [16]. They are capable of covalently modifying proteins at nucleophilic sites including Cys, His and Lys through Michael-type addition or Schiff base mechanisms, which can lead to enzymatic inhibition, increased ROS production, and contribute to a cataclysmic cycle of oxidative stress induced cellular damage. Scheme 1.1 shows examples of Michael adduct and Schiff base between peptides and lipid peroxidation products.

Mitochondria are known to play a key role in the regulation of the cellular death mechanisms of apoptosis and necrosis [17]. Damage induced by ROS and lipid peroxidation products can lead to compromised mitochondrial integrity and the release of proteins from the intermembrane space leading to cell death [18]. The involvement of the mitochondrial permeability transition (MPT) in cell death is a complex detailed subject which is outside the scope of this paper but has been covered in many reviews [17, 19-22]. Basically oxidative stress can trigger MPT, in which nonspecific pores are opened in the mitochondrial membrane leading to a drop in the mitochondrial membrane potential ($\Delta\Psi$) and release of molecules such as cytochrome C and Ca^{2+} that then activate programmed cell death pathways [23]. MPT is known to play a role in several pathological conditions including

ischemia, stroke and myocardial infarction. The voltage dependent anion selective channel (VDAC) and adenine nucleotide transporter (ANT) are both proteins known to be important in the formation of MPT pores, and oxidative damage to these proteins could play a role in the MPT process [24].

Protein Oxidation

The oxidative modification of proteins is a complex phenomenon, taking on many forms and depending on a multitude of various factors. The accumulation of oxidized proteins has been associated with a number diseases as well as the general aging process. However the role of these modified proteins in the etiology of disease is not well understood. Oxidative modification to proteins can take many forms including radical induced cleavage of the peptide backbone, direct oxidation of amino acid residue side chains, nitration and nitrosylation by peroxynitrite, and conjugation with bioactive aldehydes such as lipid peroxidation products.

The formation of protein carbonyl derivatives is widely used as a marker to assess ROS induced damage during oxidative stress related to aging or age-related diseases. Protein carbonylation can occur as a result of direct oxidation of the side chains of lysine, arginine, proline, and threonine by ROS such as $HO^{\cdot}$, resulting in the formation of α-amino adipic semialdehyde for the case of lysine, γ-glutamic semialdehyde for the case of proline and arginine, and

aminoketobutyrate for the case of threonine. Furthermore, carbonylated proteins are formed by the reaction between the side chains of cysteine, histidine, and lysine with α，β-unsaturated aldehydes such as HNE and acrolein. The C3 atom of α，β-unsaturated aldehydes is electrophilic and readily reacts with the nucleophilic sulfhydryl group of cysteine, the imidazole group of histidine and the amino group of lysine, to form a Michael-type addition product. Regardless of how the carbonyl group is introduced, they exist as relatively reactive sites on the protein molecule and can contribute to protein crosslinking by forming Schiff base products with free amino groups in the same protein or on neighboring proteins. Oxidatively crosslinked proteins are often enzymatically inactive and resistant to proteolytic degradation [25-27]. It comes as no surprise that diseases associated with an increase in protein carbonylation often also see an increase in protein aggregate formation due to crosslinking.

Analytical methods for measuring protein carbonylation

Protein carbonylation is frequently used as a measure of oxidative stress induced damage. Therefore, a myriad of techniques have been developed for the analysis of protein carbonyls. Some of the earliest developed, and most widely employed methods rely on spectrophotometric analysis following derivatization with thiobarbituric acid (TBARS) or 2, 4-dinitrophenylhydrazine (DNPH) [28, 29]. These methods are able to provide a measure of the global level of protein

carbonylation within a biological sample and are therefore useful in assessing the degree of oxidative damage. However they are not able to conclusively identify the protein, specific amino acid site, or chemical nature of the oxidative modification. Several methods have been developed to identify the carbonylated proteins using the traditional proteomics analysis tools of gel electrophoresis and Western blotting. Perhaps the most widely employed of these methods again relies on the use DNPH as a labeling agent followed by immunochemical detection with an anti-DNPH antibody [30]. Similar approaches have used biotin hydrazide instead of DNPH, as a labeling agent, which can then be detected with the use of avidin analogs and fluorescence or chemiluminescence detection [31, 32]. However, due to the lack of specificity of these hydrazine based reagents towards the various types of carbonylation (e.g. 2-alkenal-protein adduct vs. directly oxidized amino acid side chain), the chemical nature of the modification remains unknown. To this end several studies have employed immunological detection using antibodies specific for the different types of alkenal-protein adducts (i.e. anti-HNE or anti-acrolein antibodies) [33-36]. While these methods can be highly specific for the differing forms of oxidative modification the identity of the amino acid residue site of modification remains tentative at best. Technological advances in mass spectrometry have provided researchers with powerful tools to characterize post translational modifications (PTM) to proteins. Mass spectrometry provides several advantages over other approaches for the

characterization of PTMs including the ability for unequivocal identification of the amino acid site, chemical nature of PTM, discovery of novel PTMs, and the ability to quantify relative changes in PTMs [37]. A variety of studies have employed mass spectrometry to study protein carbonylation in model systems in which purified proteins are incubated with LPO products or subjected to metal-catalyzed oxidation reactions [38-44]. These studies are useful for developing new analytical methods or for detailed structural and functional analysis of proteins of interest, however the ultimate goal remains the analysis of protein carbonyls in complex biological matrices. Several gel-free, mass spectrometric methods have been developed in which researchers are able to identify the protein target, amino acid site, and type of carbonylation in biological samples. Due to the low abundance of endogenously carbonylated proteins and the extreme complexity of biological samples, affinity enrichment is necessary prior to detection. Even still, many studies add exogenous agents to carbonylate proteins *in vitro* before identifying the protein targets. Using the biotin-tagged electrophile probes N-iodoacetyl-N-biotinylhexylene-diamine (IAB) and 1-biotinamido-4-(4'-[maleimidoethylcyclohexane]-carboxamido) butane (BMCC) researchers from the Liebler group were able to identify 897 different cysteine residues from 539 proteins from nuclear and cytosolic fractions, and 1693 different cysteine residues from 809 proteins from the mitochondria [45, 46]. Several studies have employed the use of biotin-hydrazide derivatives as labeling

reagents for the enrichment and subsequent mass spectrometric analysis of protein carbonyls [47-49]. Recently, our group has developed an analogous technique employing N'-aminooxymethylcarbonylhydrazino-D-biotin (Aldehyde Reactive Probe, ARP) to label, enrich and characterize oxidative modifications to proteins [50]. This method represents an attractive alternative to hydrazine-based derivatization methods for oxidized peptides and proteins because the reduction step necessary for the transformation of the hydrazone bond to the chemically more stable hydrazine bond can be omitted. Incubating mitochondrial proteins with HNE followed by biotin hydrazide labeling, affinity enrichment and mass spectrometric detection, Condreanu et al. were able to identify 18 specific sites of HNE adduction. The flexibility of modern mass spectrometers allows for different data-dependent acquisition methods combined with different dissociation techniques including CID and ECD, to be applied for the identification of carbonylated positions in peptides and proteins [38, 51-53]. Stevens el al. identified 24 sites of Michael-type histidine-HNE adducts on 15 unique proteins using neutral loss driven MS^3 on a LTQ-FT mass spectrometer [53]. Employing a solid phase hydrazide enrichment strategy and neutral loss driven MS^3 analysis Roe et al. mapped 125 sites of HNE adduction to 67 proteins from a yeast cell lysate to which HNE had been added [52]. These in vitro studies demonstrate the powerful potential of mass spectrometry in proteomics, and have proven useful for identifying putative sites and protein targets of oxidative modification,

however it is still important to characterize the carbonyl modifications to proteins occurring endogenously in complex biological systems. Applying our ARP based analytical strategy to proteins isolated from rat cardiac mitochondria, we were able to identify 39 unique sites on 27 proteins as being modified by a variety of 2-alkenal products including acrolein, β -hydroxyacrolein, crotonaldehyde, 4-hydroxy-2-hexenal, 4-hydroxy-2-nonenal and 4-oxo-2-nonenal (unpublished results in Appendix B).

Quantitative analysis of carbonylated proteins based on mass spectrometry

Mass-spectrometry-based protein quantification has been developed greatly recently. One major approach is based on isotope-labeled amino acids or peptides, which can be recognized by a mass spectrometer according to their mass difference [54-57]. Another major approach is label-free quantification including two different strategies: (i) measuring and comparing signal intensity of peptides from proteins; (ii) counting and comparing the number of identified-peptide spectra from a particular protein [6, 58-62] (for an excellent review, see Ref [63]). All these approaches can be applied to quantification for carbonylated proteins as long as the targeted peptides are replaced by carbonylatd ones. However low abundance of carbonylated proteins in biological samples requires enrichment methods not only for identification but also for quantification. Light and heavy isotope labeled Girard's P reagents, which can enrich carbonylated peptides by ion

exchange columns, were applied to establish the linear dynamic range for quantification of a model carbonylated peptide by LC-MS [64].

Griffin's group applied Multiplexed iTRAQ reagents to label digested peptides of oxidized proteins from rat muscle mitochondria to establish the quantitative reproducibility of the avidin enrichment strateg by LC-MS/MS [65]. Recently, our group designed and synthesized an aldehyde-reactive, hydrazide-functionalized, isotope-coded affinity tag (HICAT) and applied it to mitochondrial proteins modified in vitro with HNE for quantitative analysis by nanoLC-MALDI-MS [53]. One acrolein modified peptide from ADP/ATP translocase from rat mitochondria was also successfully quantified between young and old rats in vivo. A new quantitative method without isotope-labeling is also being developed in our group. The reagent N'-aminooxymethylcarbonylhydrazino-D-biotin (ARP) and iodoacetyl-PEO_2-Biotin (IPB) were used to enrich acrolein-modified Cys-containing peptides and the corresponding unmodified ones from mitochondrial samples. The ratios between them are determined by nanoLC-SRM analysis using a hybrid linear ion trap mass spectrometer. While there have been significant advances in the mass spectrometric identification and quantification of carbonylated proteins, there is still much room for improvement on the current methods. More efficient and specific enrichment methods are critical since most of quantitative MS analysis of endogenously carbonylated proteins only works well for the most abundant of the low abundance target proteins, and there is

frequently significant interference from the very abundant non-modified proteins.

References

[1] M. Geiszt, J.B. Kopp, P. Varnai, T.L. Leto, Proc. Natl. Acad. Sci. U. S. A., 97 (2000) 8010.

[2] L.M. Sayre, M.A. Smith, G. Perry, Curr. Med. Chem., 8 (2001) 721.

[3] R.E. Pacifici, K.J. Davies, Gerontology, 37 (1991) 166.

[4] B. D'Autreaux, M.B. Toledano, Nat. Rev. Mol. Cell Biol., 8 (2007) 813.

[5] S. Nemoto, K. Takeda, Z.X. Yu, V.J. Ferrans, T. Finkel, Mol. Cell Biol., 20 (2000) 7311.

[6] L. Fialkow, Y. Wang, G.P. Downey, Free Radic. Biol. Med., 42 (2007) 153.

[7] A. Boveris, B. Chance, Biochem. J., 134 (1973) 707.

[8] J. St-Pierre, J.A. Buckingham, S.J. Roebuck, M.D. Brand, J. Biol. Chem., 277 (2002) 44784.

[9] A.J. Lambert, M.D. Brand, Methods Mol. Biol., 554 (2009) 165.

[10] J.S. Beckman, W.H. Koppenol, Am. J. Physiol., 271 (1996) C1424.

[11] A.Y. Andreyev, Y.E. Kushnareva, A.A. Starkov, Biochemistry (Mosc), 70 (2005) 200.

[12] T. Finkel, N.J. Holbrook, Nature, 408 (2000) 239.

[13] A. Pompella, A. Visvikis, A. Paolicchi, V. De Tata, A.F. Casini, Biochem. Pharmacol., 66 (2003) 1499.

[14] J.D. Hayes, L.I. McLellan, Free Radic. Res., 31 (1999) 273.

[15] H. Esterbauer, R.J. Schaur, H. Zollner, Free Radic. Biol. Med., 11 (1991) 81.

[16] H. Esterbauer, Am. J. Clin. Nutr., 57 (1993) 779S.

[17] G. Kroemer, J.C. Reed, Nat. Med., 6 (2000) 513.

[18] S. Orrenius, V. Gogvadze, B. Zhivotovsky, Annu. Rev. Pharmacol. Toxicol., 47 (2007) 143.

[19] A. Rasola, P. Bernardi, Apoptosis, 12 (2007) 815.

[20] Y. Tsujimoto, S. Shimizu, Apoptosis, 12 (2007) 835.

[21] S. Grimm, D. Brdiczka, Apoptosis, 12 (2007) 841.

[22] M. Crompton, Biochem. J., 341 (Pt 2) (1999) 233.

[23] J.C. Yang, G.A. Cortopassi, Free Radic. Biol. Med., 24 (1998) 624.

[24] K.B. Choksi, W.H. Boylston, J.P. Rabek, W.R. Widger, J. Papaconstantinou, Biochim. Biophys. Acta, 1688 (2004) 95.

[25] B. Friguet, FEBS Lett., 580 (2006) 2910.

[26] B. Friguet, L.I. Szweda, FEBS Lett., 405 (1997) 21.

[27] T. Grune, K.J. Davies, Mol. Aspects. Med., 24 (2003) 195.

[28] H. Ohkawa, N. Ohishi, K. Yagi, Anal. Biochem., 95 (1979) 351.

[29] R. Fields, H.B. Dixon, Biochem. J., 121 (1971) 587.

[30] A. Nakamura, S. Goto, J. Biochem., 119 (1996) 768.

[31] M. Oh-Ishi, T. Ueno, T. Maeda, Free Radic. Biol. Med., 34 (2003) 11.

[32] B.S. Yoo, F.E. Regnier, Electrophoresis, 25 (2004) 1334.

[33] D. Toroser, W.C. Orr, R.S. Sohal, Biochem. Biophys. Res. Commun., 363 (2007) 418.

[34] W.G. Chung, C.L. Miranda, C.S. Maier, Brain Res., 1176 (2007) 133.

[35] W.G. Chung, C.L. Miranda, J.F. Stevens, C.S. Maier, Food Chem. Toxicol., 47 (2009) 827.

[36] N. Tanaka, S. Tajima, A. Ishibashi, K. Uchida, T. Shigematsu, Arch. Dermatol. Res., 293 (2001) 363.

[37] M.R. Larsen, M.B. Trelle, T.E. Thingholm, O.N. Jensen, Biotechniques, 40 (2006) 790.

[38] N. Rauniyar, S.M. Stevens, Jr., L. Prokai, Anal. Bioanal. Chem., 389 (2007) 1421.

[39] L.M. Sayre, D. Lin, Q. Yuan, X. Zhu, X. Tang, Drug Metab. Rev., 38 (2006) 651.

[40] M.S. Bolgar, S.J. Gaskell, Anal. Chem., 68 (1996) 2325.

[41] M. Carini, G. Aldini, R.M. Facino, Mass Spectrom. Rev., 23 (2004) 281.

[42] J.A. Doorn, D.R. Petersen, Chem. Res. Toxicol., 15 (2002) 1445.

[43] A.L. Isom, S. Barnes, L. Wilson, M. Kirk, L. Coward, V. Darley-Usmar, J. Am. Soc. Mass Spectrom., 15 (2004) 1136.

[44] A. Temple, T.Y. Yen, S. Gronert, J. Am. Soc. Mass Spectrom., 17 (2006) 1172.

[45] M.K. Dennehy, K.A. Richards, G.R. Wernke, Y. Shyr, D.C. Liebler, Chem. Res. Toxicol., 19 (2006) 20.

[46] H.L. Wong, D.C. Liebler, Chem. Res. Toxicol., 21 (2008) 796.

[47] H. Mirzaei, F. Regnier, Anal. Chem., 77 (2005) 2386.

[48] B.A. Soreghan, F. Yang, S.N. Thomas, J. Hsu, A.J. Yang, Pharm. Res., 20 (2003) 1713.

[49] P.A. Grimsrud, M.J. Picklo, Sr., T.J. Griffin, D.A. Bernlohr, Mol. Cell Proteomics, 6 (2007) 624.

[50] J. Chavez, J. Wu, B. Han, W.G. Chung, C.S. Maier, Anal. Chem., 78 (2006) 6847.

[51] N. Rauniyar, S.M. Stevens, K. Prokai-Tatrai, L. Prokai, Anal. Chem., 81 (2009) 782.

[52] M.R. Roe, H. Xie, S. Bandhakavi, T.J. Griffin, Anal. Chem., 79 (2007) 3747.

[53] B. Han, J.F. Stevens, C.S. Maier, Anal. Chem., 79 (2007) 3342.

[54] S.P. Gygi, B. Rist, S.A. Gerber, F. Turecek, M.H. Gelb, R. Aebersold, Nat. Biotechnol., 17 (1999) 994.

[55] A.J. Heck, J. Krijgsveld, Expert Rev. Proteomics, 1 (2004) 317.

[56] Y. Oda, K. Huang, F.R. Cross, D. Cowburn, B.T. Chait, Proc. Natl. Acad. Sci.U. S. A., 96 (1999) 6591.

[57] K. Marley, D.T. Mooney, G. Clark-Scannell, T.T. Tong, J. Watson, T.M. Hagen, J.F. Stevens, C.S. Maier, J. Proteome Res., 4 (2005) 1403.

[58] P.V. Bondarenko, D. Chelius, T.A. Shaler, Anal. Chem., 74 (2002) 4741.

[59] D. Bylund, R. Danielsson, G. Malmquist, K.E. Markides, J. Chromatogr. A, 961 (2002) 237.

[60] A. Gilchrist, C.E. Au, J. Hiding, A.W. Bell, J. Fernandez-Rodriguez, S. Lesimple, H. Nagaya, L. Roy, S.J. Gosline, M. Hallett, J. Paiement, R.E. Kearney, T. Nilsson, J.J. Bergeron, Cell, 127 (2006) 1265.

[61] D. Lin, H.G. Lee, Q. Liu, G. Perry, M.A. Smith, L.M. Sayre, Chem. Res. Toxicol., 18 (2005) 1219.

[62] M.P. Washburn, D. Wolters, J.R. Yates, 3rd, Nat. Biotechnol., 19 (2001) 242.

[63] M. Bantscheff, M. Schirle, G. Sweetman, J. Rick, B. Kuster, Anal. Bioanal. Chem., 389 (2007) 1017.

[64] H. Mirzaei, F. Regnier, J. Chromatogr. A, 1134 (2006) 122.

[65] D.L. Meany, H. Xie, L.V. Thompson, E.A. Arriaga, T.J. Griffin, Proteomics, 7 (2007) 1150.

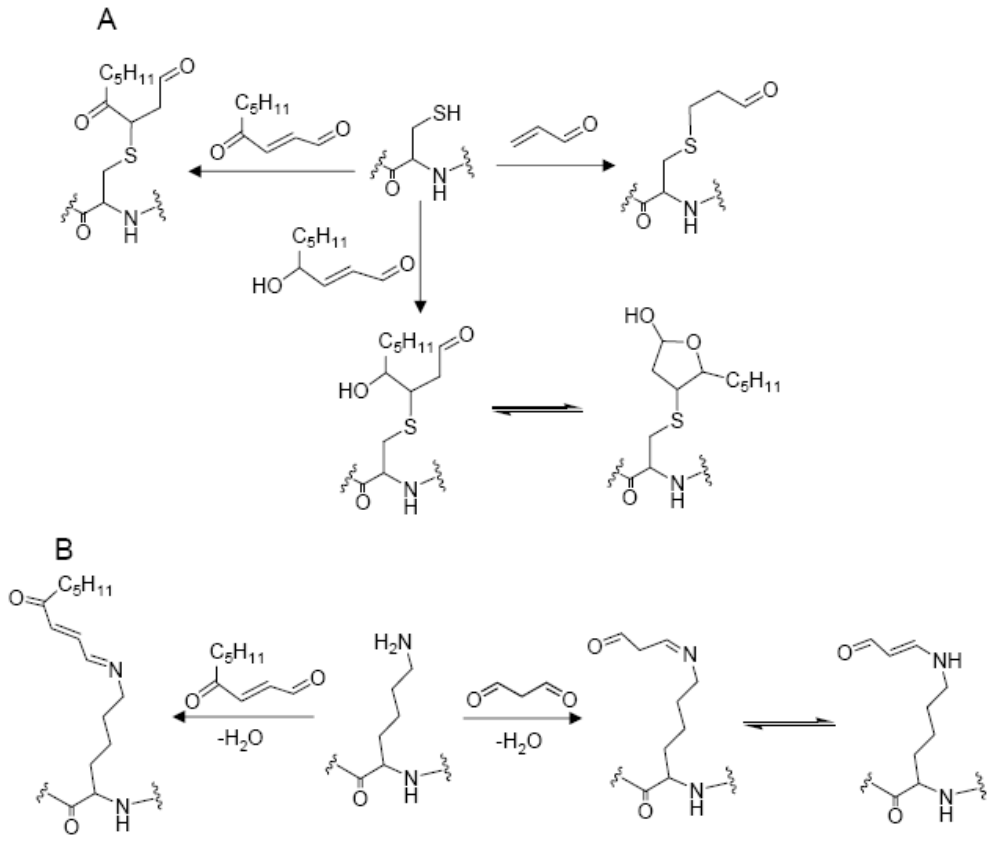

Scheme 1.1. Michael adducts formed from Cys-containing peptides with ACR, ONE and HNE (A), C-2 can also be the active site for ONE; Schiff bases formed from Lys-containing peptides with MDA and ONE (B).

CHAPTER 2. General Methods

Mass Spectrometer

A mass spectrometer consists of an ion source, a mass analyzer and detector. A sample is ionized in an ion source, and then the ions are sorted by an analyzer according to their m/z values and detected by a detector. The introduction of electrospray ionization (ESI) [1] and matrix-assisted laser/desorption ionization (MALDI) [2] in 1980's allows proteins and peptides, which are nonvolatile, to be analyzed by MS. In MALDI technique, a matrix, like α-cyano-4-hydroxycinnamic acid, is required. The matrix absorbs energy from the pulsed laser and transfers it to the analyte, which is then desorbed and forms the protonated ion in gas phase (Fig. 2.1). ESI is another popular soft ionization approach. High voltage (2-6 kV) is applied between the emitter, where samples come from, and the inlet of the mass spectrometer. The process of ESI involves the creation of an electrically charged spray followed by the reduction of the droplets' size and final liberation of totally desolvated ions (Fig. 2.2).

Modern mass analyzers include Time-of Flight (TOF), Quadrupole (Q), Quadrupole ion trap (QIT), Linear ion trap (LIT), Magnetic sector (B), Ion cyclotron resonance (ICR) and Orbitrap. In this thesis, Time-of Flight (TOF), Quadrupole (Q) and Linear Ion Trap (LIT) analyzers are employed. A quadrupole analyzer uses oscillating electrical fields to selectively stabilize or destabilize the paths of ions passing through a radio frequency (RF) quadrupole field [3]. This

analyzer can be operated under two modes: a RF-only mode or a RF/direct current (DC) mode, which allows for m/z filtering. Under RF/DC mode, a stable transmission of a narrow window of m/z can be acquired at a specified DC amplitude. This high ion transmission feature makes quadrupole a popular choice for precursor ion selection in tandem mass spectrometry. The RF-only mode is often used to transfer and focus all ions. For a full MS scan in quadrupole, only the picked ion can reach the detector and the others are wasted, thus the sensitivity is poor. Recently, a few types of LIT were developed [4-7]. One of this techniques commercialized by Applied Biosystems, Inc. is introduced here. Under this type of LIT, a RF-only mode is used to hold ions radially and an entrance potential barrier and an exit potential barrier are applied to contain ions axially. To eject the ions to the detector, the drive and auxiliary RF voltages are simultaneously ramped with an increase in amplitude, thus the ions with increasing m/z will become unstable and be ejected for detection. The sensitivity in LIT is much higher than quadrupole, since most of ions can reach the detector for full MS scans.

The construction of a TOF analyzer was described in 1946 by Stephens [8]. Ions with different m/z after moving through an acceleration voltage (U) are dispersed in time (t) when they fly along a tube with a known length (l). Here is the equation to describe this process: $t = (m/2zeU)^{1/2}l$. According to this equation, flying time is proportional to the square root of the m/z. Distribution of kinetic energy for

ions produced from an ion source makes the ions with the same m/z cannot reach the detector at the exactly same time, thus reducing the resolution. One major approach (Time-lag focusing) to reduce the distribution is to employ a delay between generation and acceleration of the ions [9]. In this approach, ions are generated in an environment without electric field and separated in space according to their different initial velocities after a time delay. Then the acceleration voltage is turned on with a fast pulse. The ions with higher initial velocities have travelled further, thus will obtain less energy from the acceleration voltage. Finally the spreads of kinetic energy for ions will be reduced. The other approach is called reflector [10]. In this method, a retarding electric field, reflector, is introduced in the ion passing way. The ions will penetrate the reflector and be expelled in the opposite direction. The ions with higher kinetic energy will penetrate deeper than those with the same m/z but having lower kinetic energy, thus the ions with higher kinetic energy will have a longer journey to reach the detector, achieving a correction in time-of-flight. TOF has become a high resolution mass analyzer after these improvements.

In this thesis, there are three mass spectrometers used, which are 4000 Q-trap, 4700 TOF/TOF Proteomics Analyzer from Applied Biosystems and Q-TOF Ultima Global from Waters. Fig. 2.3 shows schematics of these instruments. Q-TOF Ultima Global in our lab operates in MS or MS/MS modes with a nano-electrospray source. Under MS mode, the ions are generated in the ion

source and pass through the transfer optics, quadrupole (RF mode) and the collision cell (no collision) to the pusher, where the ions will be accelerated and pass the reflectron to reach the detector. Under MS/MS mode, the precursor ions are selected by the quadrupole (RF/DC mode) and accelerated to the collision cell, where collision with neutral gases happens. The fragment ions are then accelerated and detected in a reflectron mode.

4000 Q-trap is a triple quadrupole linear ion trap mass spectrometer, in which the second analyzer can function as quadrupole or LIT. LIT will be used to increase sensitivity when normal MS or MS/MS is performed; quadrupole will be applied when some special MS/MS for triple quadruple is required. In this thesis, the precursor ion scan is used to find the precursor ions which contain specific fragment ions after CID and the selected reaction monitoring (SRM) scan is applied to quantitative analysis. In these two MS/MS modes, the second analyzer is quadrupole. Under the precursor ion scan, the Q3 is fixed at a specified m/z and Q1 sweeps a mass range, so the precursor ions containing that specified fragment will be detected. Under the SRM scan, Q1 is fixed to at a specified m/z of M1 and Q3 is fixed to F1, so only precursor ion with m/z of M1 and with fragment of F1 after CID can be detected by the detector. These two filter steps greatly reduce interference making it a classic quantitative method for complex samples. SRM is also a suitable mode to determine multiple analytes (like a few hundred analytes) simultaneously because of the extremely fast switch between different SRM

transitions. Fig. 2.4 shows the schematic of these two MS/MS modes and one SRM chromatogram of a peptide from a complex mitochondrial sample. The relative low background indicates the specificity of SRM.

4700 TOF/TOF Proteomics Analyzer operates in MS or MS/MS modes with a MALDI source. Under MS mode, generated ions are accelerated in Source 1 and pass the tube in a linear way or a reflector way to reach the detector. Under MS/MS mode, the precursor ions are chosen by the ion selector according the flight time in a short linear TOF analyzer. After passing the collision cell, the fragments are accelerated again in Source 2 and reach the reflector detector in the linear way. Because of the shot first linear TOF tube, the resolution for precursor-ion selection is usually only around 10 Da, which is much lower than the previously introduced two mass spectrometers (about 1 Da) using a quadrupole.

Proteomics based on mass spectrometry

Proteomics is the large-scale study of proteins, especially their structures and functions [11, 12]. Mass spectrometry has become the most comprehensive and versatile tool for proteomics study [13, 14]. Here, identification and quantification of proteins based on mass spectrometry are mainly introduced. Right now, bottom-up proteomics is the most popular method in which proteins are digested into peptides prior to analysis of mass spectrometry. This approach usually

requires tandem spectra for peptide identification. Collision-induced dissociation (CID) is the most prominent collision method although electron capture dissociation (ECD) [15] and electron transfer dissociation (ETD) [16] become useful especially for post-translational modifications recently. Under CID, the isolated charged peptides (usually protonated) are activated by collisions with inert gases, such as argon, helium or nitrogen, and are dissociated. The fragment ions mainly are classified into two types. Ions containing N-terminus are labeled with a, b and c; ions containing C-terminus are labeled with x, y and z. B and y ions are the main fragment ions under CID although fragmentation patterns change with other parameters, such as collision energy, amino acid composition and pressure [17]. Fig. 2.5 shows the nomenclature of peptide fragmentation.

Tandem mass spectra of peptides are usually employed to identify the sequences with software such as Mascot, SEQUEST, XProteo and Peaks, which have similar principles. Here we focus on Mascot [18]. In this search engine, candidate peptides based on different digestion enzymes and their theoretical tandem spectra are generated *in silico* with protein databases and proprietary fragmentation models. The experimental tandem mass spectra are then compared with theoretical ones to calculate the probability that observed match between them is a chance event. The match with the lowest probability is considered as the best match. A widely accepted threshold is that the probability of the observed event occurring by chance is lower than 5% ($p < 0.05$). For a good match, the probability (P) is

usually an extremely small number. A probability-based score, which is $-10Log_{10}(P)$, is applied to give a convenient number. For example, the score is 60 if a probability is 10^{-6}. A higher score means a higher match. During Mascot searching, the identification score ($p < 0.05$) is important because it varies with the probability and also the size of the data base used. Thus, Mascot scores alone are not enough to show the quality of identification.

Quantification of peptides or proteins based on mass spectrometry mainly has two approaches [19]. One major approach is based on isotope-labeled amino acids or peptides, which includes reagents like ICAT or iTRAQ, methods like SILAC or AQUA. The other major approach is label-free quantification including two different strategies: (i) measuring and comparing signal intensity of peptides from proteins; (ii) counting and comparing the number of identified-peptide spectra from a particular protein. Fig. 2.6 shows these different ways, where boxes with horizontal lines indicate when samples are combined. Earlier combination of samples implies less variation involved during experiments, indicating more accurate measurement. Label-free approaches are the least accurate for quantification because all the systematic and non-systematic error happens between experiments. Here we only introduce the isotope labeled approaches.

Stable isotope labeling by amino acids in cell culture (SILAC) [20] introduced by Mann is the most popular metabolic labeling way, where the medium containing $^{13}C_6$-arginine and $^{13}C_6$-lysine are used. In this way, the tryptic peptides can carry

at least one heavy-labeled amino acid to be distinguished with the light-labeled ones. Usually, the MS intensities of heavy and light labeled peptides, which are co-eluted from LC, are compared to measure their relative amount. Since the samples are combined at the cell level, all quantitative error sources introduced by the biochemical and mass spectrometric procedures are excluded, indicating excellent accuracy. However, this method is mainly applied to immortalized cells because of the high cost and long time required for creating heavy and light labeling cells.

Chemical labeling of proteins or peptides is another way for quantification. Theoretically, any reactive amino acid can be modified with isotope-labeled chemicals [21]. Practically, side chains of lysine and cysteine are mainly applied for this purpose. ICAT (Isotope-coded affinity tag) [22] and iTRAQ (Isotope tags for relative and absolute quantification) [23] are the most popular reagents these days. The ICAT reagent (Fig. 2.7) consists of three elements: an affinity tag (biotin) that can enrich ICAT-labeled peptides by an avidin column; a linker, which can carry light or heavy isotopes; and a reactive group with high specificity to thiol groups (cysteines). Cysteines from samples react with light or heavy ICAT, and the MS intensities of the same peptides from different samples will be compared to quantify the two samples. Because cysteine residue is a relatively rare in proteins, ICAT can significantly reduce the complexity of biological samples, and meanwhile, it is not applicable to proteins which have no or few

cysteine residues.

ITRAQ reagents are specific to N-terminus of the peptides and ε-amino groups of lysine residues via the specific N-hydroxysuccinimide (NHS) chemistry. Fig. 2.8 shows iTRAQ chemistry and application principle in mass spectrometry. The iTRAQ consists of a reporter group, a mass balance group, and a peptide-reactive group, which is specific with amine groups. The total masses for iTRAQ reagents are the same and the masses for the reporter groups are different because of the ^{13}C, ^{15}N and ^{18}O atoms. The same peptides from different samples can be labeled with iTRAQ containing different reporter groups. These labeled peptides have the same precursor masses, while different fragment ions for reporter groups in MS/MS. The relative concentration of the peptides can be measured from the relative intensities of the corresponding reporter ions after CID. Since there are up to eight different reporter groups available in iTRAQ today, this reagent is qualified to quantify up to eight samples simultaneously, which is valuable for biological samples with different ages.

Gerber et al. [24] developed a method called AQUA (absolute quantification of protein) in 2004. In this approach, a known amount of synthesized isotope-labeled peptide is added in a protein sample. After digestion, the relative intensity of this peptide in heavy and light form is measured to figure out the absolute amount of the protein containing this peptide. Unlike the other metabolic or chemical labeling methods, where relative quantification is obtained for a large number of

proteins, AQUA method can obtain absolute quantification for one or a few interested proteins depending on the number of the synthetic peptides added in a sample. The other limitation for this approach is that the protein digestion efficiency is assumed to 100 %, which is not the case for most biological samples. Thus, Beynon et al. [25] refined this approach by creation of genes, which express concatenated isotope-labeled peptides. These long peptides have close digestion efficiency with proteins and multiple standard peptides after digestion can be applied for multiple proteins of interest.

For all these quantitative approaches, MS usually is applied for the measurements except the iTRAQ method, where MS/MS is used. One limitation for MS analysis is the specificity since there usually are multiple isobaric peptides present in complex samples. Another limitation is the dynamic range especially for a TOF analyzer by using a micro-channel plate (MCP) detector with a time-to-digital converter (TDC), which is easier to be saturated comparing with some other detectors. Recently, SRM becomes popular for great reduction of these two limitations [19, 26]. Two filter steps involved in SRM reduce interference and only one fragment ion from the precursor ion is allowed to reach the detector, reducing the chance of saturation.

Identification and quantification of carbonylated peptides were performed in this thesis. An enrichment step was necessary before mass spectrometry analysis because of their low abundances in mitochondrial samples. The reagents,

N'-aminooxymethylcarbonylhydrazino-D-biotin (ARP) and iodoacetyl-PEO_2-Biotin (IPB) were used to label acrolein-modified Cys-containing peptides and the corresponding unmodified ones for enrichment. The ratios between them are determined by nanoLC-SRM analysis.

Mitochondrial isolation

The experimental protocol for the animal studies was approved by the Institutional Animal Care and Use Committee at Oregon State University. Male F344 rats (Harlan, Indianapolis, IN) were housed in individual plastic cages covered with Hepa filter and allowed free access to standard animal chow and water *ad libitum*. Rats were anesthetized with ether and the hearts were perfused with phosphate-buffered saline (PBS), removed, rinsed in saline, blotted dry, and weighed. Subsarcolemmal (SSM) and interfibrillar (IFM) mitochondria were isolated by the method used by Palmer et al. [27] with slight modification [28]. After trimming excess fat and removing the atria, the ventricles were minced and homogenized 1:5 (w/v) with buffer A1 (200 mM mannitol, 5 mM MOPS, 2 mM EDTA, 0.2 % BSA, pH 7.4). The heart tissues were homogenized with a glass homogenizer and pestle attached to a drill. The homogenates were then centrifuged at 500 × *g* for 10 min at 4°C (all remaining centrifugation steps were also performed at 4°C). The supernatant was saved and the pellet was resuspended in 10 volume of Buffer A1 and centrifuged at 500 × *g* for 10 min. The two

supernatants were subsequently pooled and centrifuged at 3000 × *g* for 10 min to obtain SSM, while the pellet obtained in the second low-speed centrifugation step was saved for IFM isolation. This pellet was resuspended in 3 volumes of Buffer B1 (100 mM KCl, 50 mM MOPS, 2 mM EDTA, 0.2 % BSA, pH 7.4), nagarse (3 mg/g wet weight tissue) was added to the tissue pellet, incubated on ice for 0.5 min, and homogenized. The homogenate was then diluted 7-fold with Buffer B 1 and centrifuged at 5000 × *g* for 5 min. The supernatant was discarded and the pellet resuspended in the original volume of buffer. The resuspended pellet was centrifuged at 500 × *g* for 10 min to yield the nuclear pellet. The supernatant was saved and the pellet was resuspended and centrifuged at 500 × *g* for 10 min. This step was repeated once more with the supernatant being saved after each spin. The supernatants from the three low-speed spins were combined and centrifuged at 3000 × *g* for 10 min to obtain the IFM pellet. The simple flow chart for this procedure is listed in scheme 2.1.

Protein extraction from mitochondria

To obtain protein, the mitochondrial membranes needed to be broken. There were two methods of protein extraction from mitochondria in this thesis. The freeze/thaw method involved freezing mitochondria in a liquid nitrogen bath and then thawing them at ice water with mild sonication. The second method involved the melting the mitochondrial membranes by the 1% Triton - 100 detergent with

mild sonication at ice water. Finally, the proteins would be obtained by centrifugation. The former method could extract 0.351 mg protein from two vials of mitochondria; the latter one could obtain 0.585 mg. Detergent with mild sonicatin had the higher efficiency and would be mainly used in this thesis.

Avidin affinity enrichment

Avidin is a tetrameric protein. Each identical subunit can bind to biotin with a high degree of specificity and affinity. This avidin-biotin system can be applied to enrich compounds with biotin tags. The avidin-biotin bond is one of the strongest non-covalent bonds since the dissociation constant of avidin is about 10^{-15} M [29]. The native avidin has to be denatured to break the bond to release compounds with biotin tags. This non-reversible nature of the avidin-biotin system can limit its application in affinity enrichment. Thus, monomeric avidin with a reduced affinity for biotin ($K_D \approx 10^{-7}$ M) was developed [30]. This modified avidin allows elution conditions from the avidin matrix much milder. In this thesis, monomeric avidin is used and low pH conditions are used to release the target peptides with biotin tags. Scheme 2.2 shows this enrichment procedure. The samples with biotin labeled target peptides are loaded to the column with monomeric avidin beads inside. Then the peptides without biotin tags are washed away with a buffer. The final target peptides are eluted with a buffer of low pH.

Reaction properties of N'-aminooxymethylcarbonylhydrazino-D-biotin (ARP) and iodoacetyl-PEO_2-Biotin (IPB)

In this thesis, ARP and IPB were used to label the acrolein-modified peptides and Cys-containing peptides, respectively. Scheme 2.3 showed the reaction to form ARP-ACR modified and IPB-labeled peptides. The reaction yield and the stability of the products were important for quantitative analysis. Here, one mM model peptide (CLLLSAPRR) was applied to react with 2 mM IPB for one hour at room temperature under darkness at pH 8.3. One mM this model peptide was also used to react with acrolein to form the acrolein-modified peptide, which was further used to react with 2 mM ARP at pH 7.4 to form the ARP-ACR modified peptide. From the MALDI/MS spectra in Fig. 2.9, there was no native peptide signal for the IPB labeling reaction and no acrolein-labeled peptide signal for ARP labeling reaction, which indicates almost 100% reaction yield for these reactions. Three mM DTT was added to IPB-labeled solution to remove excess IPB; and three mM methanal was added to ARP labeling solution to remove excess ARP. These solutions were then diluted by 100 times to close the real concentration in biological samples. These solutions were reserved for 24 hours at pH 7.4 and 2 hours at pH 3.0 under room temperature, and then were determined by MALDI/MS spectra (data not shown). These spectra were nearly identical to them in Fig. 2.9. There was barely native peptide signal observed for the IPB labeling solution or acrolein-labeled peptide signal for ARP labeling solution, which

indicated these products were stable enough for sample preparation and LC-MS analysis.

References

[1] J.B. Fenn, M. Mann, C.K. Meng, S.F. Wong, C.M. Whitehouse, Science, 246 (1989) 64.

[2] M. Karas, F. Hillenkamp, Anal. Chem., 60 (1988) 2299.

[3] W. Paul, Angew. Chem. , 102 (1990) 780.

[4] B.A. Collings, W.R. Stott, F.A. Londry, J. Am. Soc. Mass Spectrom., 14 (2003) 622.

[5] J.W. Hager, Rapid Commun. Mass Spectrom. , 16 (2002) 512.

[6] Y. Huang, S. Guan, H.S. Kim, A.G. Marshall, Int. J. Mass Spectrom. Ion Processes 152 (1996) 121.

[7] J.C. Schwartz, M.W. Senko, J.E. Syka, J. Am. Soc. Mass Spectrom., 13 (2002) 659.

[8] W.E. Stephens, Bull. Am. Phys. Soc., 21 (1946) 22.

[9] W.C. Wiley, I.H. McLaren, Rev. Sci. Instrum. , 26 (1955) 1150.

[10] B.A. Mamyrin, Int. J. Mass Spectrom. Ion Processes, 131 (1994) 1.

[11] N.L. Anderson, N.G. Anderson, Electrophoresis, 19 (1998) 1853.

[12] W.P. Blackstock, M.P. Weir, Trends Biotechnol., 17 (1999) 121.

[13] R. Aebersold, M. Mann, Nature, 422 (2003) 198.

[14] J.R. Yates, C.I. Ruse, A. Nakorchevsky, Annu. Rev. Biomed. Eng., 11 (2009) 49.

[15] R.A. Zubarev, Curr. Opin. Biotechnol., 15 (2004) 12.

[16] J.J. Coon, J.E. Syka, J. Shabanowitz, D.F. Hunt, Biotechniques, 38 (2005) 519.

[17] B. Paizs, S. Suhai, Mass Spectrom. Rev., 24 (2005) 508.

[18] D.N. Perkins, D.J. Pappin, D.M. Creasy, J.S. Cottrell, Electrophoresis, 20 (1999) 3551.

[19] M. Bantscheff, M. Schirle, G. Sweetman, J. Rick, B. Kuster, Anal. Bioanal. Chem., 389 (2007) 1017.

[20] S.E. Ong, B. Blagoev, I. Kratchmarova, D.B. Kristensen, H. Steen, A. Pandey, M. Mann, Mol. Cell Proteomics, 1 (2002) 376.

[21] S.E. Ong, M. Mann, Nat. Chem. Biol., 1 (2005) 252.

[22] S.P. Gygi, B. Rist, S.A. Gerber, F. Turecek, M.H. Gelb, R. Aebersold, Nat. Biotechnol., 17 (1999) 994.

[23] P.L. Ross, Y.N. Huang, J.N. Marchese, B. Williamson, K. Parker, S. Hattan, N. Khainovski, S. Pillai, S. Dey, S. Daniels, S. Purkayastha, P. Juhasz, S. Martin, M. Bartlet-Jones, F. He, A. Jacobson, D.J. Pappin, Mol. Cell Proteomics, 3 (2004) 1154.

[24] S.A. Gerber, J. Rush, O. Stemman, M.W. Kirschner, S.P. Gygi, Proc. Natl. Acad. Sci. U. S. A., 100 (2003) 6940.

[25] R.J. Beynon, M.K. Doherty, J.M. Pratt, S.J. Gaskell, Nat. Methods, 2 (2005) 587.

[26] J. Malmstrom, H. Lee, R. Aebersold, Curr. Opin. Biotechnol., 18 (2007) 378.

[27] J.W. Palmer, B. Tandler, C.L. Hoppel, J. Biol. Chem., 252 (1977) 8731.

[28] J.M. Duan, M. Karmazyn, Mol. Cell Biochem., 90 (1989) 47.

[29] N.M. Green, Biochem. J., 89 (1963) 585.

[30] R.A. Kohanski, M.D. Lane, Methods Enzymol., 184 (1990) 194.

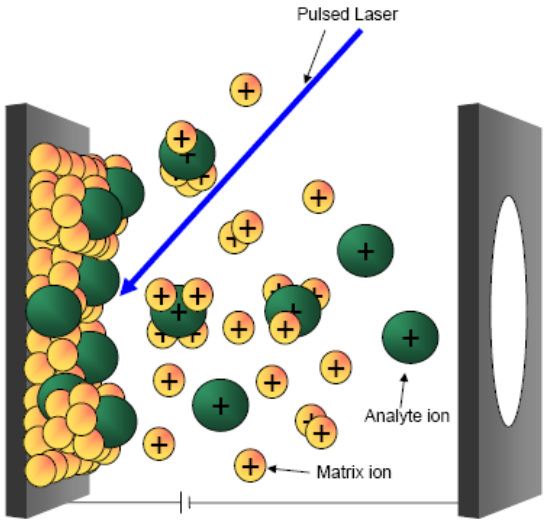

Figure 2.1. Schematic of the MALDI process.

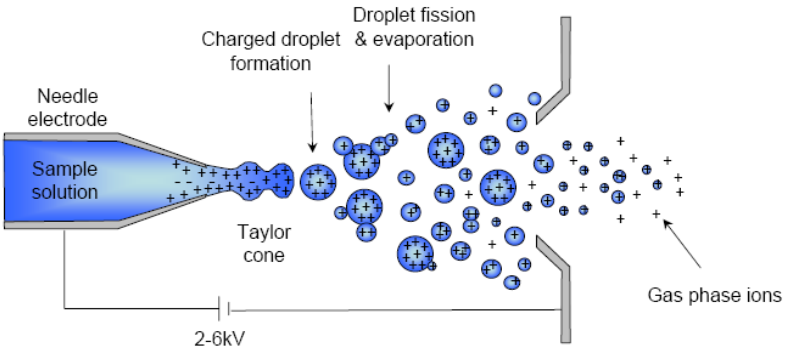

Figure 2.2. Schematic of the ESI process under a positive mode.

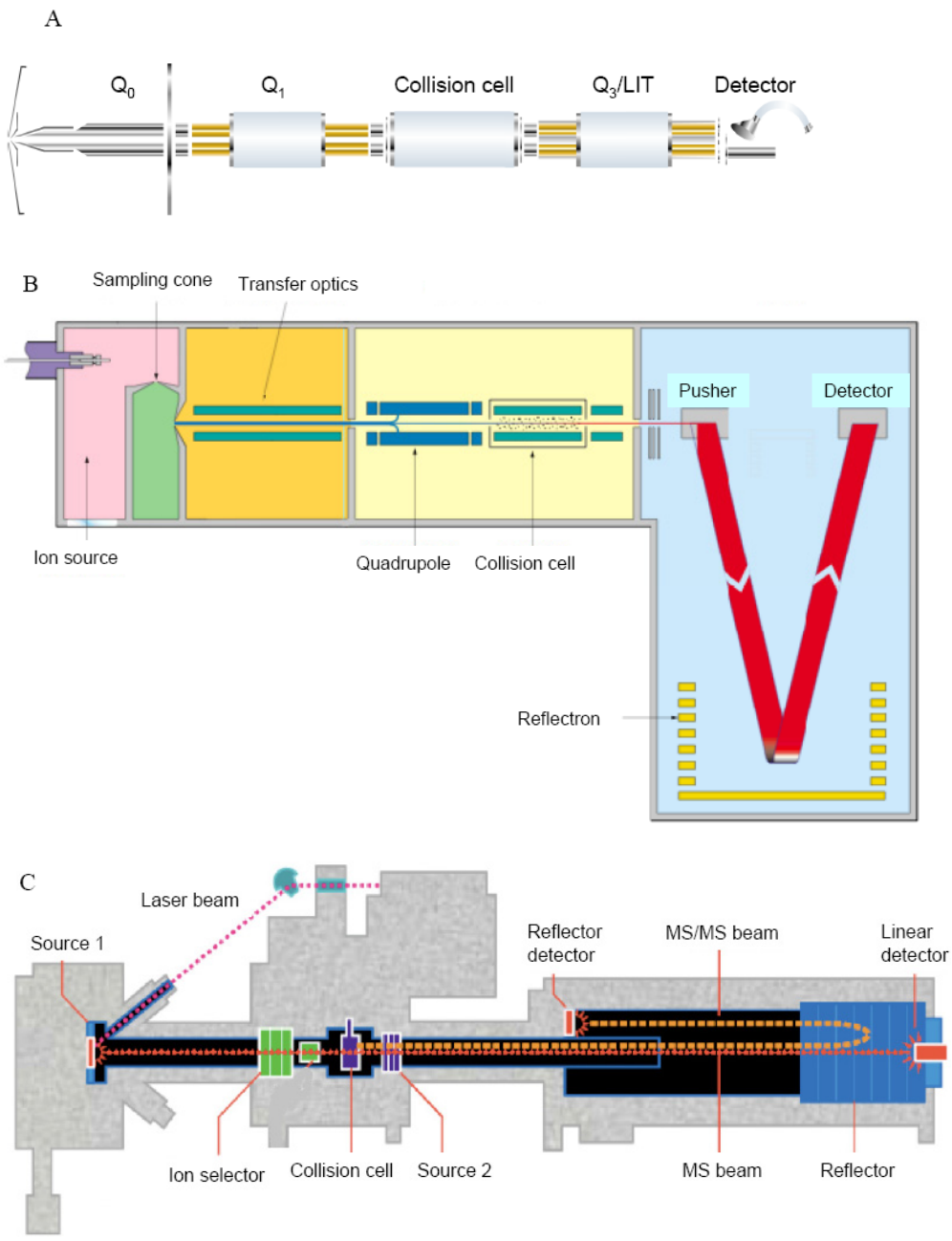

Figure 2.3 A. Schematic of 4000 Q-Trap (Picture modified from Applied Biosystems, Inc. Concord, Ontario, Canada); B. Schematic of Q-TOF Ultima Global (Picture modified from Micromass/ Waters, Manchester, UK); C. Schematic of 4700 TOF/TOF Proteomics Analyzer (Picture modified from Applied Biosystems, Inc. Framingham, MA).

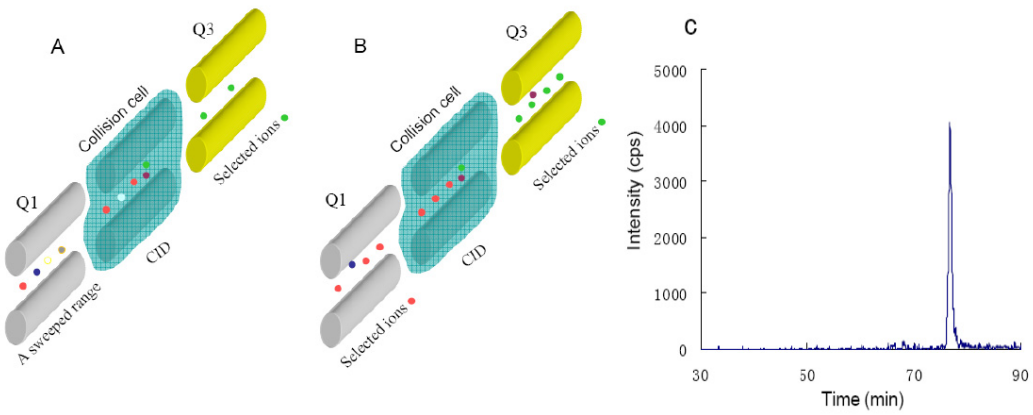

Figure 2.4. Two MS/MS modes often used for triple quadruples: A, Precursor Ion Scan; B, Selected Reaction Monitoring (SRM) Scan. C, one SRM chromatogram of a peptide from a complex mitochondrial sample.

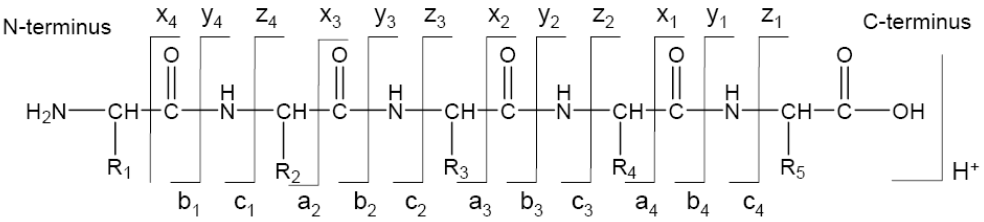

Figure 2.5. The nomenclature of peptide fragmentation. Y and b ions are the main ions under CID.

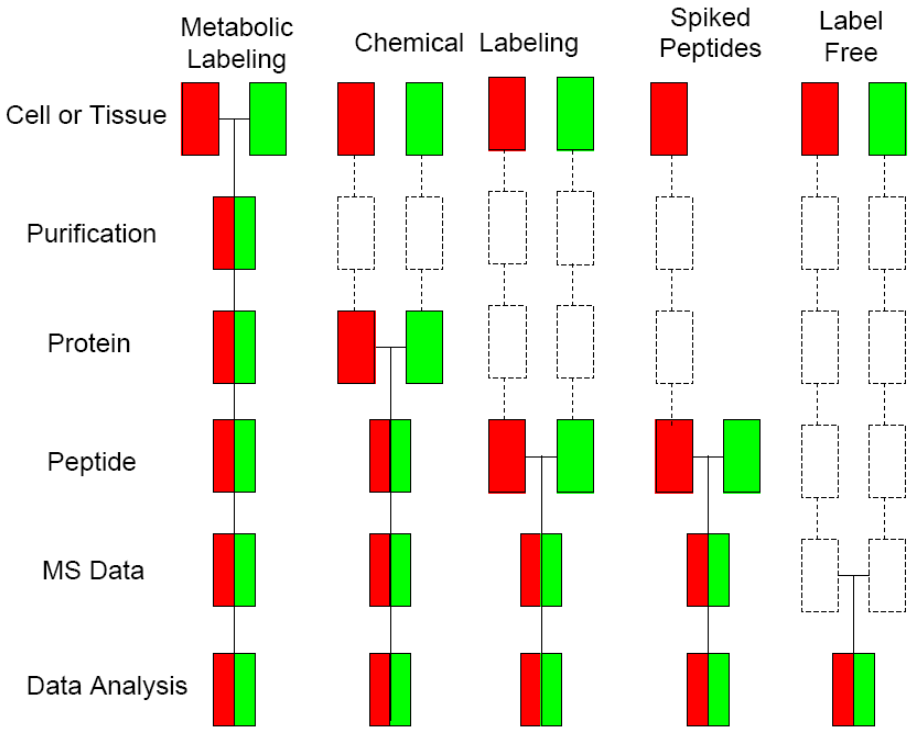

Figure 2.6. Common quantitative mass spectrometry workflows. Boxes in red and green represent two experimental conditions. Horizontal lines indicate when samples are combined. Dashed lines indicate points at which experimental variation and thus quantification errors can occur. (Figure is modified from Bantscheff et al. [19].)

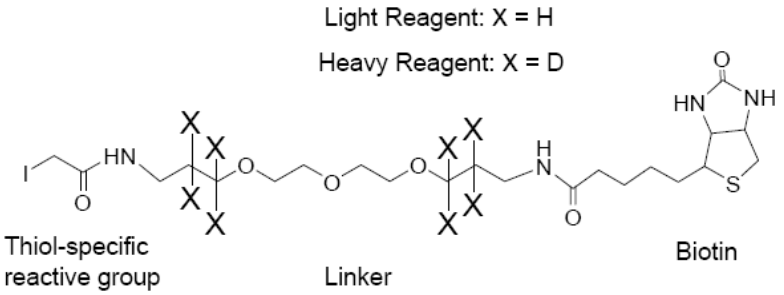

Figure 2.7. Structure of the ICAT reagent. The reagent exists in two forms: heavy and light. (Figure is modified from Gygi et al. [22].)

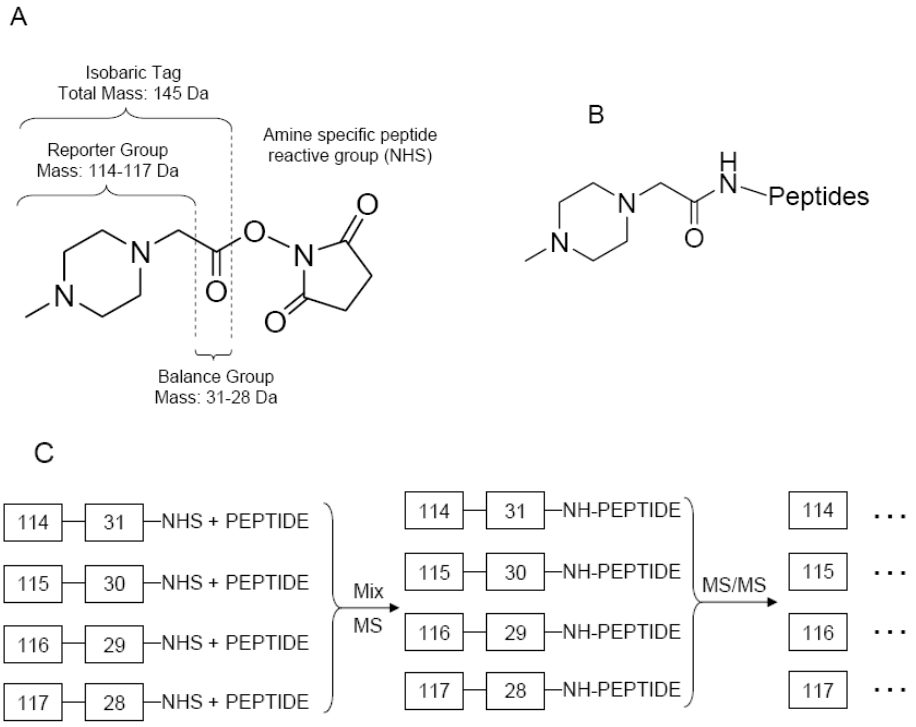

Figure 2.8. ITRAQ chemistry and application principle in mass spectrometry. A, Three parts for iTRAQ: a reporter group, a mass balance group (carbonyl), and a peptide-reactive group (NHS ester). B, Structure after reaction between iTRAQ and four peptides, the total masses are the same and the masses for the reporter groups are different because of the ^{13}C, ^{15}N and ^{18}O atoms. C, Four different reporter groups under MS/MS are used to quantify the same peptide from four different samples. (Figure is modified from Ross et al. [23].)

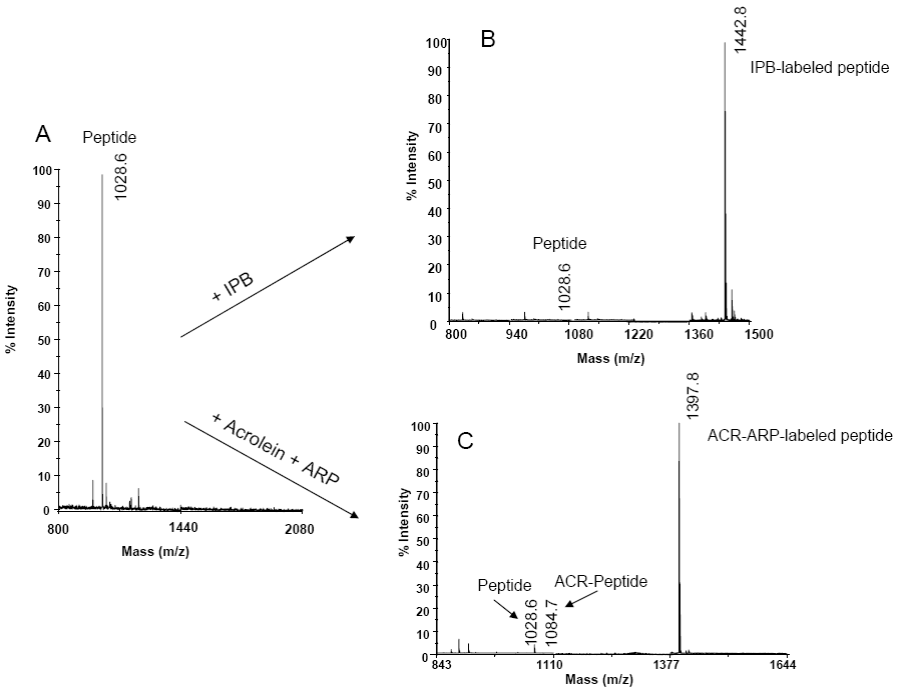

Figure 2.9 MALDI/MS spectra of the model native peptide (A); the reaction products with IPB (B); the reaction products with acrolein and ARP (C).

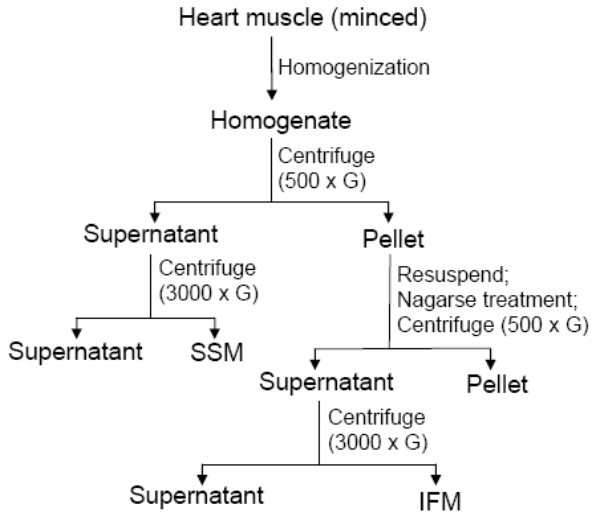

Scheme 2.1. Flow chart of mitochondrial isolation.

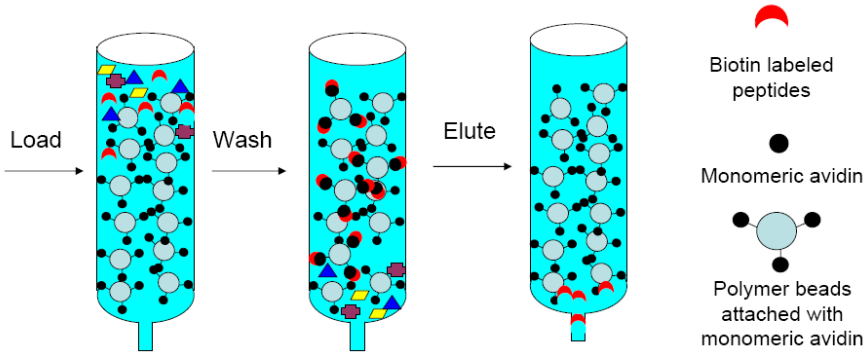

Scheme 2.2. Flow chart of avidin affinity enrichment for biotin labeled peptides.

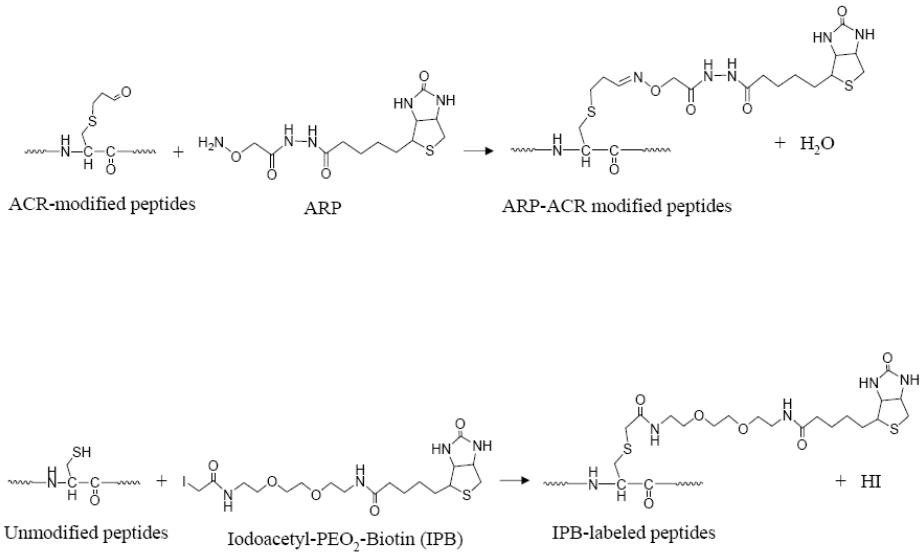

Scheme 2.3 The reactions to form ARP-ACR modified and IPB-labeled peptides.

CHAPTER 3.

Modification of Peptides by Lipid Peroxidation Products Studied by MALDI-MS/MS using a TOF/TOF Instrument

Jianyong Wu, Jie Zhang, Michael Hare, Claudia S. Maier*

Department of Chemistry, Oregon State University, Corvallis OR, 97330

* Corresponding. author. Tel.: +1 541 737 9533; fax: +1 541 737 2062.
E-mail address: claudia.maier@oregonstate.edu (C. S. Maier).

Abstract

The adduction of proteins and biomolecules by 4-hydroxy-2-nonenal and/or other lipid aldehydes is thought to be an initiating or propagating factor in the pathophysiology of several diseases, such as athereosclerosis and diabetes, and aging-related disorders e.g. Alzheimer's disease (AD) and Parkinson's disease. The identification of protein sites modified by oxylipids is of key relevance for advancing our understanding how oxidative damage affects structure and function of proteins. Based on nucleophilicity indexes from quantum calculations and percentages of reactive forms, the rank order of reactivity for amino acids at pH 7.4 is: Cys > His > Lys > Arg and the rank order of reactivity for lipid peroxidation products is: 4-oxo-2-nonenal > acrolein > 4-hydroxy-2-nonenal. Three synthesized model peptides containing one nucleophilic residue (i.e. Cys, His or Lys) were reacted with malondialdehyde, 4-hydroxy-2-nonenal, 4-oxo-2-nonenal and acrolein. MALDI-MS analysis and MS/MS analysis under high energy collision-induced dissociation (CID) were performed to confirm the adduct type and the modification sites. Michael adducts and Schiff bases were the predominant products under pH 7.4 within 2 hours. All MS/MS spectra of Michael adducts contain the neutral loss of the oxylipid moiety ions. Cys-containing peptide oxylipid conjugates have additional characteristic neutral loss of HS-oxylipid moiety ions. His-containing peptide oxylipid conjugates have characteristic oxylipid-containing His immonium ions. Lys-containing peptide

oxylipid conjugates (Schiff base) also show oxylipid-containing Lys immonium ions. However, there is no neutral loss of the oxylipid moiety ion for these Schiff bases.

Introduction

Reactive oxygen species (ROS), produced by various normal and abnormal processes in the cell, can result in deleterious modification of proteins, DNA, and lipids [1-5]. Oxidative stress due to ROS is counteracted by an intricate antioxidant system, and the degree of oxidative stress is determined by the balance of ROS production and antioxidant defenses [1]. Protein modifications due to ROS have been implicated in age-related disorders and in the etiology and pathology of inflammatory diseases. Oxidative modification of proteins can result in both backbone peptide bond cleavage and side-chain modifications [3, 4, 6-8]. An important side-chain modification is the introduction of protein carbonyls by secondary reaction of histidine (His), cysteine (Cys), lysine (Lys) and arginine (Arg) residues with lipid peroxidation products, which are produced from polyunsaturated fatty acids (PUFA) and their esters under oxidative stress [9-12]. Scheme 3.1 shows examples of lipid peroxidation products produced through oxidized PUFA. The adduction of these lipid peroxidation products to proteins and other biomolecules is thought to be an initiating or propagating factor in the pathophysiology of several diseases, including atherosclerosis, cancer,

diabetes-related complications and neurodegenerative diseases [2, 13-18].

Malondialdehyde (MDA), 4-hydroxy-2-nonenal (HNE), 4-oxo-2-nonenal (ONE) and acrolein (ACR) are four major lipid peroxidation products. The conjugation of the double bond with the aldehyde group in HNE, ACR and ONE makes C-3 a strong electrophilic center to form Michael adducts with nucleophilic sites in proteins, such as histidine imidazole moieties, cysteine sulfhydryls and ε-amino groups of lysine residues. C-2 can be another active site for Michael adducts in ONE since the double bond is also conjugated with the ketone group [11]. In addition to forming Michael adducts, these lipid peroxidation products are able to form Schiff bases when the aldehyde group reacts with ε-amino groups of lysine residues in proteins [2, 18-21]. Scheme 3.2 shows examples of Michael adduct and Schiff base forming reactions of peptides with lipid peroxidation products.

The reaction rate of Michael addition of the nucleophilic side chains of Cys, His, Lys, and Arg to ONE, HNE, and ACR have been determined experimentally [21-26]. In addition, LoPachin et al. have used calculated quantum mechanical parameters in conjunction with frontier molecular orbital (FMO) theory to rationalize the observed reactivities [25-27]. In FMO theory, covalent bonding occurs when an electron pair from the highest occupied molecular orbital (HOMO) of the nucleophile is donated into the lowest unoccupied molecular orbital (LUMO) of the electrophile. In a recently developed application of FMO theory, calculated energies for the HOMO and LUMO are used to determine a

nucleophilicity index (ω^-) which was shown to correlate with the relative reaction rate for some nucleophilic reactions [28]. LoPachin et al. calculated nucleophilic indexes for ACR and HNE reaction with unprotected Cys, His and Lys. In the present study, nucleophilicity indexes for the reaction of protected Cys, His, Lys, and Arg with ACR, HNE, and ONE have been calculated. Protected amino acids were used for quantum calculations because the protected amino acid is expected to better reflect its reactivity in a peptide.

Tandem mass spectrometry has emerged as the premier technology for the identification of post-translational oxidative modification sites [29]. However, the use of MALDI tandem mass spectrometry with high energy collision-induced dissociation (CID) on a TOF/TOF instrument for sequencing oxylipid-peptide conjugates has not been systematically studied. In this study, the adduction type of oxylipid peptide conjugates was determined by MALDI-MS analysis. We also systematically investigated the mass spectrometric fragmentation behavior of synthetic oxylipid peptide conjugates containing different nucleophilic amino acid residues modified by four different lipid peroxidation products using a TOF/TOF instrument.

Material and methods

Chemicals

HNE (10 mg mL^{-1} in ethanol) and ONE (10 mg mL^{-1} in methyl acetate) were

obtained from Cayman Chemical, Ann Arbor, MI. 1,1,3,3-tetraethoxypropane and acrolein were from Sigma, St. Louis, MO. 9-Fluoroenylmethoxy-carbonyl (Fmoc) derivatized amino acids were from SynPep Co. (Dublin, CA). Fmoc-Arg(pbf)-Rink Amide-MBHA resin with bound C-terminal residues was purchased from AnaSpec Inc. (San Jose, CA).

Synthesis of MDA and modified peptides.

The peptides Ac-SVVDLTCR-amide, Ac-SVVDLTHR-amide, Ac-SVVDLTKR-amide were synthesized using a PS3 automated solid phase peptide synthesizer (Protein Technologies, Inc., Tucson, AZ). MDA was synthesized by reacting 1,1,3,3-tetraethoxypropane with HCl according to the procedures in Guy et al. [30]. The MDA solution was neutralized with NaOH before reacting with peptides. To synthesize oxylipid-peptide conjugates, 1 μmol peptide in 1 mL 10 mM tricine buffer, pH 7.4, was reacted with 10 μmol lipid peroxidation products at 37 ^{o}C for two hours. Oxylipid peptide conjugates were analyzed by MALDI-MS and MALDI-MS/MS.

Mass spectrometry

MALDI-MS and MALDI-MS/MS analysis was performed on an ABI 4700 Proteomics Analyzer with TOF/TOF optics equipped with a 200-Hz frequency-tripled Nd:YAG laser operating at a wavelength of 355 nm (Applied

Biosystems, Inc. Framingham, MA). The reflector mode was used for all peptide mass spectra. The accelerating voltage was set to 20 kV for MS, and 8 kV for MS/MS. For MS/MS experiments, the collision energy was 1 kV, defined by the potential difference between the source acceleration voltage (8 kV) and the floating collision cell (7 kV). The precursor ion was selected by operating the timed gate window with a nominal resolution of 50 ppm. Gas pressure (air) in the collision cell was set to 6 x 10^{-7} Torr. Fragment ions were accelerated by 15 kV into the reflector. Mass data were acquired in a mass range of 700-4000 Th with external calibration using AB's 4700 calibration mixture consisting of the following peptides: des-Arg^1-bradykinin ($[M+H]^+$ at m/z_{calc} 904.4675), angiotensin 1 ($[M+H]^+$ at m/z_{calc} 1296.6847, Glu^1-fibrinopeptide B ($[M+H]^+$ at m/z_{calc} 1570.6768), and ACTH 18-39 ($[M+H]^+$ at m/z_{calc} 2465.1983). The MALDI matrix was α-cyano-4-hydroxycinnamic acid (Pierce, Rockford, IL).

Quantum mechanical calculations

Lowest unoccupied molecular orbital (LUMO) and highest occupied molecular orbital (HOMO) energies (E_{LUMO} and E_{HOMO}) were calculated using Gaussian 03 software [31]. The molecular geometries were optimized with a 6-31G* basis set and single-point energies were calculated using density functional theory (DFT) with a B3LYP-6-31G* basis set. Hardness (η) was calculated as $\eta = (E_{LUMO} - E_{HOMO})/2$ and chemical potential (μ) was calculated as $\mu = (E_{LUMO} + E_{HOMO})/2$.

The nucleophilicity index (ω^-) was calculated as $\omega^- = \eta_A(\mu_A-\mu_B)^2/2(\eta_A+\eta_B)^2$, where A is the reacting nucleophile and B is the reacting electrophile. Higher nucleophilicity indexes are correlated with higher reaction rates between nucleophiles and electrophiles [28].

Results and discussion

Adduction of peptides by lipid peroxidation products

The three model peptides Ac-SVVDLTCR-amide, Ac-SVVDLTHR-amide, and Ac-SVVDLTKR-amide were chosen as representative of the tryptic peptides typically encountered in proteomics. Arginine was selected as the less reactive of the two possible tryptic C-terminal residues. The N-terminus of the three model peptides was acetylated to prevent possible interferences with the ε-amino group of lysine and the imidazole of histidine. Arginine was selected as the C-terminal residue for the model peptides to mimic tryptic peptides, which were widely produced in proteomics study. The adduction type of oxylipid peptide conjugates was determined by the differing mass increment for Michael adduct and Schiff base formation. As shown in Fig. 3.1, the Michael adduct, with a mass increment of 156.1 Da, is the predominant product of the reaction of the His-containing peptide with HNE. Cys-containing and Lys-containing peptides also form Michael adducts with HNE (MS spectra not shown). Arg has not been observed to react with HNE. These results are consistent with our calculations and experimental

results of Doorn et al. [23].

The more electrophilic compounds ONE and ACR form Michael adducts with all three model peptides. ONE and ACR have 154.1 Da and 56.0 Da adduct mass increments, respectively (MS spectra not shown). There is no Michael adduction observed between MDA and peptides, since MDA exists primarily as the less electrophilic enolate anion ($^{-}$O-CH=CH-CH=O) at pH 7.4. However, MDA and ONE form Schiff bases with the Lys-containing peptide, and 54.0 Da and 136.1 Da adduct mass increments for MDA and ONE respectively are observed (MS spectra not shown). The adduction products are summarized in Table 3.3. In this chapter we have focused on the Michael adducts and Schiff bases. Other products are known to be produced after longer reaction times with higher concentration of oxylipid [32-34].

Reactivity of lipid peroxidation products and amino acids to form adducts

To form adducts, ONE, HNE and ACR are electrophiles and deprotonated Cys, neutral His, Lys, Arg are nucleophiles although only some of them exit as these reactive forms at pH 7.4 according to their pKa values from side chains. Acetylation of N-termini and amidation of the C-termini of these amino acids mimic peptide bonds and prevent interferences from these available lone electron pairs as nucleophilic centers. Table 3.2 shows nucleophilicity indexes (ω^{-}) for lipid peroxidation product reactions with possible nucleophilic targets using

orbital energies of E_{LUMO} and E_{HOMO} from Table 3.1. Nucleophilicity indexes for ONE with nucleophilic targets are higher than those for ACR and HNE indicating that ONE is the most reactive. ACR and HNE have similar nucleophilic indexes, however, HNE has a slower rate of Michael addition due to the steric effect of the alkane tail as discussed by LoPachin et al. [35]. Table 3.2 also shows that nucleophilic indexes with Cys are the highest and those with His, Lys and Arg are very close and much lower than Cys, which makes the Cys the most reactive although the deprotonated Cys accounts for about 10% according to its pKa value of 8.2. Because of the side chain pKa values for His, Lys and Arg (His 6.0; Lys 10.5; Arg 12.5), about 90% of His, 0.1 % of Lys and 0.001% of Arg exit as neutral forms at pH 7.4, which are nucleophilic. Considering the similarity of the nucleophilic indexes and the huge percentage differences of reactive forms for His, Lys and Arg, His is the most reactive and Arg is the least. Higher pH will increase percentage of neutral forms of Lys and Arg and increase their reactivity. Thus, the rank order of reactivity for these four amino acids at pH 7.4 is: Cys > His > Lys > Arg. The reactivity predicted mainly by the quantum mechanical calculations and the percentages of reactive forms under pH 7.4 are agreement with those based on reaction rates induced from experiments [21-24].

Characteristics of MALDI MS/MS spectra of oxylipid-modified peptides

Oxylipid-modified Cys-containing peptides

The MALDI MS/MS spectra of oxylipid peptide conjugates in our experiments show that the oxylipid can be well retained with many fragments, which is a prerequisite for peptide identification based on the use of uninterpreted tandem mass spectra acquired in conjugation with automated database searching. For example, the MS/MS spectrum of the HNE Cys-containing peptide conjugate in Fig. 3.2 shows the first C-terminal y_1 ion and fragment ions, y_2*-y_5*, which retain the HNE moiety. Obviously, these peptide fragment ions confirm that the Cys residue is modified by HNE. The strong y_4* fragment ion is observed because of the presence of Asp residue in the peptide. Scheme 3.3 shows one explanation by charge-remote peptide fragmentation pathway (Paizs et al. [36]). This spectrum exhibits two characteristic fragment ions at 933.4 Th and 899.4 Th, which indicates neutral loss of HNE moiety and HS-HNE ($C_9H_{18}O_2S$) moiety from the conjugate, respectively. The possible pathways are based on a reversal Michael adduction mechanism and a β-elimination mechanism, which are shown in Scheme 3.4. MS/MS spectra of the other two oxylipid-modified Cys-containing peptides show ions with oxylipid and HS-oxylipid neutral losses too (Fig. 3.S-1, 2). These neutral losses make the identification of oxylipid-modified peptides more challenging. However, this feature can also be used to indentify HNE-modified peptides with neutral loss-driven MS^3 technique by Roe et al. [37]

and Rauniyar et al. [38].

Oxylipid-modified His-containing peptides

The MS/MS spectrum of the HNE His-containing peptide conjugate in Fig. 3.3 shows two characteristic fragment ions at 967.6 Th and 266.2 Th, which are the neutral loss of HNE moiety from the conjugate and the HNE-containing His immonium ion, respectively. Spectra for ACR and ONE His-containing peptide conjugates also exhibit neutral loss of oxylipid moiety ions and oxylipid-containing His immonium ions, which are 166.1 Th and 264.2 Th, respectively (Fig. 3.S-3, 4). The pathway for neutral losses of oxylipid moieties from the conjugates is the same with the one in Scheme 3.3 since they have the $–CH_2CH_2CH=O$ structure in common. MALDI-TOF/TOF spectra did not show the protonated dehydrated HNE moiety (139.1 Th), which commonly appeared in low energy-CID tandem mass spectra [37, 39, 40].

Oxylipid-modified Lys-containing peptides

The MS/MS spectrum of the ONE Lys-containing peptide conjugate (Michael adduct) in Fig. 3.4 shows a neutral loss of ONE moiety ion from the conjugate at 958.6 Th, Lys immonium ion with neutral loss of NH_3 at 84.1 Th and ONE-containing Lys immonium ion with neutral loss of NH_3 at 238.2 Th. The MS/MS spectra of the ACR and HNE Lys-containing peptide conjugates (Michael

adduct) indicate the same characteristic fragment ions showing the ACR/HNE-containing Lys immonium ion with neutral loss of NH_3 at 140.1/240.2 Th (Fig. 3.S-5,6). The pathway for neutral losses of oxylipid moieties from the conjugates is the same with the one in Scheme 3.3 when the S element in side chain of Cys was replaced by the N element in Lys.

The MS/MS spectrum of the MDA Lys-containing peptide conjugate (Schiff base) in Fig. 3.5 only shows one strong characteristic fragment ion at 138.1 Th, which is MDA-containing Lys immonium ion with neutral loss of NH_3. There was no neutral loss of MDA moiety or Lys immonium related ions from the conjugate. The MS/MS spectrum of the ONE Lys-containing peptide conjugate (Schiff base) also only shows one ONE-containing Lys immonium characteristic ion at 237.2 Th and no neutral loss of ONE moiety ion (Fig. 3.S-7). These results imply there is no reasonable pathway to remove the oxylipd moiety part from Schiff bases. These MS/MS spectrum differences between Michael adducts and Schiff bases can be used to determine the adduction type of peptides modified by oxylipids under high energy-CID. However, under low energy-CID, Rauniyar et al. observed ions resulting from the neutral loss of HNE moiety from an HNE–modified Lys-containing peptide (Schiff base) with a linear ion trap [41].

Conclusions

Based on nucleophilic indexes from quantum calculations and percentages of

reactive forms in solution, the rank order of reactivity for amino acids at pH 7.4 is: Cys > His > Lys > Arg. The rank order of reactivity for lipid peroxidation products at pH 7.4 is: ONE > ACR > HNE. In our study, the MS/MS spectra allow obtaining sequence information for oxylipid-peptide conjugates which, at least in favorable cases, enables unambiguous localization of the modification sites by lipid peroxidation products. Compared with tandem mass spectrum under low energy-CID, no protonated dehydrated HNE moiety (139.1 Th) is observed for His-containing peptide oxylipid conjugates under high energy-CID. All the MS/MS spectra of Michael adducts show the neutral loss of the oxylipid moiety ions because they have $–CH_2CH_2CH=O$ structure in common. Spectra of Cys-containing peptide conjugates exhibit additional characteristic neutral loss of HS-oxylipid moiety ions. In addition to neutral loss of oxylipid moiety ions, spectra of His/Lys-containing peptide conjugates (Michael adduct) show characteristic oxylipid-containing His/Lys immonium or related ions. Spectra of Lys-containing peptide conjugates (Michael adduct) show an additional Lys immonium ion with neutral loss of NH_3. Spectra of Lys-containing peptide conjugates (Schiff base) also show oxylipid-containing Lys immonium ions or ions with neutral loss of NH_3. All characteristic fragment ions are summarized in Table 3.4.

Acknowledgements

This work was supported by grants from the NIH/NIA (AG025372). The mass spectrometry core facility of the Environmental Health Sciences Center at Oregon State University is supported in part by a grant from NIEHS (ES00210).

References

[1] T. Finkel, N.J. Holbrook, Nature, 408 (2000) 239.

[2] L.J. Marnett, J.N. Riggins, J.D. West, J. Clin. Invest., 111 (2003) 583.

[3] R.L. Levine, E.R. Stadtman, Exp. Gerontol., 36 (2001) 1495.

[4] E.R. Stadtman, Ann. N. Y. Acad. Sci., 928 (2001) 22.

[5] J.D. West, L.J. Marnett, Chem. Res. Toxicol., 19 (2006) 173.

[6] R.T. Dean, S. Fu, R. Stocker, M.J. Davies, Biochem. J., 324 (Pt 1) (1997) 1.

[7] R.L. Levine, Free Radic. Biol. Med., 32 (2002) 790.

[8] B.S. Berlett, E.R. Stadtman, J. Biol. Chem., 272 (1997) 20313.

[9] H. Esterbauer, M. Dieber-Rotheneder, G. Waeg, G. Striegl, G. Jurgens, Chem. Res. Toxicol., 3 (1990) 77.

[10] H. Esterbauer, R.J. Schaur, H. Zollner, Free Radic. Biol. Med., 11 (1991) 81.

[11] L.M. Sayre, D. Lin, Q. Yuan, X. Zhu, X. Tang, Drug Metab. Rev., 38 (2006) 651.

[12] C. Schneider, K.A. Tallman, N.A. Porter, A.R. Brash, J. Biol. Chem., 276 (2001) 20831.

[13] J.M. Gutteridge, B. Halliwell, Trends Biochem. Sci., 15 (1990) 129.

[14] R. Bucala, A. Cerami, Adv. Pharmacol., 23 (1992) 1.

[15] G. Jurgens, J. Lang, H. Esterbauer, Biochim. Biophys. Acta, 875 (1986) 103.

[16] W. Palinski, M.E. Rosenfeld, S. Yla-Herttuala, G.C. Gurtner, S.S. Socher, S.W. Butler, S. Parthasarathy, T.E. Carew, D. Steinberg, J.L. Witztum, Proc. Natl. Acad. Sci. U. S. A., 86 (1989) 1372.

[17] N. Traverso, S. Menini, L. Cosso, P. Odetti, E. Albano, M.A. Pronzato, U.M. Marinari, Diabetologia, 41 (1998) 265.

[18] K. Uchida, Free Radic. Biol. Med., 28 (2000) 1685.

[19] J.R. Requena, M.X. Fu, M.U. Ahmed, A.J. Jenkins, T.J. Lyons, J.W. Baynes, S.R. Thorpe, Biochem. J., 322 (Pt 1) (1997) 317.

[20] L.M. Sayre, M.A. Smith, G. Perry, Curr. Med. Chem., 8 (2001) 721.

[21] D. Lin, H.G. Lee, Q. Liu, G. Perry, M.A. Smith, L.M. Sayre, Chem. Res. Toxicol., 18 (2005) 1219.

[22] J.A. Doorn, S.K. Srivastava, D.R. Petersen, Chem. Res. Toxicol., 16 (2003) 1418.

[23] J.A. Doorn, D.R. Petersen, Chem. Res. Toxicol., 15 (2002) 1445.

[24] X. Zhu, L.M. Sayre, Chem. Res. Toxicol., 20 (2007) 165.

[25] R.M. LoPachin, D.S. Barber, T. Gavin, Toxicol. Sci., 104 (2008) 235.

[26] R.M. LoPachin, T. Gavin, B.C. Geohagen, S. Das, Toxicol. Sci., 98 (2007) 561.

[27] R.M. LoPachin, T. Gavin, D.R. Petersen, D.S. Barber, Chem. Res. Toxicol., 22 (2009) 1499.

[28] P. Jaramillo, P. Perez, R. Contreras, W. Tiznado, P. Fuentealba, J. Phys. Chem. A, 110 (2006) 8181.

[29] C.M. Spickett, A.R. Pitt, N. Morrice, W. Kolch, Biochim. Biophys. Acta, 1764 (2006) 1823.

[30] F. Fenaille, P. Mottier, R.J. Turesky, S. Ali, P.A. Guy, J. Chromatogr. A, 921 (2001) 237.

[31] Gaussian, Revision C.02, Gaussian, Inc., Wallingford CT (2004).

[32] A.K. Yocum, T. Oe, A.L. Yergey, I.A. Blair, J. Mass Spectrom., 40 (2005) 754.

[33] X. Zhu, V.E. Anderson, L.M. Sayre, Rapid Commun. Mass Spectrom., 23 (2009) 2113.

[34] A. Furuhata, T. Ishii, S. Kumazawa, T. Yamada, T. Nakayama, K. Uchida, J. Biol. Chem., 278 (2003) 48658.

[35] R.M. LoPachin, B.C. Geohagen, T. Gavin, Toxicol. Sci., 107 (2009) 171.

[36] B. Paizs, S. Suhai, Mass Spectrom. Rev., 24 (2005) 508.

[37] M.R. Roe, H. Xie, S. Bandhakavi, T.J. Griffin, Anal. Chem., 79 (2007) 3747.

[38] N. Rauniyar, S.M. Stevens, K. Prokai-Tatrai, L. Prokai, Anal. Chem., 81 (2009) 782.

[39] A.L. Isom, S. Barnes, L. Wilson, M. Kirk, L. Coward, V. Darley-Usmar, J. Am. Soc. Mass Spectrom., 15 (2004) 1136.

[40] M.S. Bolgar, S.J. Gaskell, Anal. Chem., 68 (1996) 2325.

[41] N. Rauniyar, L. Prokai, Proteomics, 9 (2009) 5188.

Full citation for Reference [31]:
Gaussian 03, Revision C.02, Frisch, M. J.; Trucks, G. W.; Schlegel, H. B.; Scuseria, G. E.; Robb, M. A.; Cheeseman, J. R.; Montgomery, Jr., J. A.; Vreven, T.; Kudin, K. N.; Burant, J. C.; Millam, J. M.; Iyengar, S. S.; Tomasi, J.; Barone, V.; Mennucci, B.; Cossi, M.; Scalmani, G.; Rega, N.; Petersson, G. A.; Nakatsuji, H.; Hada, M.; Ehara, M.; Toyota, K.; Fukuda, R.; Hasegawa, J.; Ishida, M.; Nakajima, T.; Honda, Y.; Kitao, O.; Nakai, H.; Klene, M.; Li, X.; Knox, J. E.; Hratchian, H. P.; Cross, J. B.; Bakken, V.; Adamo, C.; Jaramillo, J.; Gomperts, R.; Stratmann, R. E.; Yazyev, O.; Austin, A. J.; Cammi, R.; Pomelli, C.; Ochterski, J. W.; Ayala, P. Y.; Morokuma, K.; Voth, G. A.; Salvador, P.; Dannenberg, J. J.; Zakrzewski, V. G.; Dapprich, S.; Daniels, A. D.; Strain, M. C.; Farkas, O.; Malick, D. K.; Rabuck, A. D.; Raghavachari, K.; Foresman, J. B.; Ortiz, J. V.; Cui, Q.; Baboul, A. G.; Clifford, S.; Cioslowski, J.; Stefanov, B. B.; Liu, G.; Liashenko, A.; Piskorz, P.; Komaromi, I.; Martin, R. L.; Fox, D. J.; Keith, T.; Al-Laham, M. A.; Peng, C. Y.; Nanayakkara, A.; Challacombe, M.; Gill, P. M. W.; Johnson, B.; Chen, W.; Wong, M. W.; Gonzalez, C.; and Pople, J. A.; Gaussian, Inc., Wallingford CT, 2004.

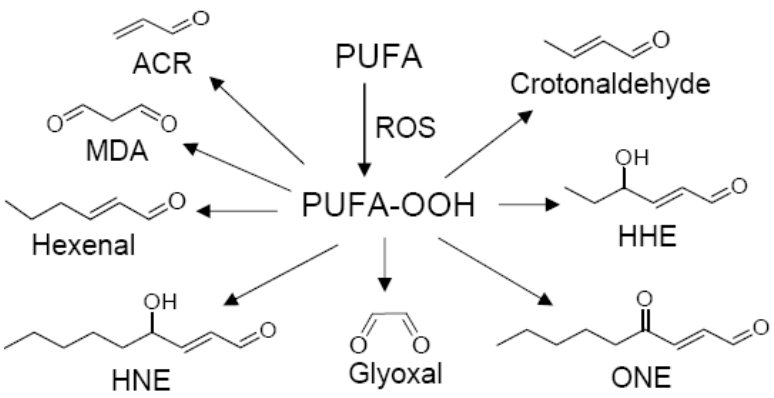

Scheme 3.1. Lipid peroxidation products generated from PUFA, including α,β-unsaturated aldehydes: 4-hydroxy-2-nonenal (HNE), 4-oxo-2-nonenal (ONE), 4-hydroxyhexanal (HHE), hexenal, crotonaldehyde, and acrolein (ACR) as well as the dialdehydes: malondialdehyde (MDA) and glyoxal. They are formed by a variety of mechanisms. For example, HNE can be produced through the β-cleavage of hydroperoxides from ω-6 polyunsaturated fatty acids.

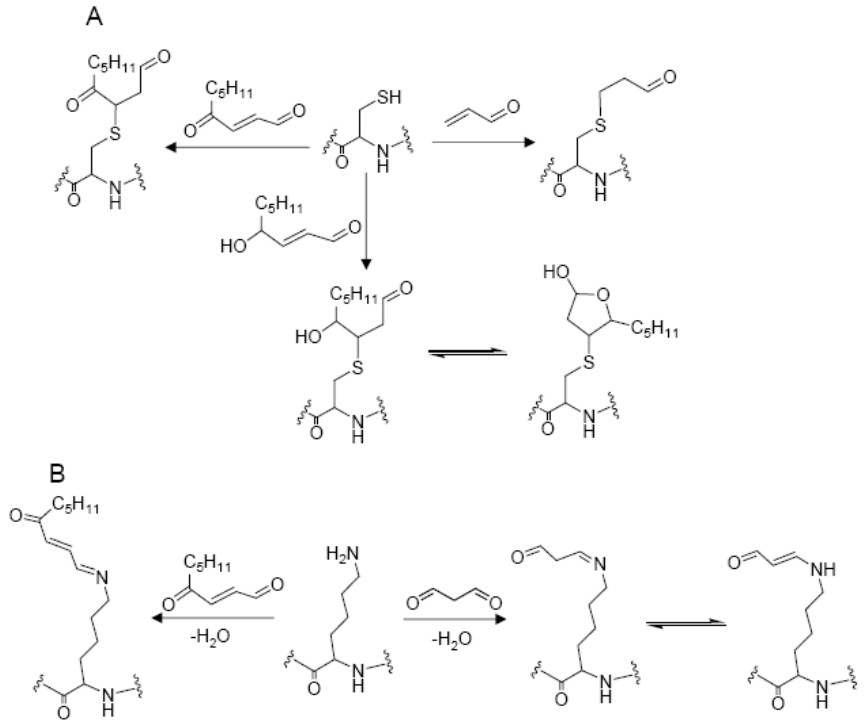

Scheme 3.2. Michael adducts formed from Cys-containing peptides with ACR, ONE and HNE (A), C-2 can also be the active site for ONE; Schiff bases formed from Lys-containing peptides with MDA and ONE (B).

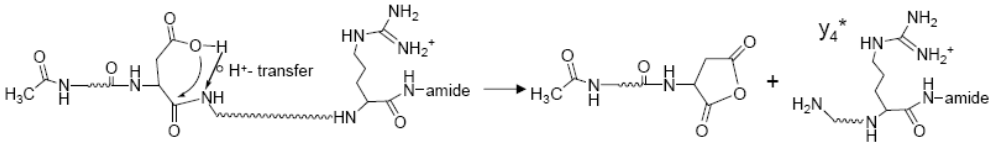

Scheme 3.3. The aspartic acid effect explained by the charge-remote peptide fragmentation pathway [36].

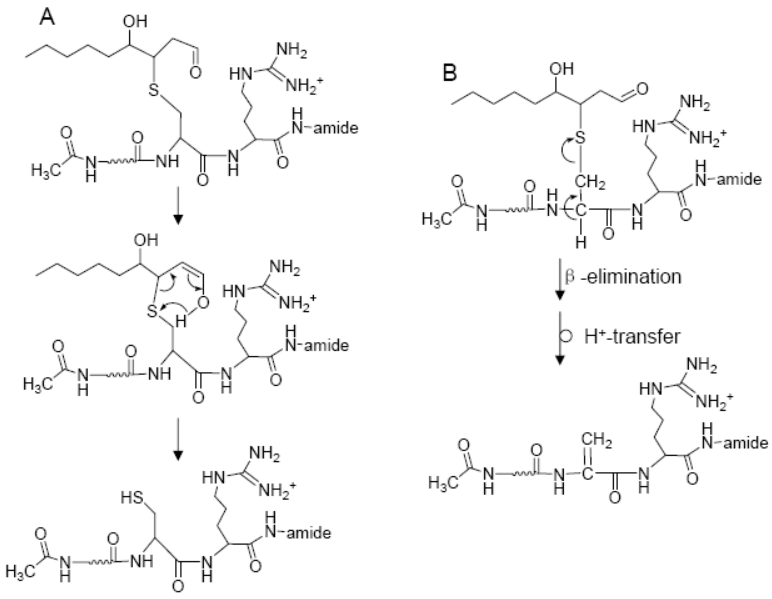

Scheme 3.4. Proposed pathways from Cys-containing peptide conjugate for (A) neutral loss of HNE moiety according to a reversal Michael adduction mechanism, and (B) neutral loss of HS-HNE ($C_9H_{18}O_2S$) moiety according to a β-elimination mechanism.

Table 3.1. Calculated E_{LUMO} and E_{HOMO} for three lipid peroxidation products and amino acids. N and C termini of the amino acids are protected. The numbers behind the amino acids indicate the charge state.

Electrophile	E_{LUMO} (eV)	E_{HOMO} (eV)	Nucleophile	E_{LUMO} (eV)	E_{HOMO} (eV)
ONE	-3.020	-7.238	Cys (-1)	2.776	-1.143
ACR	-2.429	-7.434	His (0)	-0.747	-6.650
HNE	-2.422	-7.374	Lys (0)	-0.748	-6.289
			Arg (0)	-0.619	-6.169

Table 3.2. Calculated nucleophilicity indexes (ω^-) for lipid peroxidation product reactions with possible nucleophilic targets. N and C termini of the amino acids are protected. The numbers behind the amino acids indicate the charge state.

Electrophile	ω^- Cys (-1)	ω^- His (0)	ω^- Lys (0)	ω^- Arg (0)
ONE	2.092 eV	0.118 eV	0.151 eV	0.175 eV
ACR	1.626 eV	0.076 eV	0.099 eV	0.117 eV
HNE	1.626 eV	0.072 eV	0.096 eV	0.113 eV

Table 3.3. Peptide adduction type by lipid peroxidation products under reaction conditions: reaction time 2 h, reaction temperature 37 ℃, pH 7.4. Cys, His and Lys are the reactive residue for the peptides. MA = Michael Adduct, SB = Schiff Base, NCO = No Conjugate Observed.

Peptide	HNE Conjugate	ONE Conjugate	ACR Conjugate	MDA Conjugate
Ac-SVVDLTCR-amide	MA	MA	MA	NCO
Ac-SVVDLTHR-amide	MA	MA	MA	NCO
Ac-SVVDLTKR-amide	MA	MA, SB	MA	SB

Table 3.4. Characteristic fragment ions for oxylipid-peptide conjugates observed in MALDI-MS/MS spectra.

Oxylipid-peptide conjugates	Neutral loss fragment ions	Specific fragment ions
Ac-SVVDLTCR-amide (MA)	933.4 Th (Oxylipid neutral loss); 899.4 Th (HS- oxylipid Neutral loss)	NO
Ac-SVVDLTHR-amide (MA)	967.6 Th (Oxylipid neutral loss)	Oxylipid-containing His immonium ions: 266.2 Th for HNE; 264.2 Th for ONE; 166.1 Th for ACR
Ac-SVVDLTKR-amide (MA)	958.6 Th (Oxylipid neutral loss)	Lys immonium related ion: 84.1Th. Oxylipid-containing Lys related immonium ions: 238.2 Th for ONE; 140.1 Th for ACR; 240.2 Th for HNE
Ac-SVVDLTKR-amide (SB)	NO	Oxylipid-containing Lys immonium or related ions: 237.2 Th for ONE; 138.1 Th for MDA

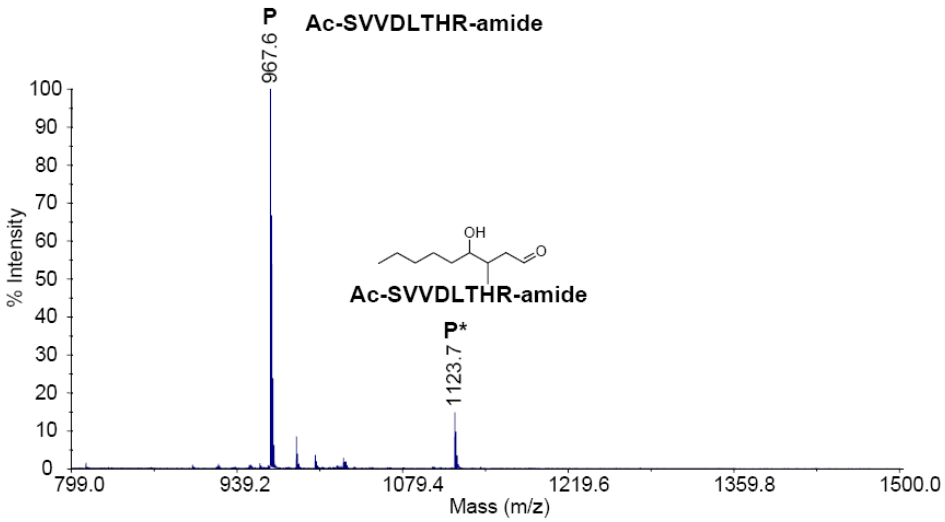

Figure 3.1. MALDI MS demonstrating adduction type of the Ac-SVVDLTHR-amide peptide by HNE. P annotates the original peptide; asterisk * annotates the oxylipid labeling.

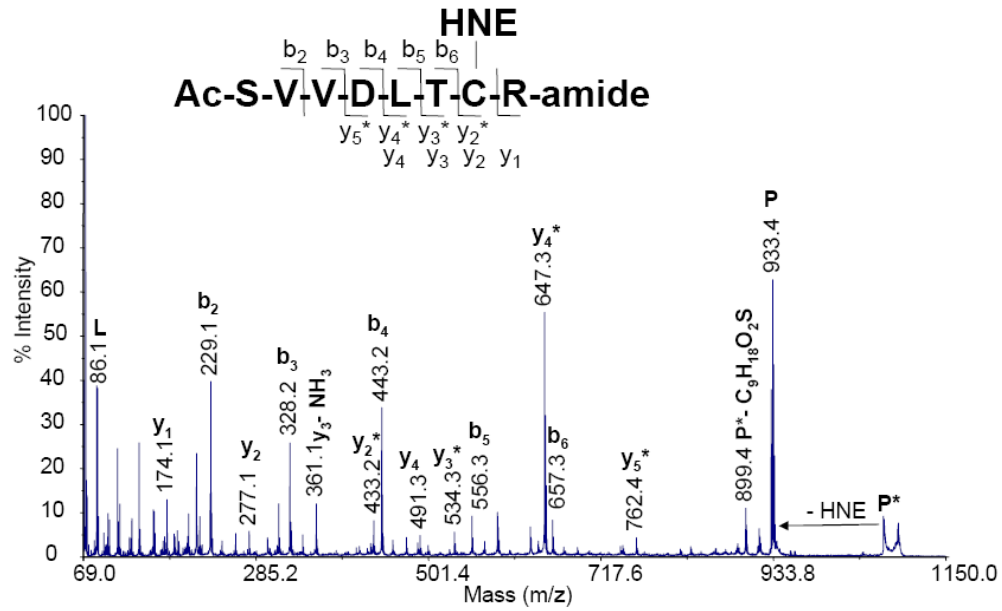

Figure 3.2. MALDI MS/MS spectrum of HNE-peptide conjugate (Michael adduct) Ac-SVVDLTCR-amide. Precursor, P* = 1089.6 Th, L, a Leu immonium ion.

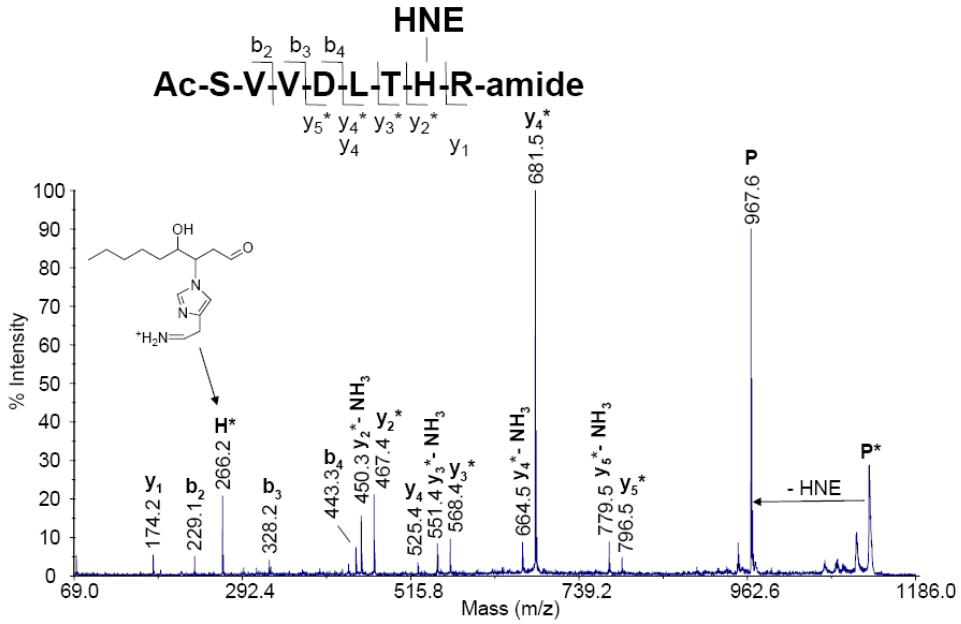

Figure 3.3. MALDI MS/MS spectrum of HNE-peptide conjugate (Michael adduct) Ac-SVVDLTHR-amide. Precursor, P* = 1123.7 Th; H, a His immonium ion.

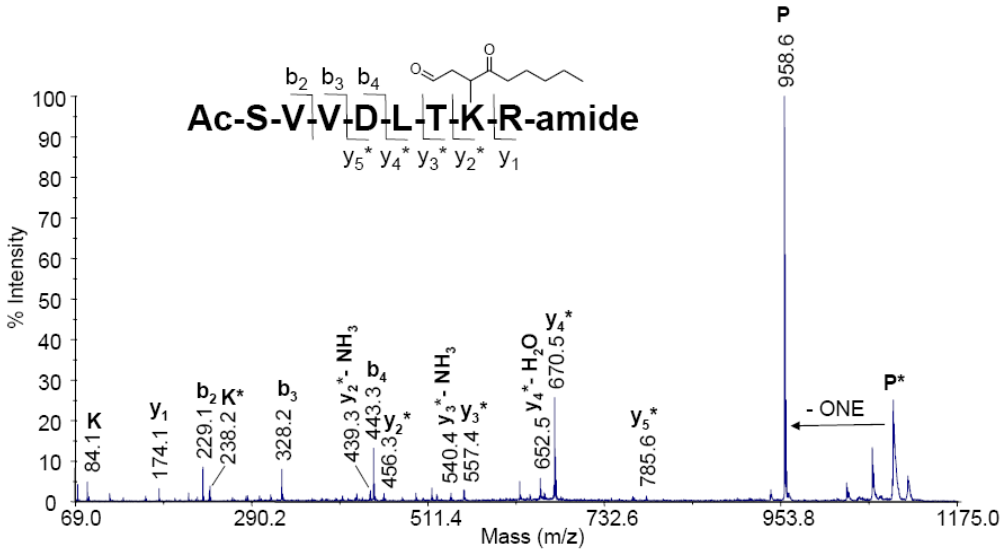

Figure 3.4. MALDI MS/MS spectrum of ONE-peptide conjugate (Michael adduct) Ac-SVVDLTKR-amide. Precursor, P* = 1112.7 Th; K, a Lys immonium ion with neutral loss of NH3.

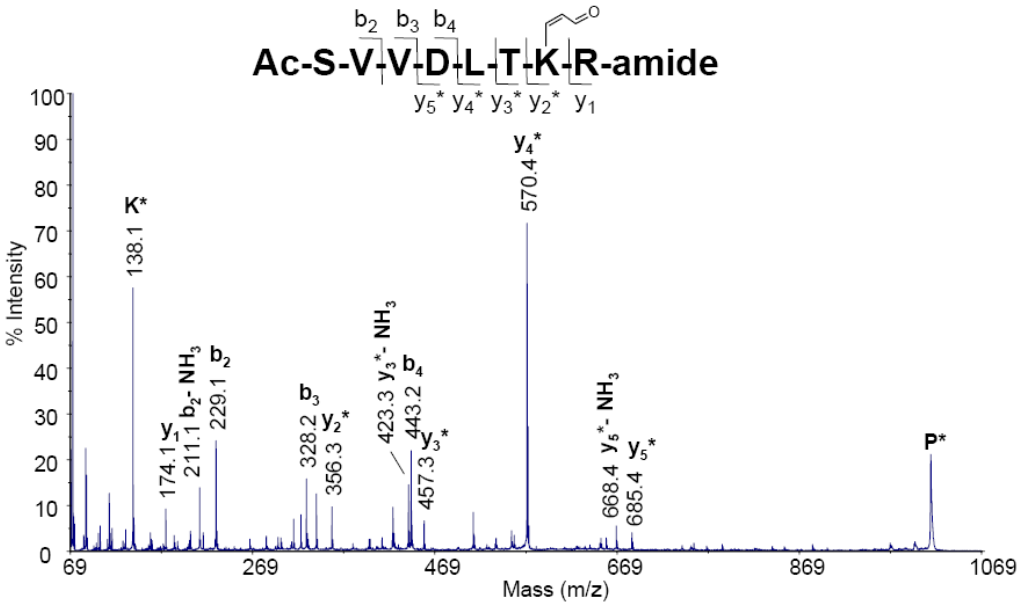

Figure 3.5. MALDI MS/MS spectrum of MDA-peptide conjugate (Schiff base) Ac-SVVDLTKR-amide. Precursor, P* = 1012.6 Th; K, a Lys immonium ion with neutral loss of NH3.

Supporting information

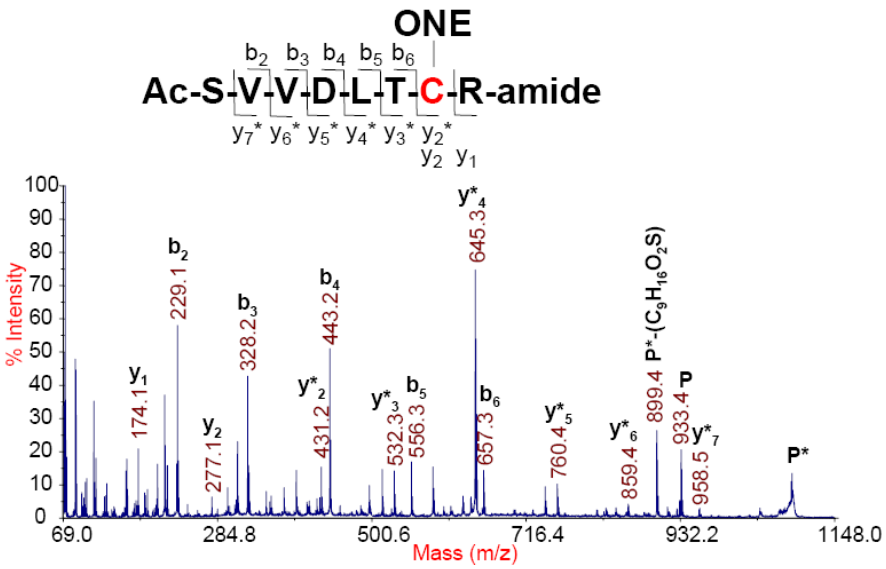

Figure 3.S-1. MALDI MS/MS spectrum of ONE-peptide conjugate (Michael adduct) Ac-SVVDLTCR-amide. P annotates the original peptide; asterisk * annotates the oxylipid labeling. Precursor, P* = 1087.5 Th.

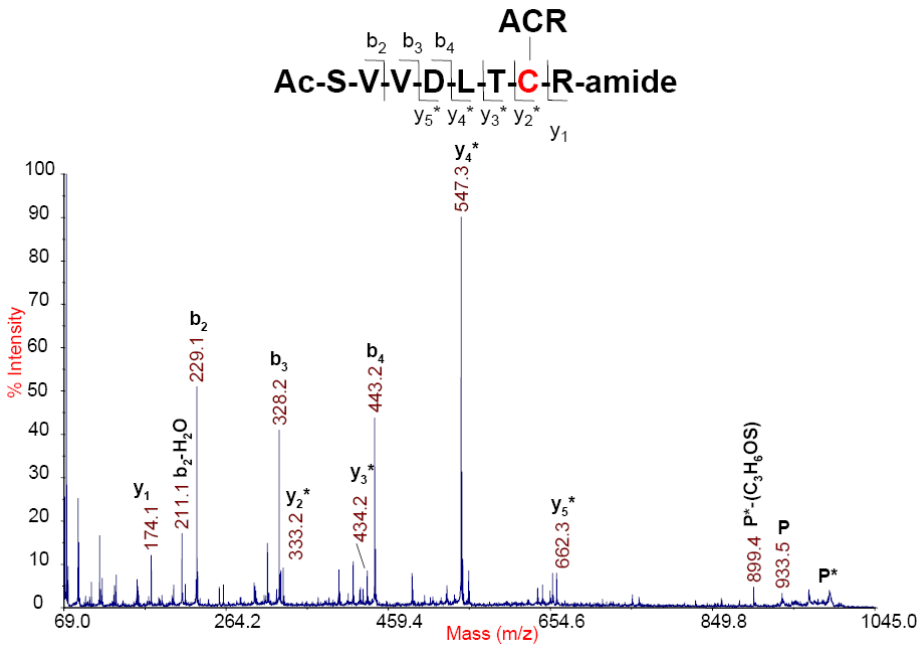

Figure 3.S-2. MALDI MS/MS spectrum of ACR-peptide conjugate (Michael adduct) Ac-SVVDLTCR-amide. Precursor, P* = 989.4 Th.

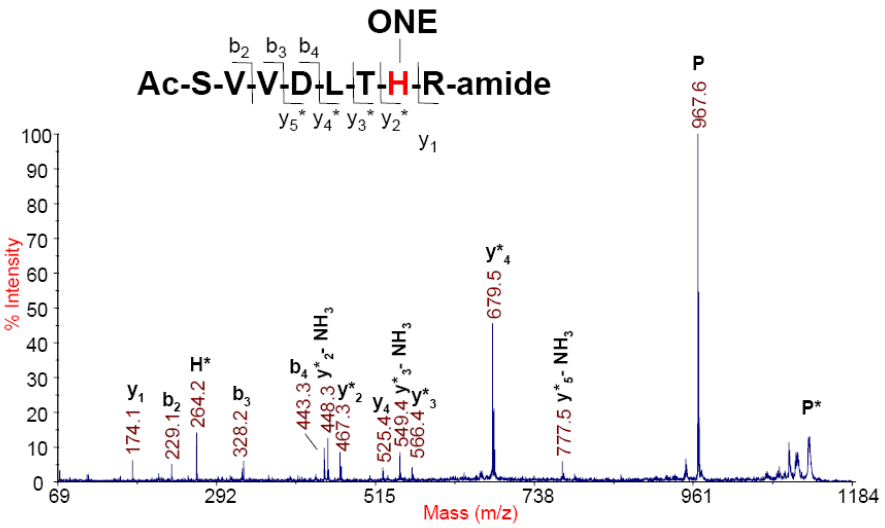

Figure 3.S-3. MALDI MS/MS spectrum of ONE-peptide conjugate (Michael adduct) Ac-SVVDLTHR-amide. Precursor, P* = 1121.7 Th; H, a His immonium ion.

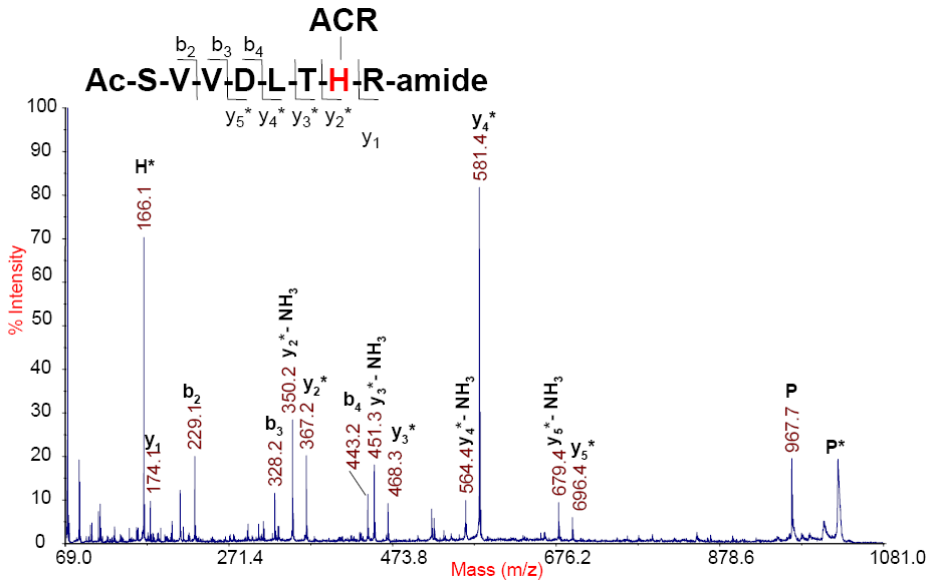

Figure 3.S-4. MALDI MS/MS spectrum of ACR-peptide conjugate (Michael adduct) Ac-SVVDLTHR-amide. Precursor, P* = 1023.4 Th; H, a His immonium ion.

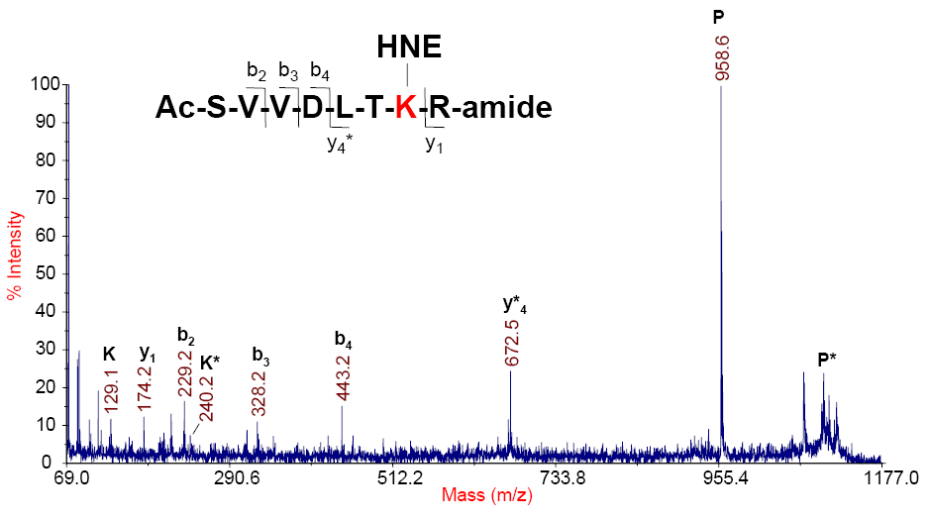

Figure 3.S-5. MALDI MS/MS spectrum of HNE-peptide conjugate (Michael adduct) Ac-SVVDLTKR-amide. Precursor, P* = 1114.7 Th; K, a Lys immonium ion with neutral loss of NH_3.

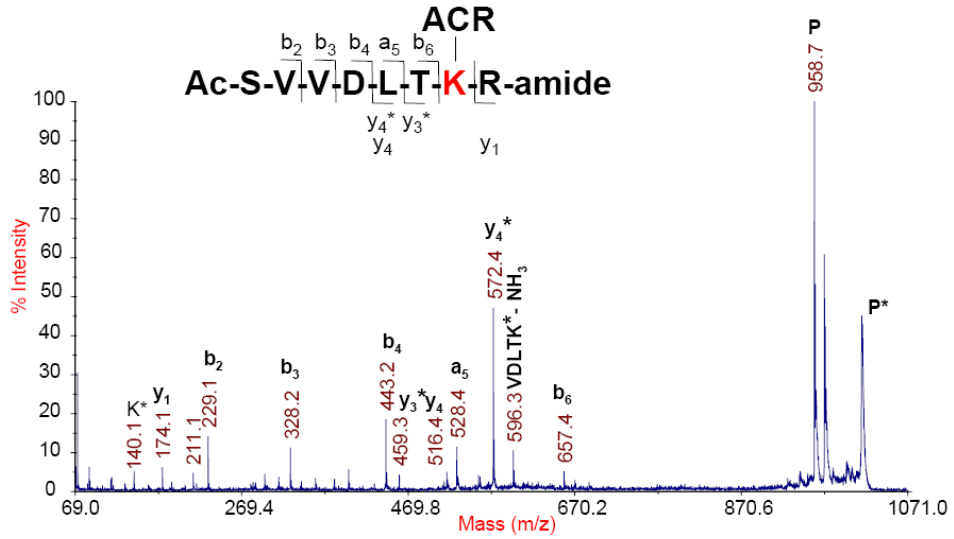

Figure 3.S-6. MALDI MS/MS spectrum of ACR-peptide conjugate (Michael adduct) Ac-SVVDLTKR-amide. Precursor, P* = 1014.5 Th; K, a Lys immonium ion with neutral loss of NH_3.

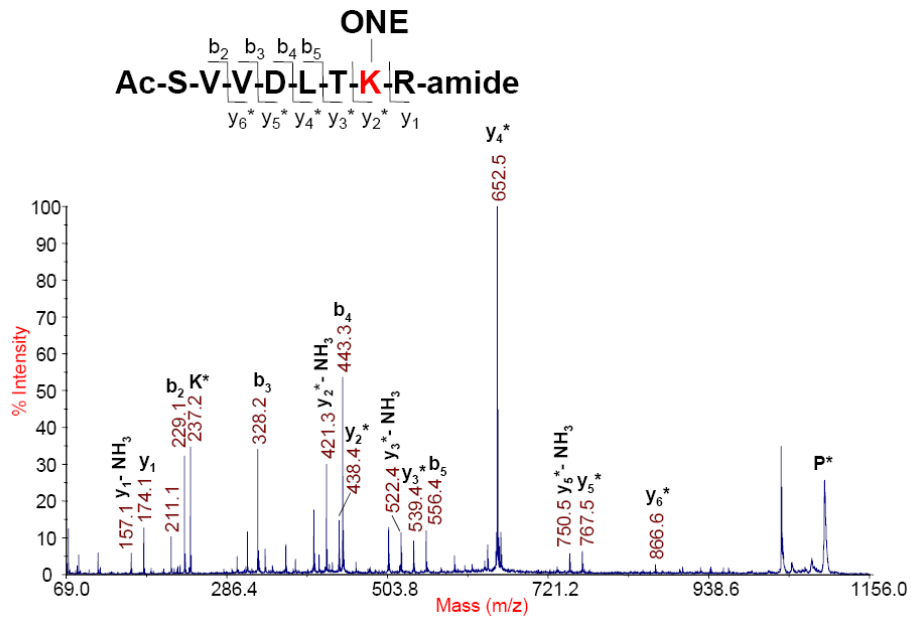

Figure 3.S-7. MALDI MS/MS spectrum of ONE-peptide conjugate (Schiff base) Ac-SVVDLTKR-amide. Precursor, P* = 1094.7 Th; K, a Lys immonium ion.

CHAPTER 4.

Mass Spectrometry-based Quantification of Acrolein-modified Cys-containing Peptides in an *In Vivo* Model of Oxidative Stress

Jianyong Wu and Claudia S. Maier*

Department of Chemistry, Oregon State University, Corvallis OR, 97330

* Corresponding author.

Email: Claudia.maier@oregonstate.edu

Fax: 541-737-2062

Abstract

The adduction of proteins and other biomolecules by electrophilic lipid peroxidation products such as 4-hydroxy-2-nonenal (HNE), 4-oxo-2-nonenal (ONE) or acrolein (ACR) is thought to be an initiating and/or propagating factor in the pathophysiology of several diseases such as atherosclerosis, diabetes, Alzheimer's, Parkinson's and other age-related disorders. Determining the extent or relative amounts of this oxidative damage could provide valuable insights into the molecular mechanisms of these disorders. Relative quantitation of oxylipid-modified proteins in biological samples is a challenging problem because of the complexity and extreme dynamic range that characterize these samples. In this study, the reagents, N'-aminooxymethylcarbonylhydrazino-D-biotin and iodoacetyl-PEO_2-biotin, were used to enrich acrolein-modified Cys-containing peptides and the corresponding unmodified ones from mitochondrial samples. The ratios between them were determined by nanoLC-SRM analysis. Model Cys-containing peptides labeled with ARP-acrolein and IPB were employed to demonstrate this method. Seven acrolein-modified Cys-containing peptides from five mitochondrial proteins were quantified. The ratios for those seven peptides from the CCl_4 treated rats are higher than the control ones indicating that the ratios of acrolein-modified peptides to unmodified ones are potential markers of oxidative stress *in vivo*.

Introduction

Mitochondria are cell's powerhouse through oxidative phosphorylation. 2% [1] of oxygen escapes in the respiration chain from mitochondria and forms superoxide radical, a reactive oxygen species (ROS) which can initiate radical-mediated oxygenations. Free-radical injury is crucial to age-related disorders and etiology and pathology of inflammatory diseases. ROS is counteracted by an intricate antioxidant system and the degree of oxidative stress is determined by the extent of the imbalance of ROS production and antioxidant defenses [2]. Proteins, DNA and lipids can be modified because of oxidative stress in biological system [2-6]. Oxidative modification of proteins occur according to a variety of mechanisms [3, 5, 7-9]. Some of them lead to backbone peptide bond cleavage or to side-chain modifications. The latter introduces protein carbonyls by secondary reaction of histidine, cysteine and lysine reside with lipid peroxidation products, which are produced by polyunsaturated fatty acids and their esters under oxidative stress [10-13]. 4-hydroxy-2-nonenal (HNE), 4-oxo-2-nonenal (ONE) and acrolein (ACR) are the most reactive lipid peroxidation products. The adduction of proteins and other biomoleculars by these lipid peroxidation products is thought to be an initiating or propagating factor in the pathophysiology of several diseases, such as atherosclerosis, cancer, diabetes-related complications and neurodegenerative diseases [4, 14-19].

Traditionally, protein carbonyls were detected by approaches using 2,

4-dinitrophenylhydrazine (DNPH) [20] or anti-dinitrophenyl primary antibody [21, 22]. Recently, mass spectrometry is applied to identify the modification sites and types for protein carbonyls in biological samples by different research groups [23-25]. Since the protein carbonyls are only a small proportion from the complex biological samples, an enrichment method is usually required before MS analysis.

For deeper understanding of impact of those modifications to cells, quantitative analysis of those modified peptides is necessary. Quantification of peptides or proteins based on mass spectrometry mainly has two approaches [26]. One major approach is based on isotope-labeled amino acids or peptides, which includes reagents like ICAT or iTRAQ, and methods like SILAC or AQUA. The other major approach is label-free quantification including two different strategies: (i) measuring and comparing signal intensity of peptides from proteins; (ii) counting and comparing the number of identified-peptide spectra from a particular protein. Quantification of protein carbonyls in biological samples are more challenging because of the additional enrichment step involved. A few methods with stable isotope labeling were carried out to measure peptides carbonyls *in vitro* in different groups [27-29]. However, none of them determined the ratios between oxylipid-modified peptides and unmodified peptides in biological sample *in vivo*, which indicates the extent of oxylipid modification in cell. Here we introduced a method that tried to reach this goal. In our previous study [23], N'-aminooxymethylcarbonylhydrazino-D-biotin as an aldehyde reactive probe

(ARP) was used to enrich peptide carbonyls with avidin affinity columns, then the peptide carbonyls were identified by mass spectrometry. We develop this method with an additional iodoacetyl-PEO_2-Biotin (IPB) reagent to determine the ratios of seven acrolein-modified peptides to their corresponding unmodified peptides in mitochondrial samples *in vivo*. In this method, ARP was used to react with acrolein-modified peptides to form ARP-ACR modified peptides and IPB was applied to react with unmodified peptides to form IPB labeled peptides (Scheme 4.1). The prepared samples were passed through a strong cation exchange (SCX) column and an avidin affinity column for further nano-LC MS analysis. Selected reaction monitoring (SRM) was employed for quantitative analysis because of its high specificity and sensitivity in complex biological samples.

Material and methods

Materials

Sequencing grade-modified trypsin was purchased from Promega Corp. (Madison, WI). Acrolein (ACR) (≥99%) was obtained from Fluka (St. Louis, MO). Aldehyde reactive probe (ARP, *N*-aminooxymethylcarbonylhydrazino D-biotin) was purchased from Dojindo Laboratories (Kumamoto, Japan). UltraLink-immobilized monomeric avidin, iodoacetyl-IPB_2-Biotin (IPB) and triton X-100 detergent were obtained from Pierce (Rockford, IL). Bovine serum albumin (BSA) was from Calbiochem (La, CA). Macrospin strong cation

exchange (SCX) columns were from Nest Group (Southboro, MA).

Synthesis of ARP-ACR and IPB Labeled Peptides

One ml of 2-mg BSA (20 mM phosphate buffer, pH 8.3) was reacted with 25 μl of DTT (60 mM, 20 mM phosphate buffer, pH 8.3) at 95 °C for 10 min. One half of the reduced BSA was then mixed with 200 μl IPB (20 mM, 50 mM Trice buffer, pH 8.3). The mixture was kept in the dark at room temperature for 90 min to form IPB labeled BSA. The additional IPB was removed by adding 30 μl DTT (60 mM, 20 mM phosphate buffer, pH 8.3). The other half of the reduced BSA was reacted with 60 μl of ACR (80 mM, 20 mM phosphate buffer, pH 8.3) at room temperature for 60 min. Almost all of the Cys residues would be adducted with ACR and nearly non of the Lys or Arg residues would be adducted under this reaction condition according to the high difference of reactivity between them [30-33]. The excess ACR was removed by adding 40 μl DTT (60 mM, 20 mM phosphate buffer, pH 8.3). This ACR labeled BSA was then reacted with 250 μl ARP (30 mM, in H_2O) at room temperature for 60 min. Both ARP-ACR and IPB labeled BSA were digested by trypsin and passed through 10 KDa filter. The peptide (YICDNQDTISSK) labeled with ARP-ACR and IPB, respectively, will be used in the quantitative model study.

SCX Cleanup

Procedure was followed the manufacture's instructions. Acetonitrile was used to active the column and an elution buffer with 20 % acetonitrile (pH 3.0; 0.6 M KCl) was applied to condition the column. A washing buffer with 20% acetonitrile (pH 3.0; 10mM KCl) was used to equilibrate the column. The mitochondrial peptide sample (~pH 3.0, adjusted with H_3PO_4) was added into the column and washed with washing buffer three times to remove all small molecules with biotin tag and triton X-100 detergent, finally 350 µl elution buffer was added to release the peptide sample.

Affinity Chromatography

200 µl of Ultralink monomeric avidin was packed into Handee Mini Spin Columns which accommodate solvent addition with a Luer Lok syringe. The column was washed with 1.5 ml of 10 mM NaH_2PO_4, pH 7.4. Irreversible binding sites, consisting of tetrameric avidin, were blocked by washing with 600 µl of 2 mM D-biotin. To remove excess D-biotin the column was washed with 1 ml of 2 M Glycine-HCl pH2.8. The column was then re-equilibrated by washing with 2 ml of 2 x phosphate buffered saline (PBS, 20 mM NaH_2PO_4 300mM NaCl). The mitochondrial peptide sample was then slowly added to the affinity column. To remove non-labeled and non-specifically bound peptides the column was washed with 1 ml 2 x PBS followed by 1 ml of 10 mM NaH_2PO_4 and

finally 1.5 ml of 50 mM NH_4HCO_3 20% CH_3OH. The column was then rinsed with 1 ml of MilliQ H_2O before eluting the ARP labeled peptides with 0.4% formic acid 20% acetonitrile. Collected fractions were then concentrated using a freeze dryer and stored at -20^{o}C before mass spectrometric analysis.

Nano-HPLC

An Ultimate LC Packing system (Dionex, Sunnyvale, CA) was used. Peptide samples were loaded onto a 5 mm × 0.50 mm C18 trap cartridge at a washing flow rate of 20 μL/min. After 4 min the trap cartridge was automatically switched in-line with a 75 μm i.d. ×15 cm C18 PepMap 100 column (Dionex, Sunnyvale, CA). Peptides were eluted with a gradient from 9% to 18% B over 90 min (using solvent A: 1% acetonitrile with 0.1% formic acid; solvent B, 100% acetonitrile with 0.1% formic acid) at a 0.260 μL/min.

Mass Spectrometry

All experiments were carried out on a 4000 Q-Trap hybrid tandem mass spectrometer (AB/MDS SCIEX, Concord, Ontario, Canada) using nano-ESI source. The electrospray voltage was set to 2300 V and the declustering potential was 60 V. For identification of ARP labeled peptides, the precursor ion scan was performed over a mass range of 400–1300 Th at 500 Th/s (Q1 and Q3 with unit resolution). An enhanced product ion scan (MS/MS) would be performed to

identify it if an intensity of a precursor of 227 Th exceeds the threshold value of 1000 cps. The scan rate for MS/MS was set to 4000 Th/s. The SRM mode was run with Q1 and Q3 set at unit resolution to increase the specificity. Each SRM transition time is 30 ms. SRM collision energies were 50 eV and 51 eV for ARP-ACR labeled and IPB labeled model peptides. All other SRM collision energies for peptides from mitochondrial samples were listed in Table 4.2.

Animal Treatment

The experimental protocol for the animal studies was approved by the Institutional Animal Care and Use Committee at Oregon State University. Seven Male F344 rats (Harlan, Indianapolis, IN) were housed in individual plastic cages covered with Hepa filter and allowed free access to standard animal chow and water *ad libitum*. After 1 week of acclimatization, one 25-month old rat was killed for reproducibility study and the other six 3-month old rats were transferred to metabolism cages. These six animals were divided into two groups of three, with one group receiving an intraperitoneal dose of 1 ml/kg CCl_4 (dissolved in corn oil), and the other group (control) receiving the vehicle alone. The CCl_4 dose of 1 ml/kg was chosen on the basis of literature reports [34, 35]. The rats were killed 24 h after the treatment.

Preparation of ARP-ACR and IPB labeled Mitochondrial Peptides for SRM analysis

Rat cardiac mitochondria were isolated by differential centrifugation and stored at -80 ^{o}C [36]. Each sample of subsarcolemmal mitochondria (SSM) containing approximately 0.5 mg total protein was washed twice with 10 mM NaH_2PO_4 pH 7.4 at 0 ^{o}C. The mitochondria were then resuspended in 400 µl of 10 mM NaH_2PO_4 pH 7.4 with 1% of triton X-100 detergent and 3 mM DTT. DTT was used to react with free acrolein to prevent artificial results during sample preparation. The mitochondria were sonicated in ice water for 5 min. Mitochondrial proteins were separated by centrifugation at 14 K × g for 15 min at 4 ^{o}C. This sample was then filtered through an Amicon Microcon centrifugal filter (10 KDa MWCO) to remove the oxylipid, lipid and other small molecules at 4 ^{o}C. Mitochondrial proteins were then resuspended in 400 µl of 10mM NaH_2PO_4 pH 7.4 with 1 mM DTT. Further sample preparation was followed in Scheme2. by four steps.

(1) APR was added to sample to reach a final concentration of 3 mM and the proteins were digested with a 1:50 ratio of trypsin at 37 ^{o}C for 15 h.

(2) 15 µl DTT (30 mM, 20 mM phosphate buffer, pH 8.0) was added to the tryptic peptides to reduce all still existing disulfide bridge. This sample was then filtered through an Amicon Microcon centrifugal filter (10 KDa MWCO) to remove trypsin and other big molecules or particles.

(3) 40 µl of this sample was added with 120 µl IPB (5 mM, 50 mM Tris buffer, pH 8.3). This mixture was kept in dark at room temperature for 90 min to form IPB labeled peptides. 80 µl DTT (30 mM, 20 mM phosphate buffer, pH 8.0) was added to remove the additional IPB. This sample was diluted by water to reach 1750 µl.

(4) 35 µl of the sample from step 3 was mixed with 800 µl of the sample from step 2 to form a new sample for nanoLC-SRM analysis after SCX column and affinity column.

Result and discussion

CID-based Fragmentation of ARP-ACR and IPB Labeled Peptides

Low-energy collision-induced dissociation (CID) was used to obtain tandem mass spectra for ARP-ACR and IPB labeled peptides. Fig. 4.1 showes spectra of doubly charged EFNGLGDCLTK peptides with different modification from ADP/ATP translocase 1 protein. The asterisk * means the ARP-ACR labeled residue and pound # means IPB labeled one. The ions in Fig. 4.1 are mainly y and b ions, which are typical for ESI low-energy CID. The Cys-containing fragment ions always with ARP-ACR (+ 369.2 Da) or IPB (+ 414.2 Da) moiety indicated that those two modifications only slightly change the fragmentation pattern of peptides and peptide bonds are still the main bonds to be broken. The relative intensity among those y or b ions is very close between the ARP-ACR and IPB labeled

peptides. There are two characteristic ions: F_1 (227.1 Th) and F_2 (332.1 Th) from ARP in the ARP-ACR labeled peptide and also two ones: F_a (270.1 Th) and F_b (332.2 Th) from IPB in the IPB labeled peptide. The similarity of the fragmentation pattern makes SRM a possibly accurate method to compare these differently modified peptides.

Identification of Oxylipid Modified Peptides from Mitochondrial Samples

Sample preparation for identification of oxylipid modified peptides was the same as the previous study [23]. The sample was labeled with ARP and then eluted from an avidin affinity column. However, a significant amount of peptides without ARP labeling still exited after enrichment because of an overwhelming amount of native peptides in the original sample. Since a strong fragment ion of 270.1 Th from ARP exits in tandem mass spectra of APR labeled peptides, a precursor ion scan was carried out to trigger the tandem mass spectra with 4000 Q-trap for identification. Seven acrolein-modifed Cys-containing peptides labeled as **a** through **g** from five mitochondrial proteins were identified (Table 4.1). More oxylipid modified peptides were found in our group with more sensitive instruments (Appendix B). To obtain better quality of spectra, a serial of independent tandem spectra were achieved with known mass of precursor ions of ARP-ACR and IPB Labeled Peptides. These tandem spectra are shown in Fig. 4.1 and Fig. 4.S-1-14. The collision energies and retention times will be used for

further quantitative analysis.

Standard Curves for Model ARP-ACR and IPB Labeled Peptides

An enrichment method is necessary to detect acrolein-modified peptides by mass spectrometry in biological samples since the concentration of them is extremely low. APR reagent with biotin tag was used to react with acrolein-modified peptides and these labeled peptides would be captured by an avidin affinity column. In order to compare them to unmodified ones, IPB also with biotin tag was used to react with unmodified peptides. To test the reaction yields for those two reactions, a Cys-containing model peptide reacted with IPB to form an IPB labeled peptide; this model peptide also reacted with acrolein to form an ACR-modified peptide, which further reacted with ARP to form an ARP-ACR modified peptide. The MS spectra of these two crude products do not show the peaks of the native peptide or the ACR-modified peptide indicating almost 100% yield for these two reactions (more details in Chapter 2). Thus, the amounts of ARP-ACR labeled peptide and IPB labeled peptides will represent those of acrolein-modified ones and unmodified ones respectively.

Before those two reagents were applied to biological samples, the ARP-ACR and IPB labeled model peptides (YICDNQDTISSK) digested from BSA protein was tested first. The other tryptic peptides were considered matrix. The tandem mass spectra for these two modified peptides were available in 4.S-1-2. Three fragments

were selected for LC-SRM transition analysis. Fig. 4.2 showed the SRM chromatograms for the mixture of 100 fmol ARP-ACR labeled peptide and 100 fmol IPB labeled peptide. The SRM intensity areas from ARP-ACR labeled peptide were very similar with those from IPB labeled peptide, which indicates that the ionization efficiency of electrospray and fragmentation pattern for those two modified peptides are very similar. To prove this point, three SRM standard curves (Fig. 4.3) were built. The 100 fmol IPB labeled peptide was considered the reference and the amount of ARP-ACR labeled peptide started from 10.0 fmol to 1000 fmol. The R^2 was higher than 0.997, which indicated good linearity. The response factors (slopes) were 0.979, 1.102 and 1.100, which were close to 1. To simplify the later calculation, we assumed the response factor equaled to 1 thus the ratio of intensity area from SRM transition can directly represent the amount ratio between ARP-ACR and IPB labeled peptides. Considering of the extremely high yield for formations of ARP-ACR and IPB labeled peptides, the ratios of intensity area from SRM transitions can also directly represent the ratio of acrorein-modified peptides to unmodified peptides. For more accurate calculation, the ratios were needed to be multiplied by a factor, which was close to 1.

Quantification of Acrolein-modified Cys-containing Peptides in Mitochondrial Samples

Scheme 4.2 showed the sample preparation procedure, through which there were

only 0.800 μl (40×(35/1750) = 0.8) of tryptic peptide used to react with IPB to form IPB labeled peptides to represent unmodified Cys-containing peptides and 800 μl tryptic peptide to react with ARP to form ARP-ACR labeled peptides to represent acrolein-modified peptides. Thus, the ratio of ARP-ACR modified peptides to IPB labeled peptides obtained from nanoLC-SRM analysis in mixed sample should be divided by 1000 to achieve the ratio in original mitochondrial samples. In this way, we can circumvent the huge concentration difference between acrolein-modified peptides and their corresponding unmodified ones to avoid problems like overloading the nano-LC column or saturation of detector of the mass spectrometer.

From 14 tandem mass spectra of ARP-ACR and IPB labeled peptides (shown in Fig. 4.1 and 4.S-3-14), the three circled fragments for each spectrum were applied to SRM analysis. One of the SRM with the least interference was selected for quantification. Those SRM chromatograms for seven ARP-ACR modified peptides and their corresponding IPB labeled ones are shown in Fig. 4.4. From the graph, we can see the ARP-ACR modified peptides usually are eluted a little earlier than the corresponding IPB labeled ones and the peak shapes of acrolein-modifed peptides usually are broader. To compensate the mass difference (45 Da) between ARP-ACR and IPB labeled peptides, the collision energy for the IPB labeled peptide is one eV higher than the corresponding ARP-ACR modified one. Detail information of nano-LC and MS properties for APR-ACR and IPB

labeled peptides are shown in Table 4.2. Because of the long sample preparation and delicate nano-LC involved, a test for precision was necessary. Three samples from one 25-month old rat went through sample preparation and nano-LC for SRM analysis. The results are shown in Table 4.3. The CV for these three samples was around 5%. The ratio of acrolein-modified peptides to unmodified ones varied from 0.04% to 0.1%. There is still no available published data to directly compare with our results. Judge et al. [37] prepared SSM sample almost the same way and obtained 0.26 nmol protein carbonyl/mg protein using an enzyme immunoassay. All peptide carbonyls in mitochondria were identified to be acrolein-modified and Cys-containing in our experiments, which was reasonable considering much higher concentration of ACR in cell than other reactive oxylipids (ONE, HNE) and much higher reactivity for Cys than His and Lys [30-33]. If we use acrolein-modified Cys-containing peptides to replace peptide carbonyls and assume that the mass percentage of Cys in proteins is 1.5% [38] and the ratio of Cys for modification varies from 0.04% to 0.1%, the calculated protein carbonyl amount will vary from 0.06 to 0.15 nmol protein carbonyl/mg protein, which is comparable with the results from Judge et al. (0.26 nmol protein carbonyl/mg protein).

Quantification of Acrolein-modified Cys-containing Peptides under Oxidative Stress

For further demonstration of this quantitative method, rats exposed to CCl_4 as an established oxidative stress *in vivo* model [39] were used in experiments. In Fig. 4.5, the seven mean ratios of acrolein-modified peptides to unmodified ones for CCl_4 treated rats are higher than those for control rats. The difference of the ratios for b, d, f, and g peptides is statistically significant with a t-test ($p < 0.05$). The lack of statistical difference for the other three peptides could be due to the individual variation for animals. Those results indicate that those ratios not only represent the extent of modification for the peptides from acrolein but also could serve as markers of oxidative stress *in vivo*.

Conclusions

In our study, a method to measure ratios of acrolein-modified Cys-containing peptides to unmodified ones in mitochondrial samples *in vivo* was developed. Seven acrolein-modifed Cys-containing peptides from five mitochondrial proteins were quantified by nano-LC SRM analysis. ARP and IPB reagents were successfully used to label our target peptides for enrichment. The dilution step during sample preparation circumvented the huge concentration difference between acrolein-modified peptides and their corresponding unmodified ones. ARP-ACR and IPB labeled peptides show similar elctrospray ionization

efficiency and fragmentation pattern in low-energy CID, which makes LC-SRM an appropriate way to measure the ratios between them. The ratios for those seven peptides from the CCl_4 treated rats are higher than the control ones, which indicates the ratios of acrolein-modified peptides to unmodified ones are potential markers of oxidative stress *in vivo*. This quantification method can also be possibly applied to protein carbonyls in bodily fluids and tissues in oxidative stress-related diseases.

Acknowledgements

This work was supported by grants from the NIH/NIA (AG025372). The mass spectrometry core facility of the Environmental Health Sciences Center at Oregon State University is supported in part by a grant from NIEHS (ES00210).

References

[1] A. Boveris, N. Oshino, B. Chance, Biochem. J., 128 (1972) 617.

[2] T. Finkel, N.J. Holbrook, Nature, 408 (2000) 239.

[3] R.L. Levine, E.R. Stadtman, Exp. Gerontol., 36 (2001) 1495.

[4] L.J. Marnett, J.N. Riggins, J.D. West, J. Clin. Invest., 111 (2003) 583.

[5] E.R. Stadtman, Ann. N. Y. Acad. Sci., 928 (2001) 22.

[6] J.D. West, L.J. Marnett, Chem. Res. Toxicol., 19 (2006) 173.

[7] B.S. Berlett, E.R. Stadtman, J. Biol. Chem., 272 (1997) 20313.

[8] R.T. Dean, S. Fu, R. Stocker, M.J. Davies, Biochem. J., 324 (Pt 1) (1997) 1.

[9] R.L. Levine, Free Radic. Biol. Med., 32 (2002) 790.

[10] H. Esterbauer, M. Dieber-Rotheneder, G. Waeg, G. Striegl, G. Jurgens, Chem. Res. Toxicol., 3 (1990) 77.

[11] H. Esterbauer, R.J. Schaur, H. Zollner, Free Radic. Biol. Med., 11 (1991) 81.

[12] C. Schneider, K.A. Tallman, N.A. Porter, A.R. Brash, J. Biol. Chem., 276 (2001) 20831.

[13] L.M. Sayre, D. Lin, Q. Yuan, X. Zhu, X. Tang, Drug Metab. Rev., 38 (2006) 651.

[14] R. Bucala, A. Cerami, Adv. Pharmacol., 23 (1992) 1.

[15] J.M. Gutteridge, B. Halliwell, Trends Biochem. Sci., 15 (1990) 129.

[16] W. Palinski, M.E. Rosenfeld, S. Yla-Herttuala, G.C. Gurtner, S.S. Socher, S.W. Butler, S. Parthasarathy, T.E. Carew, D. Steinberg, J.L. Witztum, Proc. Natl. Acad. Sci. U. S. A., 86 (1989) 1372.

[17] N. Traverso, S. Menini, L. Cosso, P. Odetti, E. Albano, M.A. Pronzato, U.M. Marinari, Diabetologia, 41 (1998) 265.

[18] K. Uchida, Free Radic. Biol. Med., 28 (2000) 1685.

[19] G. Jurgens, J. Lang, H. Esterbauer, Biochim. Biophys. Acta, 875 (1986) 103.

[20] R.L. Levine, D. Garland, C.N. Oliver, A. Amici, I. Climent, A.G. Lenz, B.W. Ahn, S. Shaltiel, E.R. Stadtman, Methods Enzymol., 186 (1990) 464.

[21] M.A. Korolainen, G. Goldsteins, I. Alafuzoff, J. Koistinaho, T. Pirttila, Electrophoresis, 23 (2002) 3428.

[22] T. Reinheckel, S. Korn, S. Mohring, W. Augustin, W. Halangk, L. Schild, Arch. Biochem. Biophys., 376 (2000) 59.

[23] J. Chavez, J. Wu, B. Han, W.G. Chung, C.S. Maier, Anal. Chem., 78 (2006) 6847.

[24] M.R. Roe, H. Xie, S. Bandhakavi, T.J. Griffin, Anal. Chem., 79 (2007) 3747.

[25] S.M. Stevens, Jr., N. Rauniyar, L. Prokai, J. Mass Spectrom., 42 (2007) 1599.

[26] M. Bantscheff, M. Schirle, G. Sweetman, J. Rick, B. Kuster, Anal. Bioanal. Chem., 389 (2007) 1017.

[27] B. Han, J.F. Stevens, C.S. Maier, Anal. Chem., 79 (2007) 3342.

[28] D.L. Meany, H. Xie, L.V. Thompson, E.A. Arriaga, T.J. Griffin, Proteomics, 7 (2007) 1150.

[29] H. Mirzaei, F. Regnier, J. Chromatogr. A, 1134 (2006) 122.

[30] J.A. Doorn, D.R. Petersen, Chem. Res. Toxicol., 15 (2002) 1445.

[31] J.A. Doorn, S.K. Srivastava, D.R. Petersen, Chem. Res. Toxicol., 16 (2003) 1418.

[32] D. Lin, H.G. Lee, Q. Liu, G. Perry, M.A. Smith, L.M. Sayre, Chem. Res. Toxicol., 18 (2005) 1219.

[33] X. Zhu, L.M. Sayre, Chem. Res. Toxicol., 20 (2007) 165.

[34] H. Chung, D.P. Hong, J.Y. Jung, H.J. Kim, K.S. Jang, Y.Y. Sheen, J.I. Ahn, Y.S. Lee, G. Kong, Toxicol. Appl. Pharmacol., 206 (2005) 27.

[35] R. Srinivasan, M.J. Chandrasekar, M.J. Nanjan, B. Suresh, J. Ethnopharmacol., 113 (2007) 284.

[36] J.W. Palmer, B. Tandler, C.L. Hoppel, J. Biol. Chem., 252 (1977) 8731.

[37] S. Judge, Y.M. Jang, A. Smith, T. Hagen, C. Leeuwenburgh, FASEB J., 19 (2005) 419.

[38] D. Voet, J.G. Voet, Biochemistry, John Wiley & Sons, Inc., Hoboken, 2004.

[39] B. Halliwell, Gutteridge, T., Free Radicals in Biology and Medicine, Oxford University Press, London, 2007.

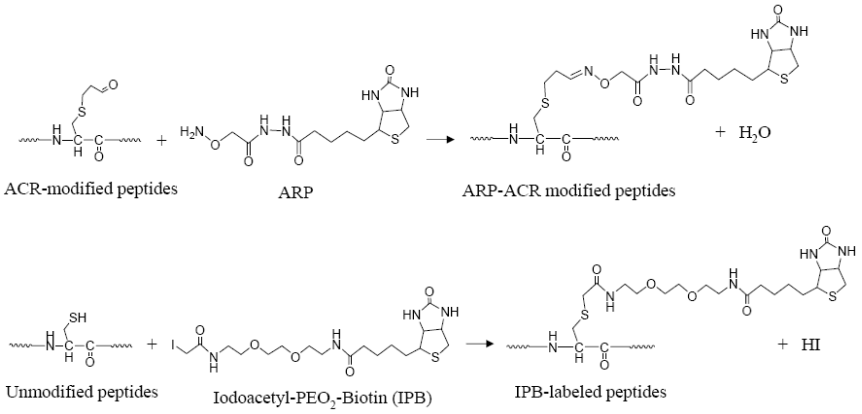

Scheme 4.1. Structures and formations of ARP-ACR modified and IPB-labeled peptides.

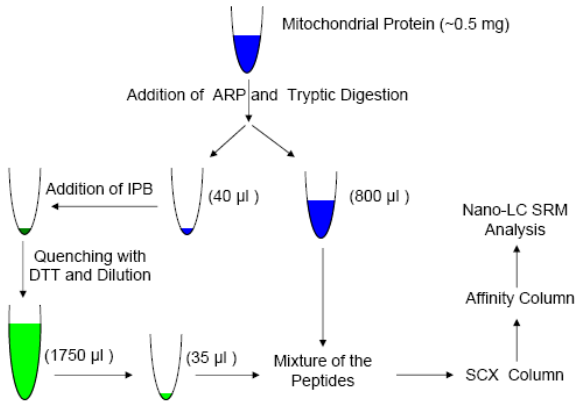

Scheme 4.2. Relative quantitation procedure for acrolein-modified peptides in mitochondrial protein samples.

Table 4.1. Summary of the seven acrolein-modified peptides labeled as **a** through **g** from five mitochondrial proteins. Peptide sequences, biological and functional assignments were made on the basis of information from the NCBI (http://www.ncbi.nlm.nih.gov/Pubmed) and the UniPort Knowledgebase (http://www.uniprot.org) websites.

Peptide	Modified residue	Protein name	Biological function
a. EFNGLGD**C**LTK	**C** 159	ADP/ATP translocase 1	Transport
b. GADIMYTGTVD**C**WR	**C** 256		
c. N**C**AQFVTGSQAR	**C** 100	ATP synthase D chain	Respiratory chain
d. GGDVSV**C**EWYR	**C** 54	Cytochrome c oxidase subunit VIb isoform 1	Respiratory chain
e. LVEG**C**LVGGR	**C** 142	NADH dehydrogenase [ubiquinone] flavoprotein 1	Respiratory chain
f. G**C**DVVVIPAGVPR	**C** 93	Malate dehydrogenase	TCA cycle
g. TIIPLISQ**C**TPK	**C** 212		

Table 4.2. LC and MS properties for ARP-ACR (*) and IPB ($^{\#}$) labeled peptides.

Peptide	SRM transition Precursor →Fragment ion	Collision energy (eV)	Retention time (Min)
a*	783.5 Th →1005.5 Th	40	63.5
a$^{\#}$	805.8 Th →1050.5 Th	41	65
b*	978.9 Th →1205.6 Th	49	75
b$^{\#}$	1001.4Th →1250.6 Th	50	76.5
c*	825.8 Th →619.3Th	42	42.5
c$^{\#}$	848.4 Th →619.3 Th	43	45
d*	820.3 Th →1125.5 Th	42	64.5
d$^{\#}$	842.8 Th →1170.5 Th	43	66
e*	686.3 Th →289.2 Th	36	50
e$^{\#}$	708.9 Th →289.2 Th	37	54
f*	825.9 Th →596.3 Th	42	67
f$^{\#}$	848.5 Th →596.3 Th	43	68.5
g*	842.0 Th →678.3 Th	43	72
g$^{\#}$	864.5 Th →700.9 Th	44	72

Table 4.3. Reproducibility test for our method with three samples from one 25-month old rat.

Peptide	Ratios of acrolein-modified peptides to unmodified ones				
	Sample A (%)	Sample B (%)	Sample C (%)	Average (%) ± SD (%)	CV (%)
a	0.0951	0.1000	0.1052	0.1001 ± 0.0050	5.0
b	0.1057	0.0973	0.0990	0.1007 ± 0.0044	4.4
c	0.0920	0.1010	0.0920	0.0950 ± 0.0052	5.5
d	0.0434	0.0452	0.0408	0.0431 ± 0.0022	5.1
e	0.0642	0.0673	0.0605	0.0640 ± 0.0034	5.3
f	0.0543	0.0490	0.0480	0.0504 ± 0.0034	6.7
g	0.1000	0.0992	0.0931	0.0974 ± 0.0038	3.9

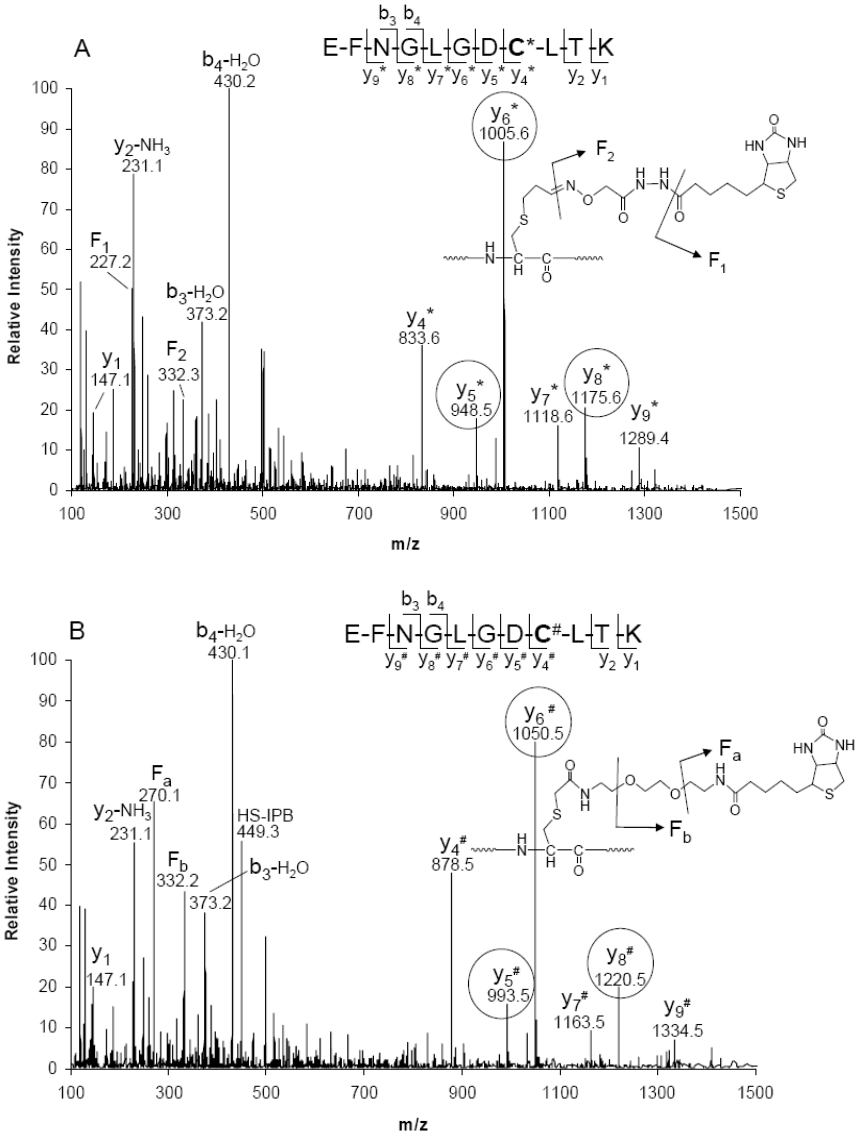

Figure 4.1. Tandem mass spectra of the doubly charged Peptide **a** with different modification from ADP/ATP translocase 1 protein by ESI Low-energy CID: A, ARP-ACR modified (MH_2^{2+}, 783.5 Th); B, IPB labeled (MH_2^{2+}, 805.8 Th). The circled fragments were used for SRM analysis.

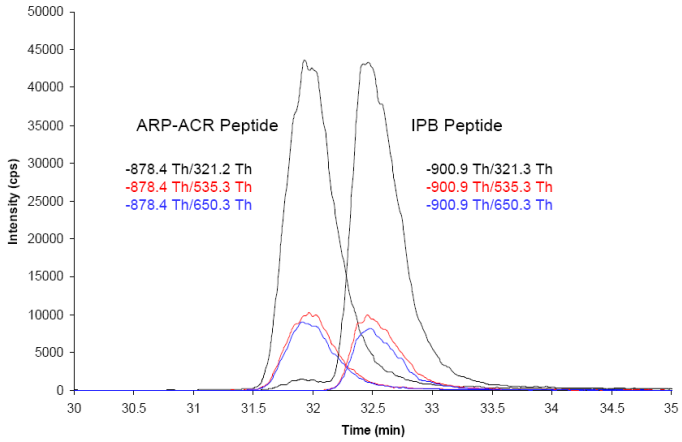

Figure 4.2. SRM chromatograms for the ARP-ACR modified model peptide (MH_2^{2+}, 878.4 Th, 100 fmol) and IPB-labeled model peptide (MH_2^{2+}, 900.9 Th, 100 fmol).

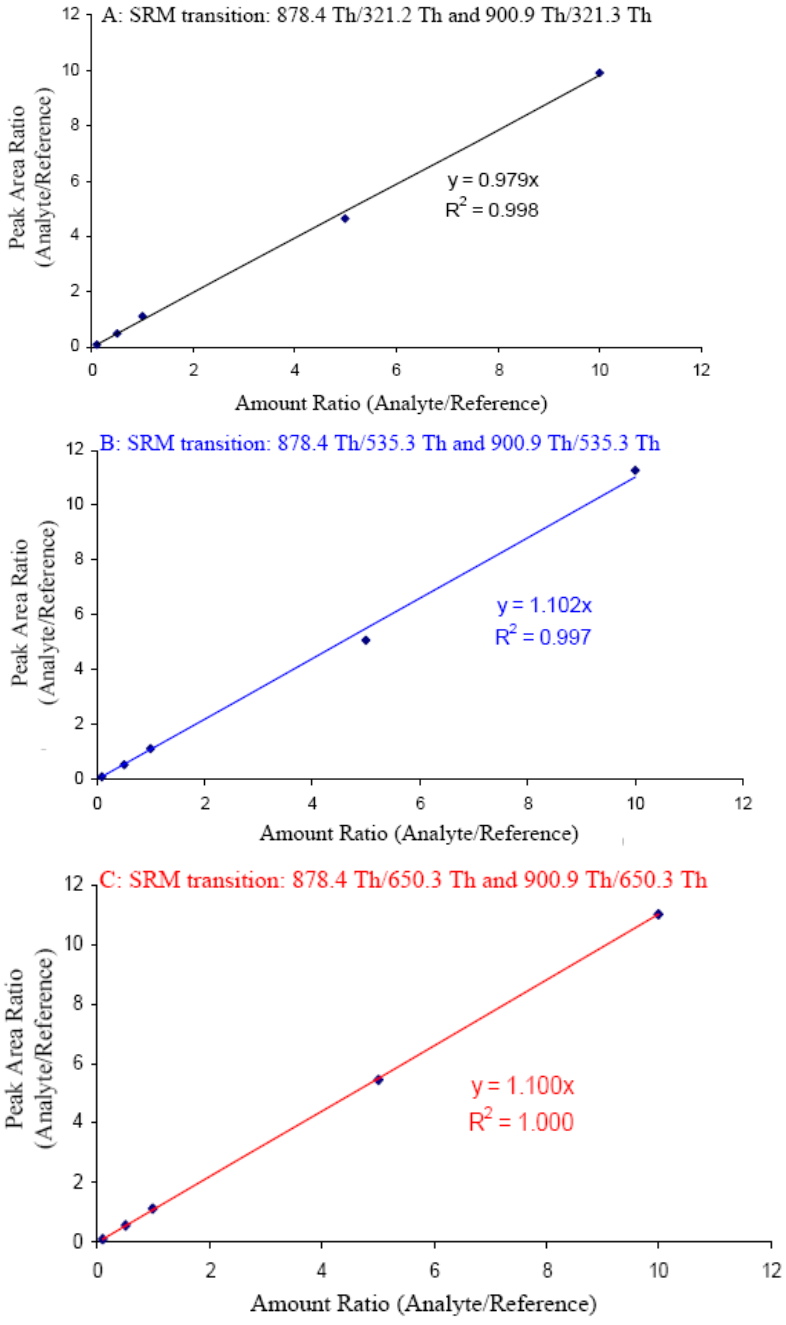

Figure 4.3. Calibration curves for the ARP-ACR modified model peptide with three SRM transsitions; the IPB modified model peptide (100 fmol) was used as the internal standard.

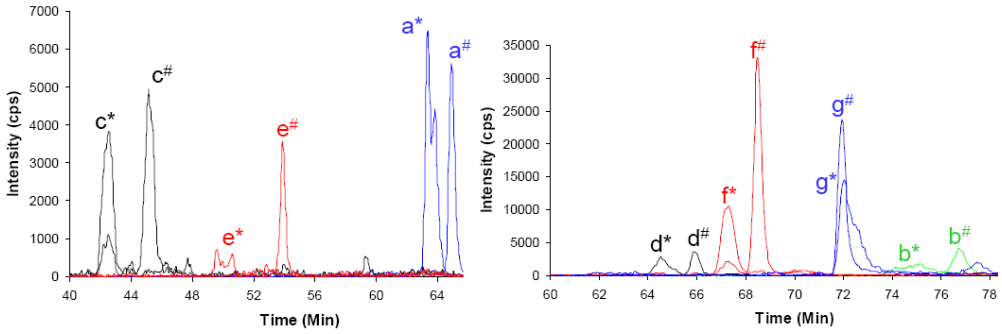

Figure 4.4. SRM chromatograms for ARP-ACR modified peptides and PEO-labeled peptides from mitochondrial samples (* means ARP-ACR modified and # means IPB labeled).

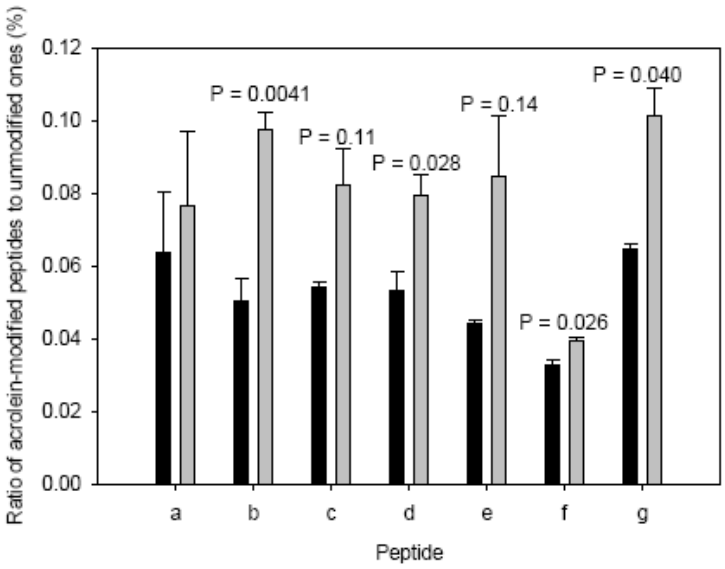

Figure 4.5. Ratios of acrolein-modified peptides to unmodified ones for control rats (n = 3) and rats (n = 3) oxidatively stressed by CCl_4. All results are presented as the mean ± SEM. (Black bars indicate control rats and gray bars indicate CCl_4 treated ones).

Supporting information

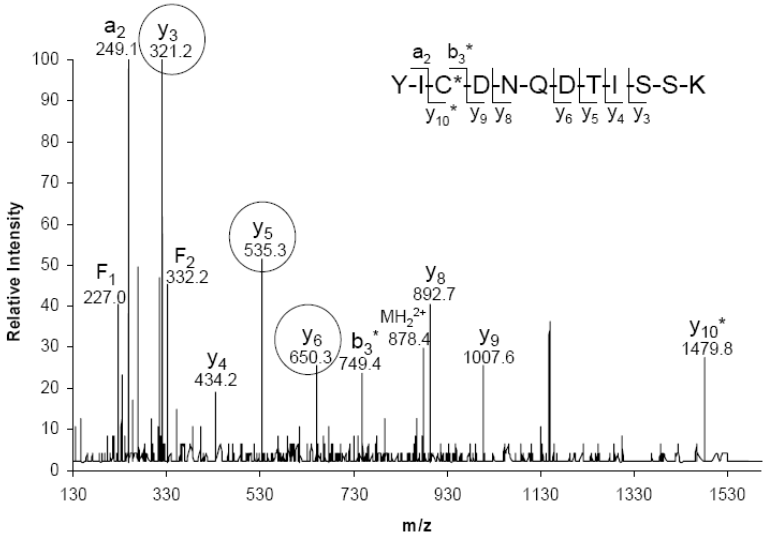

Figure 4.S-1. Tandem mass spectrum of the doubly charged model peptide with ARP-ACR modification (MH_2^{2+}, 878.4 Th). The circled fragments were used for SRM analysis.

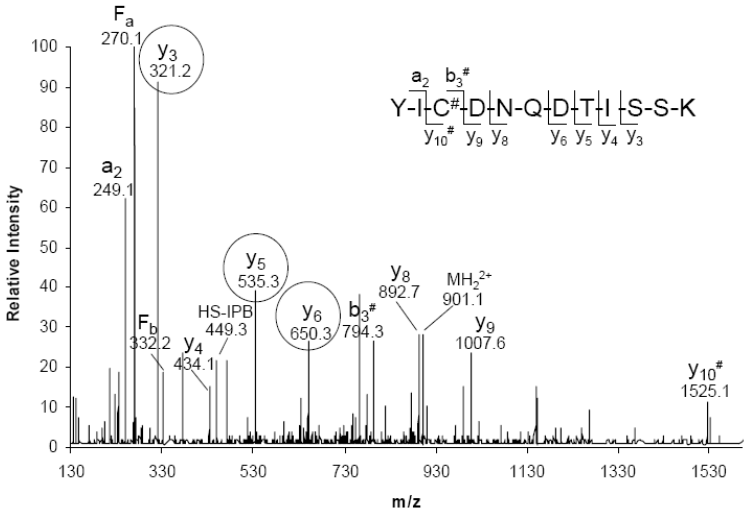

Figure 4.S-2. Tandem mass spectrum of the doubly charged model peptide with IPB modification (MH_2^{2+}, 900.9 Th). The circled fragments were used for SRM analysis.

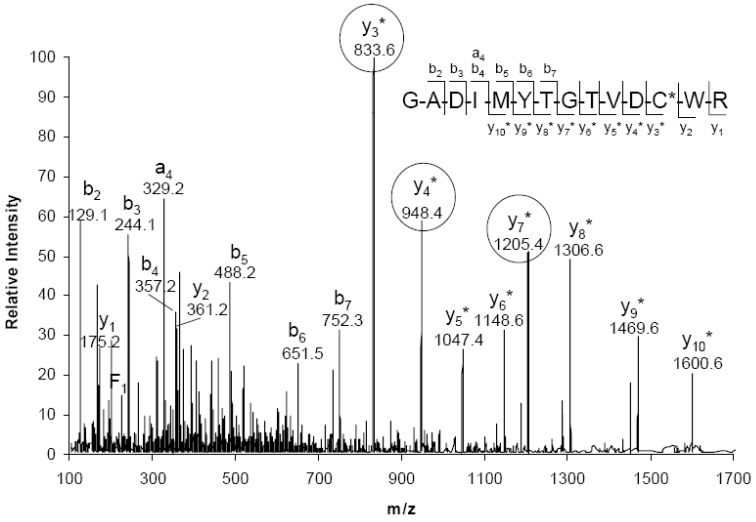

Figure 4.S-3. Tandem mass spectrum of doubly charged Peptide **b** with ARP-ACR modification (MH_2^{2+}, 978.9 Th). The circled fragments were used for SRM analysis.

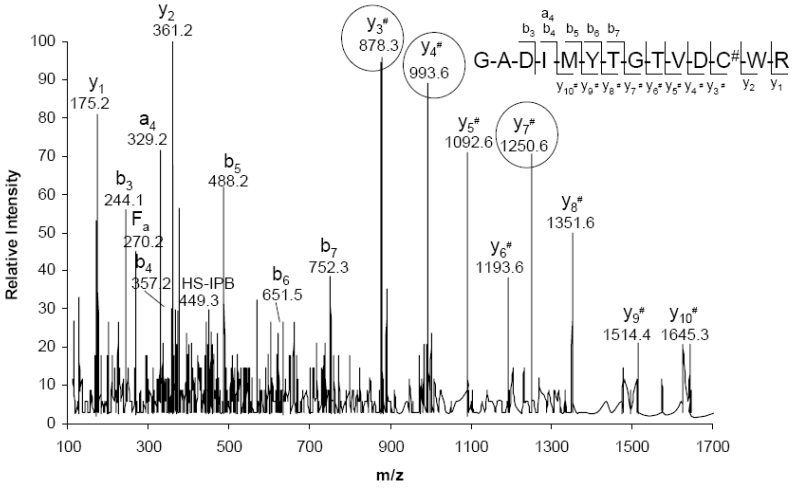

Figure 4.S-4. Tandem mass spectrum of doubly charged Peptide **b** with IPB modification (MH_2^{2+}, 1001.4 Th). The circled fragments were used for SRM analysis.

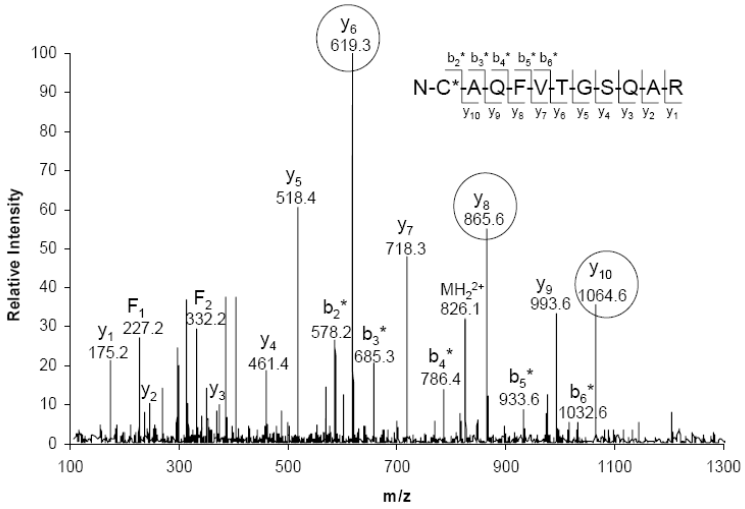

Figure 4.S-5. Tandem mass spectrum of doubly charged Peptide **c** with ARP-ACR modification (MH_2^{2+}, 825.8 Th). The circled fragments were used for SRM analysis.

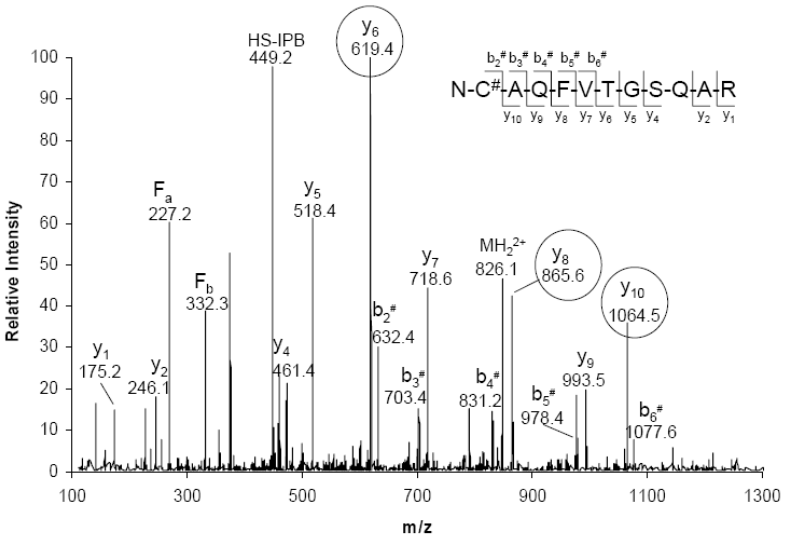

Figure 4.S-6. Tandem mass spectrum of doubly charged Peptide **c** with IPB modification (MH_2^{2+}, 848.4 Th). The circled fragments were used for SRM analysis.

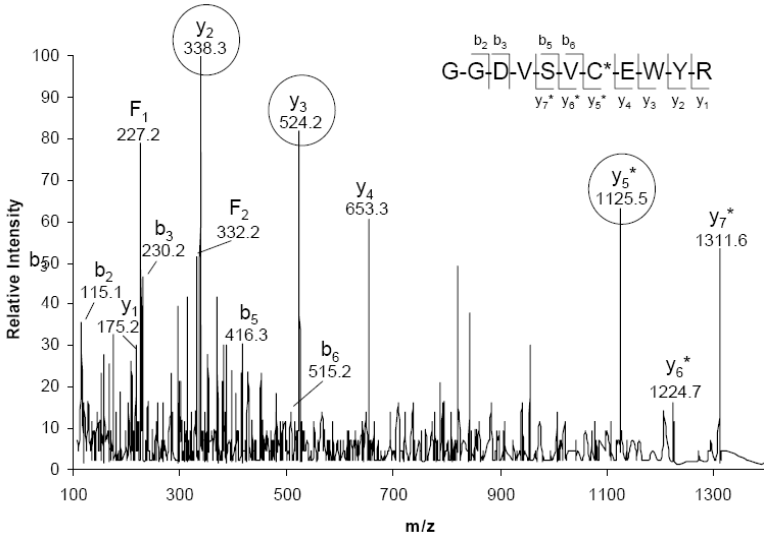

Figure 4.S-7. Tandem mass spectrum of doubly charged Peptide **d** with ARP-ACR modification (MH_2^{2+}, 820.3 Th). The circled fragments were used for SRM analysis.

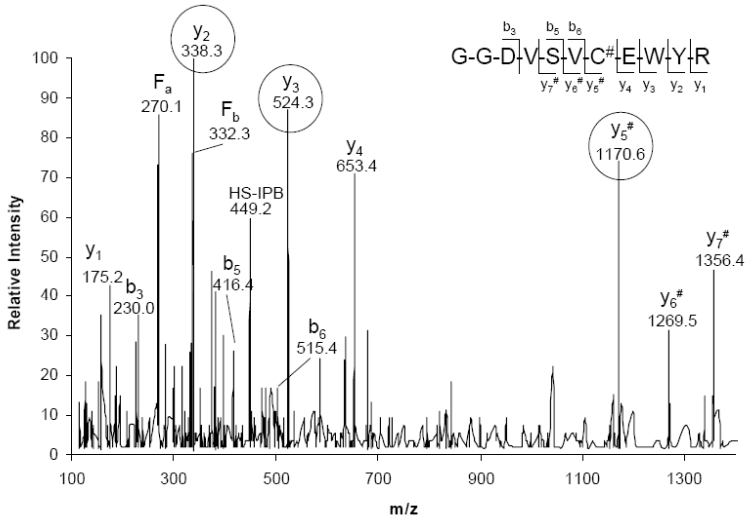

Figure 4.S-8. Tandem mass spectrum of doubly charged Peptide **d** with IPB modification (MH_2^{2+}, 842.8 Th). The circled fragments were used for SRM analysis.

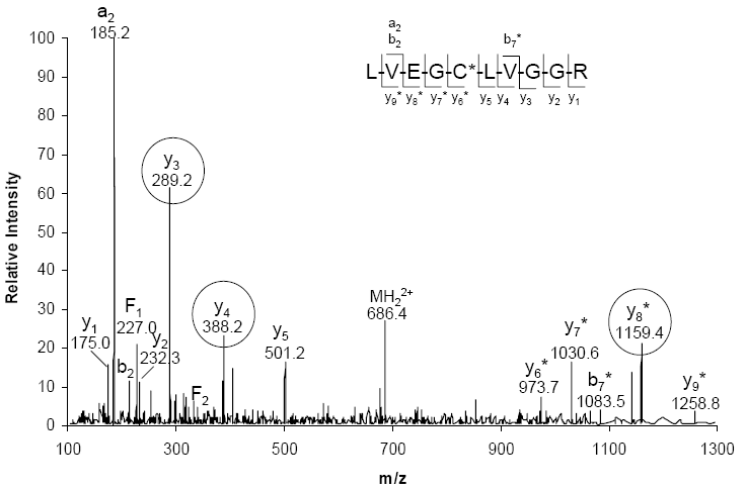

Figure 4.S-9. Tandem mass spectrum of doubly charged Peptide **e** with ARP-ACR modification (MH_2^{2+}, 686.3 Th). The circled fragments were used for SRM analysis.

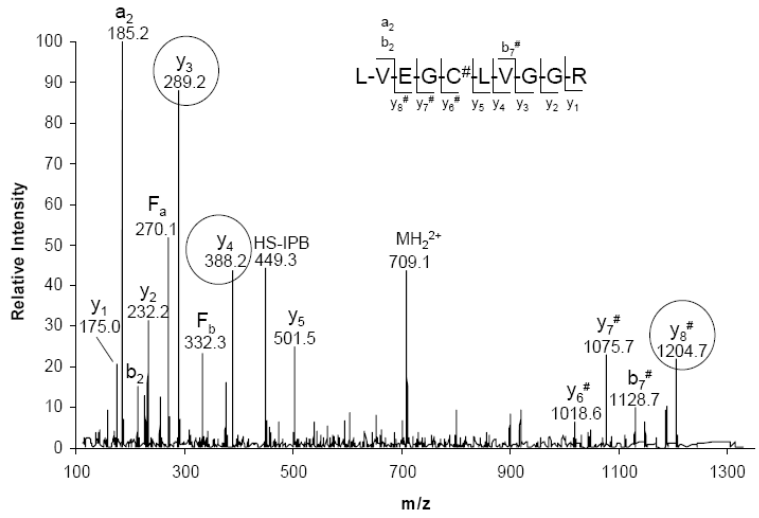

Figure 4.S-10. Tandem mass spectrum of doubly charged Peptide **e** with IPB modification (MH_2^{2+}, 708.9 Th). The circled fragments were used for SRM analysis.

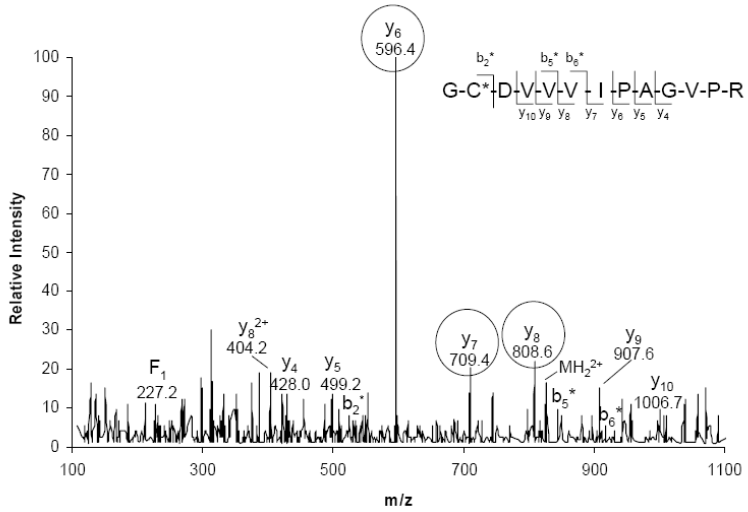

Figure 4.S-11. Tandem mass spectrum of doubly charged Peptide **f** with ARP-ACR modification (MH_2^{2+}, 825.9 Th). The circled fragments were used for SRM analysis.

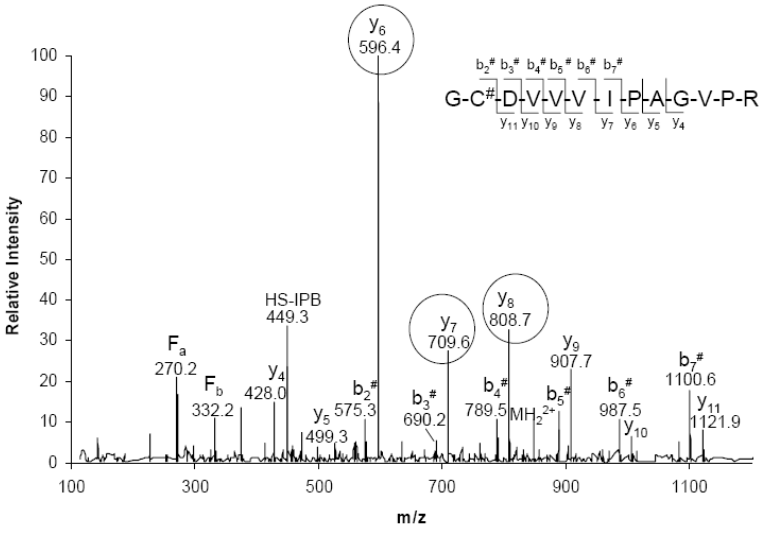

Figure 4.S-12. Tandem mass spectrum of doubly charged Peptide **f** with IPB modification (MH_2^{2+}, 848.5 Th). The circled fragments were used for SRM analysis.

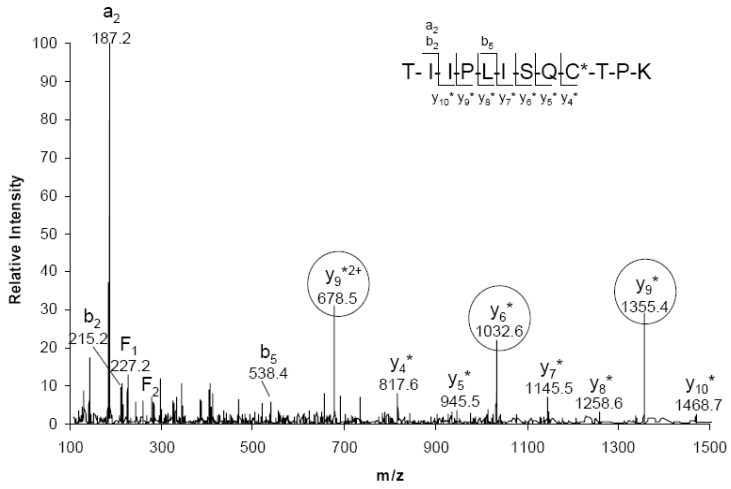

Figure 4.S-13. Tandem mass spectrum of doubly charged Peptide **g** with ARP-ACR modification (MH_2^{2+}, 842.0 Th). The circled fragments were used for SRM analysis.

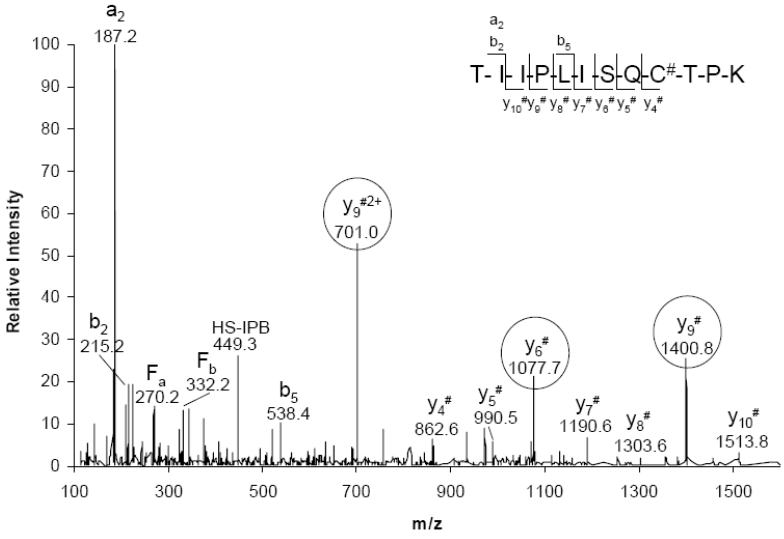

Figure 4.S-14. Tandem mass spectrum of doubly charged Peptide **g** with IPB modification (MH_2^{2+}, 864.5 Th). The circled fragments were used for SRM analysis.

CHAPTER 5.

Quantification of Peptide Adducts of Acrolein in Subsarcolemmal Mitochondria in Aging Rats

Jianyong Wu, Cristobal Miranda, Kristina Jonsson and Claudia S. Maier

Department of Chemistry, Oregon State University, Corvallis OR, 97330

Abstract

The modification of proteins by lipid peroxidation products is thought to be an underlying molecular factor in the pathogenesis of many degenerative diseases and age related disorders. In myocardia, there are two distinct types of mitochondria: interfibrillar mitochondria (IFM) and subsarcolemmal mitochondria (SSM). Here, seven acrolein-modifed Cys-containing peptides in five mitochondrial proteins in SSM from young and old rats were quantified by LC–SRM (selected reaction monitoring) analysis. Western blot analysis with N'-aminooxymethylcarbonyl hydrazino-D-biotin as an aldehyde reactive probe (ARP) and anti-ACR monoclonal antibody was also applied to measure the protein carbonyls and FDP-lysine derivatives for SSM with age, respectively. The tentative age-related increase of distinct target acrolein-modified peptides in SSM was confirmed by the increase of FDP-lysine derivatives. However, total protein carbonyls measurement using ARP in Western blot analysis did not conform to this change suggesting that age-related changes in protein carbonyls are complex and would benefit from more specific measurement protocols.

Introduction

Mitochondria are cell's powerhouse through oxidative phosphorylation. About 2% [1] of oxygen escapes in the respiration chain from mitochondria and forms superoxide radical, a reactive oxygen species (ROS) which can initiate

radical-mediated oxygenations. Proteins, DNA and lipids can be modified under oxidative stress in biological system [2-6]. Oxidative modification of proteins occurs according to a variety of mechanisms [3, 5, 7-9]. Some of them lead to backbone peptide bond cleavage or to side-chain modifications. The latter introduces protein carbonyls by Michael addition reactions between lipid peroxidation products and histidine, cysteine or lysine reside. These oxylipids, including acrolein (ACR), could be produced by polyunsaturated fatty acids and their esters under oxidative stress [10-13].

In myocardia, there are two distinct types of mitochondria: interfibrillar mitochondria (IFM) and subsarcolemmal mitochondria (SSM) [14]. The former mitochondria are located between the myofibrils and the latter ones are clustered beneath the plasma membrane. Judge et al. measured protein carbonyls in SSM and IFM from rat heart using an enzyme immunoassay [15]. They found a significant increase in oxidative stress levels in IFM with age, while little change occurred for SSM. Fannin et al. also found that oxidative metabolism was impaired with age in IFM and remained unaltered in SSM [16]. Recently, our group developed a method to detect protein carbonyls in IFM by Western blot analysis with N'-aminooxymethylcarbonyl hydrazino-D-biotin as an aldehyde reactive probe (ARP) [17]. The ratios between acrolein-modified Cys-containing peptides and the corresponding unmodified ones in SSM were also successfully measured by using ARP and iodoacetyl-PEO_2-Biotin (IPB) reagents with

nanoLC-SRM analysis (Chapter 4). Here we used this method to measure seven acrolein-modifed Cys-containing peptides in five mitochondrial proteins. Western blot with ARP and anti-ACR antibody was also applied to measure the protein carbonyls and FDP-lysine derivatives, respectively, in SSM from young and old rats.

Materials and methods

Materials

N'-aminooxymethylcarbonyl hydrazino-D-biotin (ARP) was purchased from Dojindo Molecular Technologies Inc. (Rockville, MD). Ultralink Monomeric Avidin and SuperSignal West Pico Chemiluminescent substrate were purchased from Thermo Scientific (Rockford, IL). Neutravidin-HRP, UltraLink-immobilized monomeric avidin, iodoacetyl-IPB$_2$-Biotin (IPB) and Triton X-100 detergent were obtained from Pierce (Rockford, IL). Sequencing grade modified trypsin was purchased from Promega (Madison, WI). Tris-HCl (10%) Ready Gels were purchased from Bio-Rad. Immobilon-P PVDF membranes were purchased from Millipore. Goat anti-mouse IgG–HRP conjugate was obtained from Bio-Rad Laboratories (Hercules, CA). Monoclonal anti-acrolein IgG was from COSMO BIO Co. Ltd. (Carlsbad, CA)

Animal Treatment

The experimental protocol for the animal studies was approved by the Institutional Animal Care and Use Committee at Oregon State University. Six 3-month and six 25-month male F344 rats (Harlan, Indianapolis, IN) were housed in individual plastic cages covered with Hepa filter and allowed free access to standard animal chow and water *ad libitum*. After 1 week of acclimatization, these twelve rats were killed for study.

SDS-PAGE and Western Blot with Anti-ACR Antibody and ARP

Rat cardiac mitochondria were isolated by differential centrifugation and stored at -80 ^{o}C [14]. Each sample of subsarcolemmal mitochondria (SSM) was washed twice with 10 mM NaH_2PO_4, pH 7.4, at 0 ^{o}C. The mitochondria were then resuspended in 200 µl of 10 mM NaH_2PO_4, pH 7.4, with 1% of SDS detergent and 10 mM DTT. DTT was used to react with free acrolein to prevent artificial results during sample preparation. The mitochondria were sonicated at room temperature for 5 min and then were mixed with Laemmli sample buffer (BioRad) with 5% 2-mercaptoethanol. The proteins were denatured at 95 ^{o}C for 5 min. One dimension SDS-PAGE was accomplished by loading about 15 µg of mitochondrial protein per well of Bio-Rad 10%Tris-HCl ReadyMade gels and running them at a constant 130V for 70 minutes. For visualization of the protein bands the gels were incubated with Biosafe Coomassie dye for 1 hr.

Western blotting with anti-ACR antibody was accomplished by transferring the proteins from the gel to a PVDF membrane by applying a constant current of 300 mA for 2 hours. The membrane was blocked in 5% non-fat milk in TBS-T (TBS buffer with 0.1% Tween-20) and then reacted with monoclonal anti-acrolein IgG for one hour. After extensive washing, the membrane was incubated with goat anti-mouse IgG–HRP conjugate for 1 hr. After several additional wash steps, the membrane was exposed to the West Pico Chemiluminescent substrate for 5 minutes and developed using Kodak BioMax X-Ray film.

For Western blotting with ARP, ARP was added to reach a final concentration of 5 mM to label the protein carbonyls before the proteins were totally denatured. After one dimension SDS-PAGE, the proteins were transferred from the gel to a PVDF membrane by applying a constant current of 300 mA for 2 hours. The blot was then blocked in TBS buffer with 0.5% Tween-20 and then washed extensively before being incubated with 40 ng/mL of HRP-NeutrAvidin for 1 hr. After several additional wash steps, the membrane was exposed to the West Pico Chemiluminescent substrate for 5 minutes and developed using Kodak BioMax X-Ray film. For these two Western blottings, optical densities (OD) of all the bands within a given lane from the stained gel and the membrane were calculated with Kodak ID Image Analysis software.

Preparation of ARP-ACR and IPB labeled Mitochondrial Peptides for SRM analysis

Because of the low abundance of ACR-modified mitochondrial proteins, an enrichment method is necessary for SRM analysis. ARP and IPB were used to react with ACR-modified peptides and Cys-containing peptides, respectively (Scheme 5.1). The resulting products with biotin tags were able to be enriched by an avidin column. The Scheme 5.2 shows the sample preparation procedure. More details are in Chapter 4.

Nano-HPLC and Mass Spectrometry

An Ultimate LC Packing system and a 75 μm i.d. ×15 cm C18 PepMap 100 column (Dionex, Sunnyvale, CA) were used. Peptides were eluted with a gradient from 9% to 18% B over 90 min (using solvent A: 1% acetonitrile with 0.1% formic acid; solvent B, 100% acetonitrile with 0.1% formic acid) at a 0.260 μL/min. SRM analysis was carried out on a 4000 Q-Trap hybrid tandem mass spectrometer (AB/MDS SCIEX, Concord, Ontario, Canada) using nano-ESI source. More details are in Chapter 4.

Results and discussion

Quantification of Acrolein-modified Cys-containing Peptides in SSM for Young and Old Rats by SRM analysis

Seven acrolein-modifed Cys-containing peptides from five mitochondrial proteins

were identified previously by mass spectrometry (Chapter 4). These modified peptides can also represent acrolein-modifed Cys-containing peptides in SSM. Table 5.1 shows these peptides labeled as **a** through **g**. Nano-LC SRM analysis was used to quantify these seven modified peptides from six young (3-month) and six old (25-month) rats. Fig. 5.1 shows the ratios of acrolein-modified peptides to unmodified ones from young and old rats. The ratios were around 0.1%. There was a tentative increase of ACR-modified peptides with age. However, statistical analysis using a t-test (p-values < 0.05) indicating that there was no significant difference between levels of ACR-modified peptides for young and old rats.

Measurement of Protein Carbonyls in SSM for Young and Old Rats by Western Blot with ARP

As an alternative to the 2,4-dinitrophenylhydrazine-based assays for protein carbonyls measurement, our group developed an approach, in which ARP reacted with carbonyl group to form a biotinylated oxime derivatives [17]. After ARP treatment, the SSM proteins were separated by 1D-SDS-PAGE followed by Western blotting on a PVDF membrane. HRP conjugated NeutrAvidin was used with PicoWest chemilumiinescent reagents to visualize the ARP reactive bands (Fig. 5.2). Some ARP reactive protein bands are visible based on the Western blot. The control sample without ARP addition shows relatively weak signals for two bands. These two HRP-NeutrAvidin reactive protein bands in the control could be

due to naturally biotinylated proteins, such as one of the mitochondrial carboxylase enzymes. Optical densities (OD) of all the bands within a given lane from the stained gel and the Western blot membrane indicate the total amount of protein and protein carbonyl, respectively. After correction of protein amount in each lane, there is no significant difference of protein carbonyls in SSM based on OD analysis with age in Fig. 5.3. Little concentration change of protein carbonyls might be due to the undamaged anti-oxidative stress system in SSM with age [15].

Measurement of FDP-lysine Derivatives in SSM for Young and Old Rats by Western Blot with Anti-ACR Antibody

Acrolein is α,β-unsaturated aldehyde, which can react with some side chains of amino acids. One of the adducts is the formyl-dehydropiperidino-lysine (FDP-lysine) derivative [18]. Anti-ACR monoclonal antibody is specific for ACR-modified proteins, especially for FDP-lysine derivatives [19]. Here, we applied this antibody to SSM samples. Fig. 5.4 shows the images of SDS-PAGE and Western blot of FDP-lysine derivatives. After correction of protein amount from SDS-PAGE image based on OD analysis, Fig. 5.5 implies the levels of FDP-lysine derivatives in SSM in old rats are higher than young ones.

Conclusions

Ratios of ACR-modified Cys-containing peptides to unmodified ones in SSM with

age were successfully measured by LC-SRM analysis. A tentative increase of distinct Michael adducts of ACR was observed, however statistical analysis indicated that the observed difference in acrolein adduction was not significant ($p < 0.05$) for the two age groups. Complementation of the LC-SRM analysis by immunochemical analysis using an anti-ACR antibody showed that the levels of FDP-lysine derivatives were higher in SSM isolated from old animals compared to the levels determined for young animals. However, total protein carbonyls measurement using ARP in Western blot analysis did not conform to this change suggesting that age-related changes in protein carbonyls are complex and would benefit from more specific measurement protocols.

Acknowledgements

This work was supported by grants from the NIH/NIA (AG025372). The mass spectrometry core facility of the Environmental Health Sciences Center at Oregon State University is supported in part by a grant from NIEHS (ES00210).

Reference

[1] A. Boveris, N. Oshino, B. Chance, Biochem. J., 128 (1972) 617.

[2] T. Finkel, N.J. Holbrook, Nature, 408 (2000) 239.

[3] R.L. Levine, E.R. Stadtman, Exp. Gerontol., 36 (2001) 1495.

[4] L.J. Marnett, J.N. Riggins, J.D. West, J. Clin. Invest., 111 (2003) 583.

[5] E.R. Stadtman, Ann. N. Y. Acad. Sci., 928 (2001) 22.

[6] J.D. West, L.J. Marnett, Chem. Res. Toxicol., 19 (2006) 173.

[7] B.S. Berlett, E.R. Stadtman, J. Biol. Chem., 272 (1997) 20313.

[8] R.T. Dean, S. Fu, R. Stocker, M.J. Davies, Biochem. J., 324 (Pt 1) (1997) 1.

[9] R.L. Levine, Free Radic. Biol. Med., 32 (2002) 790.

[10] H. Esterbauer, M. Dieber-Rotheneder, G. Waeg, G. Striegl, G. Jurgens, Chem. Res. Toxicol., 3 (1990) 77.

[11] H. Esterbauer, R.J. Schaur, H. Zollner, Free Radic. Biol. Med., 11 (1991) 81.

[12] C. Schneider, K.A. Tallman, N.A. Porter, A.R. Brash, J. Biol. Chem., 276 (2001) 20831.

[13] L.M. Sayre, D. Lin, Q. Yuan, X. Zhu, X. Tang, Drug Metab. Rev., 38 (2006) 651.

[14] J.W. Palmer, B. Tandler, C.L. Hoppel, J. Biol. Chem., 252 (1977) 8731.

[15] S. Judge, Y.M. Jang, A. Smith, T. Hagen, C. Leeuwenburgh, FASEB J., 19 (2005) 419.

[16] S.W. Fannin, E.J. Lesnefsky, T.J. Slabe, M.O. Hassan, C.L. Hoppel, Arch. Biochem. Biophys., 372 (1999) 399.

[17] W.G. Chung, C.L. Miranda, C.S. Maier, Electrophoresis, 29 (2008) 1317.

[18] K. Uchida, M. Kanematsu, Y. Morimitsu, T. Osawa, N. Noguchi, E. Niki, J. Biol. Chem., 273 (1998) 16058.

[19] K. Uchida, M. Kanematsu, K. Sakai, T. Matsuda, N. Hattori, Y. Mizuno, D. Suzuki, T. Miyata, N. Noguchi, E. Niki, T. Osawa, Proc. Natl. Acad. Sci. U. S. A., 95 (1998) 4882.

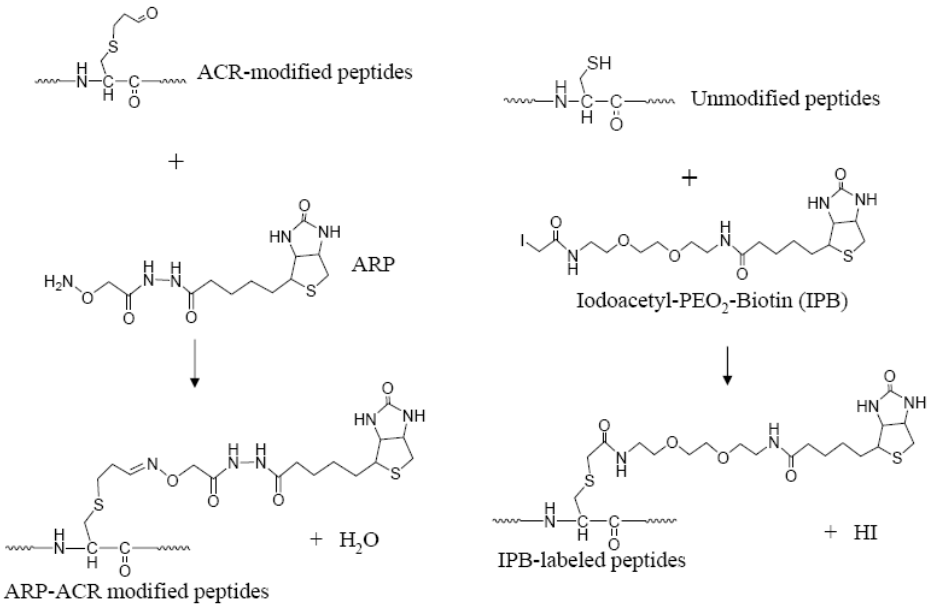

Scheme 5.1. Structures and formations of ARP-ACR modified and IPB-labeled peptides.

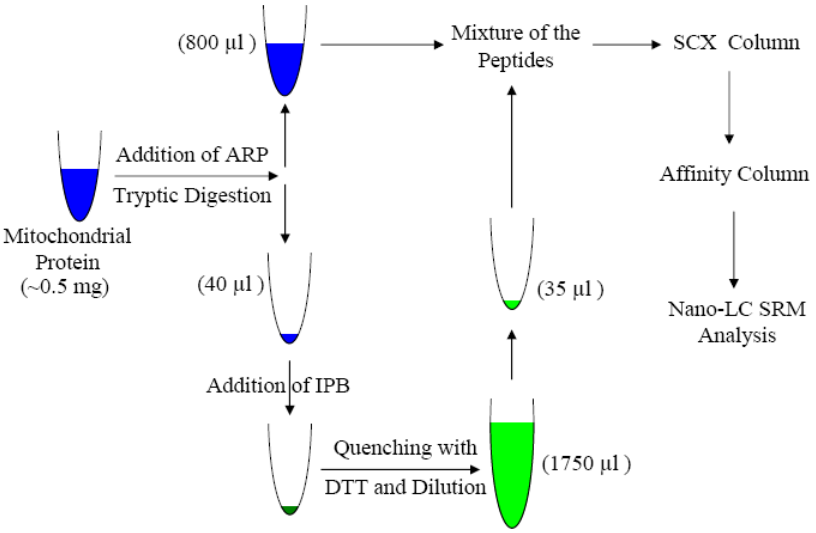

Scheme 5.2. Relative quantitation procedure for acrolein-modified peptides in mitochondrial protein samples.

Table 5.1. Summary of the seven acrolein-modifed peptides labeled as **a** through **g** from five mitochondrial proteins. Peptide sequences, biological and functional assignments were made on the basis of information from the NCBI (http://www.ncbi.nlm.nih.gov/Pubmed) and the UniPort Knowledgebase (http://www.uniprot.org) websites.

Peptide	Modified residue	Protein name	Biological function
a. EFNGLGD**C**LTK	**C** 159	ADP/ATP translocase 1	Transport
b. GADIMYTGTVD**C**WR	**C** 256		
c. N**C**AQFVTGSQAR	**C** 100	ATP synthase D chain	Respiratory chain
d. GGDVSV**C**EWYR	**C** 54	Cytochrome c oxidase subunit VIb isoform 1	Respiratory chain
e. LVEG**C**LVGGR	**C** 142	NADH dehydrogenase [ubiquinone] flavoprotein 1	Respiratory chain
f. G**C**DVVVIPAGVPR	**C** 93	Malate dehydrogenase	TCA cycle
g. TIIPLISQ**C**TPK	**C** 212		

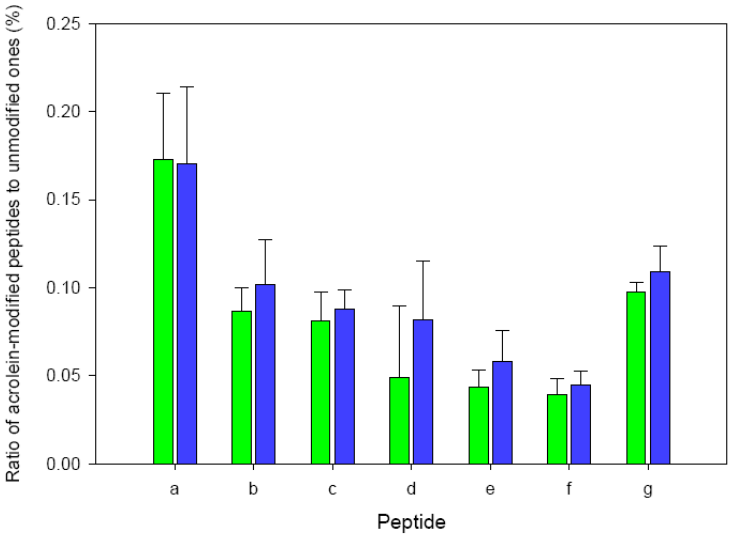

Figure 5.1. Ratios of acrolein-modified peptides to unmodified ones for young rata (n = 6) and old rats (n = 6). All results are presented as the mean ± SEM. (Green bars indicate young rats and blue bars indicate old ones).

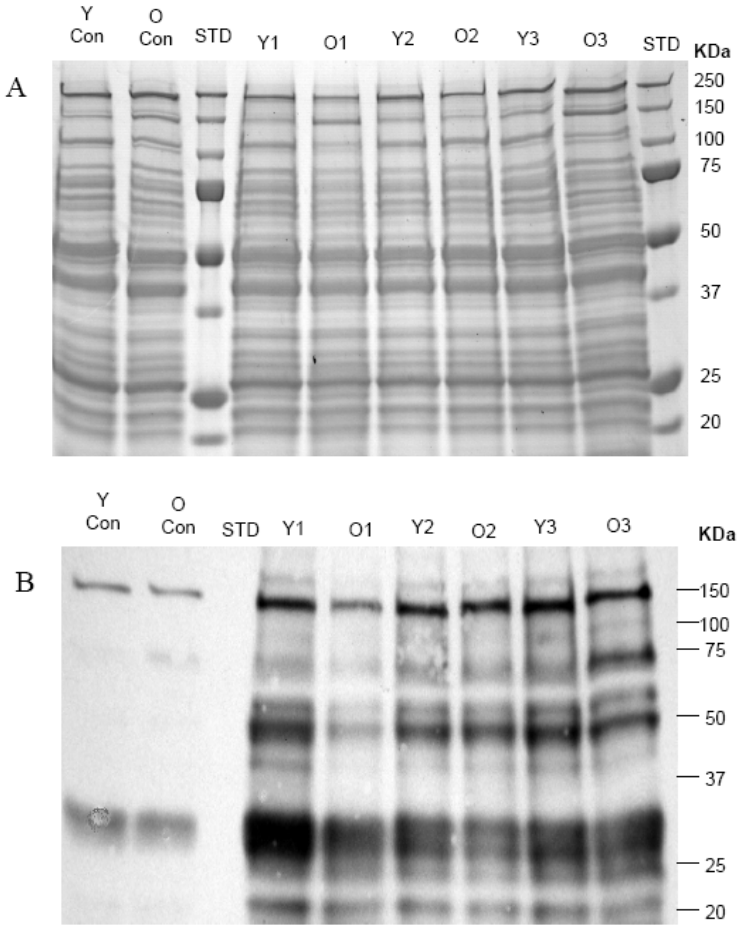

Figure 5.2. Images of SDS-PAGE (A) and Western ARP blot of protein carbonyls (B) for mitochondrial proteins from young (Y) and old (O) rats. (STD indicates standard proteins and Con indicates control sample.)

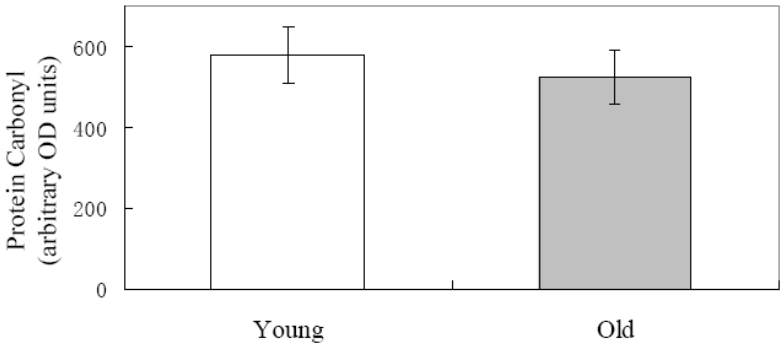

Figure 5.3. Western ARP blot analysis of protein carbonyls in SSM from young rats (n = 3) and old rats (n = 3). Optical densities (OD) of all the protein carbonyl bands within a given lane were calculated with Kodak ID Image Analysis software. All results are presented as the mean ± SEM.

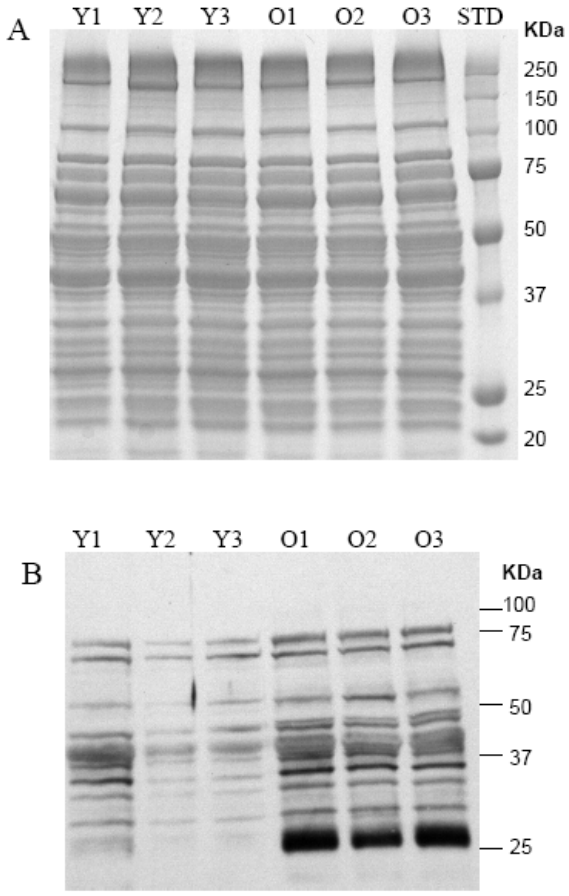

Figure 5.4. Images of SDS-PAGE (A) and Western blot of FDP-lysine Derivative (B) for mitochondrial proteins from young (Y) and old (O) rats. STD indicates standard proteins.

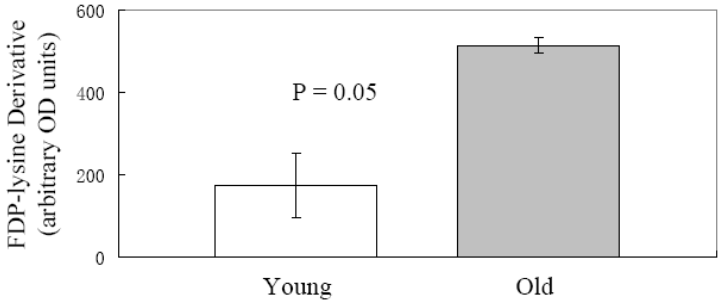

Figure 5.5. Western blot analysis of FDP-lysine derivative in SSM from young rats (n = 3) and old rats (n = 3). Optical densities (OD) of all the FDP-lysine derivative bands within a given lane were calculated with Kodak ID Image Analysis software. All results are presented as the mean ± SEM; p value is 0.05, indicating the difference.

CHAPTER 6. CONCLUSIONS

MS/MS spectra under high-energy collision-induced dissociation (CID) allow obtaining sequence information for oxylipid-peptide conjugates which, at least in favorable cases, enables unambiguous localization of the modification sites by lipid peroxidation products. The protonated dehydrated HNE moiety (139.1 Th) is not shown in tandem mass spectra for His-containing peptide oxylipid conjugates, compared with low energy CID. All MS/MS spectra of Michael adducts exhibit neutral loss of the oxylipid moiety ions because they have $–CH_2CH_2CH=O$ structure in common. Spectra of Cys-containing peptide conjugates exhibit additional characteristic neutral loss of HS-oxylipid moiety ions. In addition to neutral loss of oxylipid moiety ions, spectra of His/Lys-containing peptide conjugates (Michael adduct) show characteristic oxylipid-containing His/Lys immonium or related ions. Spectra of Lys-containing peptide conjugates (Michael adduct) show an additional Lys immonium ion with neutral loss of NH_3. Spectra of Lys-containing peptide conjugates (Schiff base) also show oxylipid-containing Lys immonium ions or ions with neutral loss of NH_3.

In our study, N'-aminooxymethylcarbonylhydrazino-D-biotin (ARP), as an enrichment probe, was successfully used to identify seven acrolein-modifed Cys-containing peptides from subsarcolemmal mitochondria (SSM) with a Q-trap

instrument. Combined with iodoacetyl-PEO_2-Biotin (IPB) reagents, these seven acrolein-modifed Cys-containing peptides were quantified by nano-LC SRM analysis. ARP and IPB reagents were successfully used to label our target peptides for enrichment. The dilution step during sample preparation circumvented the huge concentration difference between acrolein-modified peptides and their corresponding unmodified ones. ARP-ACR and IPB labeled peptides show similar elctrospray ionization efficiency and fragmentation pattern in low-energy CID, which makes LC-SRM an appropriate way to measure the ratios between them. The ratios for those seven peptides from the CCl_4 treated rats are higher than the control ones, which indicates the ratios of acrolein-modified peptides to unmodified ones are potential markers of oxidative stress *in vivo*. Age-dependent changes of protein carbonyls were also investigated in subsarcolemmal mitochondria by using this LC-SRM analysis of distinct ACR-modified Cys-containing peptides. Immunochemical analysis using an anti-ACR monoclonal antibody supported an increase of proteins modified by acrolein with age. However, total protein carbonyls measurement using ARP in Western blot analysis did not conform to this change suggesting that age-related changes in protein carbonyls are complex and would benefit from more specific measurement protocols.

ABBREVIATION

ACR	acrolein
ANT	adenine nucleotide transporter
AQUA	absolute quantification of protein
ARP	aldehyde reactive probe
B	magnetic sector
BSA	bovine serum albumin
CID	collision-induced dissociation
CV	coefficient of variation
DFT	density functional theory
DNPH	2, 4-dinitrophenylhydrazine
DTT	dithiothreitol
ECD	electron capture dissociation
ESI	electrospray ionization
ETC	electron transport chain
ETD	electron transfer dissociation
FMO	frontier molecular orbital
HNE	4-hydroxy-2-nonenal
HOMO	highest occupied molecular orbital

ABBREVIATION (Continued)

HRP	horseradish peroxidase
ICAT	isotope-coded affinity tag
ICR	ion cyclotron resonance
IFM	interfibrillar mitochondria
IPB	iodoacetyl-PEO_2-Biotin
iTRAQ	isotope tags for relative and absolute quantification
LIT	linear ion trap
LUMO	lowest unoccupied molecular orbital
MALDI	matrix assisted laser desorption ionization
MCP	micro-channel plate
MDA	malondialdehyde
MPT	mitochondrial permeability transition
OD	optical density
ONE	4-oxo-2-nonenal
PBS	phosphate buffered saline
PTM	post translational modification
PUFA	polyunsaturated fatty acid
PVDF	polyvinylidene fluoride
Q	quadrupole
QIT	quadrupole ion trap

ABBREVIATION (Continued)

RF	radio frequency
ROS	reactive oxygen species
SCX	strong cation exchange
SEM	standard error of the mean
SILAC	stable isotope labeling by amino acids in cell culture
SOD	superoxide dismutase
SRM	selected reaction monitoring
SSM	subsarcolemmal mitochondria
TBARS	thiobarbituric acid
TDC	time-to-digital converter
TOF	time-of-flight
VDAC	voltage dependent anion selective channel

BIBLIOGRAPHY

[1] R. Aebersold, M. Mann, Nature, 422 (2003) 198.

[2] N.L. Anderson, N.G. Anderson, Electrophoresis, 19 (1998) 1853.

[3] A.Y. Andreyev, Y.E. Kushnareva, A.A. Starkov, Biochemistry (Mosc), 70 (2005) 200.

[4] M. Bantscheff, M. Schirle, G. Sweetman, J. Rick, B. Kuster, Anal. Bioanal. Chem., 389 (2007) 1017.

[5] J.S. Beckman, W.H. Koppenol, Am. J. Physiol., 271 (1996) C1424.

[6] B.S. Berlett, E.R. Stadtman, J. Biol. Chem., 272 (1997) 20313.

[7] R.J. Beynon, M.K. Doherty, J.M. Pratt, S.J. Gaskell, Nat. Methods, 2 (2005) 587.

[8] W.P. Blackstock, M.P. Weir, Trends Biotechnol., 17 (1999) 121.

[9] M.S. Bolgar, S.J. Gaskell, Anal. Chem., 68 (1996) 2325.

[10] P.V. Bondarenko, D. Chelius, T.A. Shaler, Anal. Chem., 74 (2002) 4741.

[11] A. Boveris, B. Chance, Biochem. J., 134 (1973) 707.

[12] A. Boveris, N. Oshino, B. Chance, Biochem. J., 128 (1972) 617.

[13] R. Bucala, A. Cerami, Adv. Pharmacol., 23 (1992) 1.

[14] D. Bylund, R. Danielsson, G. Malmquist, K.E. Markides, J. Chromatogr. A, 961 (2002) 237.

[15] M. Carini, G. Aldini, R.M. Facino, Mass Spectrom. Rev., 23 (2004) 281.

[16] J. Chavez, J. Wu, B. Han, W.G. Chung, C.S. Maier, Anal. Chem., 78 (2006) 6847.

[17] K.B. Choksi, W.H. Boylston, J.P. Rabek, W.R. Widger, J. Papaconstantinou, Biochim. Biophys. Acta, 1688 (2004) 95.

[18] H. Chung, D.P. Hong, J.Y. Jung, H.J. Kim, K.S. Jang, Y.Y. Sheen, J.I. Ahn, Y.S. Lee, G. Kong, Toxicol. Appl. Pharmacol., 206 (2005) 27.

[19] W.G. Chung, C.L. Miranda, C.S. Maier, Brain Res., 1176 (2007) 133.

[20] W.G. Chung, C.L. Miranda, C.S. Maier, Electrophoresis, 29 (2008) 1317.

[21] W.G. Chung, C.L. Miranda, J.F. Stevens, C.S. Maier, Food Chem. Toxicol., 47 (2009) 827.

[22] B.A. Collings, W.R. Stott, F.A. Londry, J. Am. Soc. Mass Spectrom., 14 (2003) 622.

[23] J.J. Coon, J.E. Syka, J. Shabanowitz, D.F. Hunt, Biotechniques, 38 (2005) 519.

[24] M. Crompton, Biochem. J., 341 (Pt 2) (1999) 233.

[25] B. D'Autreaux, M.B. Toledano, Nat. Rev. Mol. Cell Biol., 8 (2007) 813.

[26] R.T. Dean, S. Fu, R. Stocker, M.J. Davies, Biochem. J., 324 (Pt 1) (1997) 1.

[27] M.K. Dennehy, K.A. Richards, G.R. Wernke, Y. Shyr, D.C. Liebler, Chem. Res. Toxicol., 19 (2006) 20.

[28] J.A. Doorn, D.R. Petersen, Chem. Res. Toxicol., 15 (2002) 1445.

[29] J.A. Doorn, S.K. Srivastava, D.R. Petersen, Chem. Res. Toxicol., 16 (2003) 1418.

[30] J.M. Duan, M. Karmazyn, Mol. Cell Biochem., 90 (1989) 47.

[31] H. Esterbauer, Am. J. Clin. Nutr., 57 (1993) 779S.

[32] H. Esterbauer, M. Dieber-Rotheneder, G. Waeg, G. Striegl, G. Jurgens, Chem. Res. Toxicol., 3 (1990) 77.

[33] H. Esterbauer, R.J. Schaur, H. Zollner, Free Radic. Biol. Med., 11 (1991) 81.

[34] S.W. Fannin, E.J. Lesnefsky, T.J. Slabe, M.O. Hassan, C.L. Hoppel, Arch. Biochem. Biophys., 372 (1999) 399.

[35] F. Fenaille, P. Mottier, R.J. Turesky, S. Ali, P.A. Guy, J. Chromatogr. A, 921 (2001) 237.

[36] J.B. Fenn, M. Mann, C.K. Meng, S.F. Wong, C.M. Whitehouse, Science, 246 (1989) 64.

[37] L. Fialkow, Y. Wang, G.P. Downey, Free Radic. Biol. Med., 42 (2007) 153.

[38] R. Fields, H.B. Dixon, Biochem. J., 121 (1971) 587.

[39] T. Finkel, N.J. Holbrook, Nature, 408 (2000) 239.

[40] B. Friguet, FEBS Lett, 580 (2006) 2910.

[41] B. Friguet, L.I. Szweda, FEBS Lett, 405 (1997) 21.

[42] A. Furuhata, T. Ishii, S. Kumazawa, T. Yamada, T. Nakayama, K. Uchida, J. Biol. Chem., 278 (2003) 48658.

[43] A. Furuhata, M. Nakamura, T. Osawa, K. Uchida, J. Biol. Chem., 277 (2002) 27919.

[44] Gaussian, Revision C.02, Gaussian, Inc., Wallingford CT (2004).

[45] M. Geiszt, J.B. Kopp, P. Varnai, T.L. Leto, Proc. Natl. Acad. Sci. U. S. A., 97 (2000) 8010.

[46] S.A. Gerber, J. Rush, O. Stemman, M.W. Kirschner, S.P. Gygi, Proc. Natl. Acad. Sci. U. S. A., 100 (2003) 6940.

[47] A. Gilchrist, C.E. Au, J. Hiding, A.W. Bell, J. Fernandez-Rodriguez, S. Lesimple, H. Nagaya, L. Roy, S.J. Gosline, M. Hallett, J. Paiement, R.E. Kearney, T. Nilsson, J.J. Bergeron, Cell, 127 (2006) 1265.

[48] N.M. Green, Biochem. J., 89 (1963) 585.

[49] S. Grimm, D. Brdiczka, Apoptosis, 12 (2007) 841.

[50] P.A. Grimsrud, M.J. Picklo, Sr., T.J. Griffin, D.A. Bernlohr, Mol. Cell Proteomics, 6 (2007) 624.

[51] T. Grune, K.J. Davies, Mol. Aspects. Med., 24 (2003) 195.

[52] J.M. Gutteridge, B. Halliwell, Trends Biochem. Sci., 15 (1990) 129.

[53] S.P. Gygi, B. Rist, S.A. Gerber, F. Turecek, M.H. Gelb, R. Aebersold, Nat. Biotechnol., 17 (1999) 994.

[54] J.W. Hager, Rapid Commun. Mass Spectrom., 16 (2002) 512.

[55] B. Halliwell, Gutteridge, T., Free Radicals in Biology and Medicine, Oxford University Press, London, 2007.

[56] B. Han, J.F. Stevens, C.S. Maier, Anal. Chem., 79 (2007) 3342.

[57] J.D. Hayes, L.I. McLellan, Free Radic. Res., 31 (1999) 273.

[58] A.J. Heck, J. Krijgsveld, Expert. Rev. Proteomics, 1 (2004) 317.

[59] Y. Huang, S. Guan, H.S. Kim, A.G. Marshall, Int. J. Mass Spectrom. Ion Processes, 152 (1996) 121.

[60] A.L. Isom, S. Barnes, L. Wilson, M. Kirk, L. Coward, V. Darley-Usmar, J. Am. Soc. Mass Spectrom., 15 (2004) 1136.

[61] P. Jaramillo, P. Perez, R. Contreras, W. Tiznado, P. Fuentealba, J. Phys. Chem. A, 110 (2006) 8181.

[62] S. Judge, Y.M. Jang, A. Smith, T. Hagen, C. Leeuwenburgh, FASEB J., 19 (2005) 419.

[63] G. Jurgens, J. Lang, H. Esterbauer, Biochim. Biophys. Acta, 875 (1986) 103.

[64] M. Karas, F. Hillenkamp, Anal. Chem., 60 (1988) 2299.

[65] R.A. Kohanski, M.D. Lane, Methods Enzymol., 184 (1990) 194.

[66] M.A. Korolainen, G. Goldsteins, I. Alafuzoff, J. Koistinaho, T. Pirttila, Electrophoresis, 23 (2002) 3428.

[67] G. Kroemer, J.C. Reed, Nat. Med., 6 (2000) 513.

[68] A.J. Lambert, M.D. Brand, Methods Mol. Biol., 554 (2009) 165.

[69] M.R. Larsen, M.B. Trelle, T.E. Thingholm, O.N. Jensen, Biotechniques, 40 (2006) 790.

[70] R.L. Levine, Free Radic. Biol. Med., 32 (2002) 790.

[71] R.L. Levine, D. Garland, C.N. Oliver, A. Amici, I. Climent, A.G. Lenz, B.W. Ahn, S. Shaltiel, E.R. Stadtman, Methods Enzymol., 186 (1990) 464.

[72] R.L. Levine, E.R. Stadtman, Exp. Gerontol., 36 (2001) 1495.

[73] D. Lin, H.G. Lee, Q. Liu, G. Perry, M.A. Smith, L.M. Sayre, Chem. Res. Toxicol., 18 (2005) 1219.

[74] R.M. LoPachin, D.S. Barber, T. Gavin, Toxicol. Sci., 104 (2008) 235.

[75] R.M. LoPachin, T. Gavin, B.C. Geohagen, S. Das, Toxicol. Sci., 98 (2007) 561.

[76] R.M. LoPachin, T. Gavin, D.R. Petersen, D.S. Barber, Chem. Res. Toxicol., 22 (2009) 1499.

[77] R.M. Lopachin, B.C. Geohagen, T. Gavin, Toxicol. Sci., 107 (2009) 171.

[78] J. Malmstrom, H. Lee, R. Aebersold, Curr. Opin. Biotechnol., 18 (2007) 378.

[79] B.A. Mamyrin, Int. J. Mass Spectrom. Ion Processes, 131 (1994) 1.

[80] K. Marley, D.T. Mooney, G. Clark-Scannell, T.T. Tong, J. Watson, T.M. Hagen, J.F. Stevens, C.S. Maier, J. Proteome Res., 4 (2005) 1403.

[81] L.J. Marnett, J.N. Riggins, J.D. West, J. Clin. Invest., 111 (2003) 583.

[82] D.L. Meany, H. Xie, L.V. Thompson, E.A. Arriaga, T.J. Griffin, Proteomics, 7 (2007) 1150.

[83] H. Mirzaei, F. Regnier, Anal. Chem., 77 (2005) 2386.

[84] H. Mirzaei, F. Regnier, J. Chromatogr. A, 1134 (2006) 122.

[85] A. Nakamura, S. Goto, J. Biochem., 119 (1996) 768.

[86] S. Nemoto, K. Takeda, Z.X. Yu, V.J. Ferrans, T. Finkel, Mol. Cell Biol., 20 (2000) 7311.

[87] Y. Oda, K. Huang, F.R. Cross, D. Cowburn, B.T. Chait, Proc. Natl. Acad. Sci. U. S. A., 96 (1999) 6591.

[88] M. Oh-Ishi, T. Ueno, T. Maeda, Free Radic. Biol. Med., 34 (2003) 11.

[89] H. Ohkawa, N. Ohishi, K. Yagi, Anal. Biochem., 95 (1979) 351.

[90] S.E. Ong, B. Blagoev, I. Kratchmarova, D.B. Kristensen, H. Steen, A. Pandey, M. Mann, Mol. Cell Proteomics, 1 (2002) 376.

[91] S.E. Ong, M. Mann, Nat. Chem. Biol., 1 (2005) 252.

[92] S. Orrenius, V. Gogvadze, B. Zhivotovsky, Annu. Rev. Pharmacol. Toxicol., 47 (2007) 143.

[93] R.E. Pacifici, K.J. Davies, Gerontology, 37 (1991) 166.

[94] B. Paizs, S. Suhai, Mass Spectrom. Rev., 24 (2005) 508.

[95] W. Palinski, M.E. Rosenfeld, S. Yla-Herttuala, G.C. Gurtner, S.S. Socher, S.W. Butler, S. Parthasarathy, T.E. Carew, D. Steinberg, J.L. Witztum, Proc. Natl. Acad. Sci. U. S. A., 86 (1989) 1372.

[96] J.W. Palmer, B. Tandler, C.L. Hoppel, J. Biol. Chem., 252 (1977) 8731.

[97] W. Paul, Angew. Chem., 102 (1990) 780.

[98] D.N. Perkins, D.J. Pappin, D.M. Creasy, J.S. Cottrell, Electrophoresis, 20 (1999) 3551.

[99] A. Pompella, A. Visvikis, A. Paolicchi, V. De Tata, A.F. Casini, Biochem. Pharmacol., 66 (2003) 1499.

[100] A. Rasola, P. Bernardi, Apoptosis, 12 (2007) 815.

[101] N. Rauniyar, L. Prokai, Proteomics, 9 (2009) 5188.

[102] N. Rauniyar, S.M. Stevens, Jr., L. Prokai, Anal. Bioanal. Chem., 389 (2007) 1421.

[103] N. Rauniyar, S.M. Stevens, K. Prokai-Tatrai, L. Prokai, Anal. Chem., 81 (2009) 782.

[104] T. Reinheckel, S. Korn, S. Mohring, W. Augustin, W. Halangk, L. Schild, Arch. Biochem. Biophys., 376 (2000) 59.

[105] J.R. Requena, M.X. Fu, M.U. Ahmed, A.J. Jenkins, T.J. Lyons, J.W. Baynes, S.R. Thorpe, Biochem. J., 322 (Pt 1) (1997) 317.

[106] M.R. Roe, H. Xie, S. Bandhakavi, T.J. Griffin, Anal. Chem., 79 (2007) 3747.

[107] P.L. Ross, Y.N. Huang, J.N. Marchese, B. Williamson, K. Parker, S. Hattan, N. Khainovski, S. Pillai, S. Dey, S. Daniels, S. Purkayastha, P. Juhasz, S. Martin, M. Bartlet-Jones, F. He, A. Jacobson, D.J. Pappin, Mol. Cell Proteomics, 3 (2004) 1154.

[108] L.M. Sayre, D. Lin, Q. Yuan, X. Zhu, X. Tang, Drug Metab. Rev., 38 (2006) 651.

[109] L.M. Sayre, M.A. Smith, G. Perry, Curr. Med. Chem., 8 (2001) 721.

[110] C. Schneider, K.A. Tallman, N.A. Porter, A.R. Brash, J. Biol. Chem., 276 (2001) 20831.

[111] J.C. Schwartz, M.W. Senko, J.E. Syka, J. Am. Soc. Mass Spectrom., 13 (2002) 659.

[112] B.A. Soreghan, F. Yang, S.N. Thomas, J. Hsu, A.J. Yang, Pharm. Res., 20 (2003) 1713.

[113] C.M. Spickett, A.R. Pitt, N. Morrice, W. Kolch, Biochim. Biophys. Acta, 1764 (2006) 1823.

[114] R. Srinivasan, M.J. Chandrasekar, M.J. Nanjan, B. Suresh, J. Ethnopharmacol., 113 (2007) 284.

[115] E.R. Stadtman, Ann. N. Y. Acad. Sci., 928 (2001) 22.

[116] W.E. Stephens, Phys. Rev., 69 (1946) 691.

[117] W.E. Stephens, Bull. Am. Phys. Soc., 21 (1946) 22.

[118] S.M. Stevens, Jr., N. Rauniyar, L. Prokai, J. Mass Spectrom., 42 (2007) 1599.

[119] J. St-Pierre, J.A. Buckingham, S.J. Roebuck, M.D. Brand, J. Biol. Chem., 277 (2002) 44784.

[120] N. Tanaka, S. Tajima, A. Ishibashi, K. Uchida, T. Shigematsu, Arch. Dermatol. Res., 293 (2001) 363.

[121] A. Temple, T.Y. Yen, S. Gronert, J. Am. Soc. Mass Spectrom., 17 (2006) 1172.

[122] D. Toroser, W.C. Orr, R.S. Sohal, Biochem. Biophys. Res. Commun., 363 (2007) 418.

[123] N. Traverso, S. Menini, L. Cosso, P. Odetti, E. Albano, M.A. Pronzato, U.M. Marinari, Diabetologia, 41 (1998) 265.

[124] Y. Tsujimoto, S. Shimizu, Apoptosis, 12 (2007) 835.

[125] K. Uchida, Free Radic. Biol. Med., 28 (2000) 1685.

[126] K. Uchida, M. Kanematsu, Y. Morimitsu, T. Osawa, N. Noguchi, E. Niki, J. Biol. Chem., 273 (1998) 16058.

[127] K. Uchida, M. Kanematsu, K. Sakai, T. Matsuda, N. Hattori, Y. Mizuno, D. Suzuki, T. Miyata, N. Noguchi, E. Niki, T. Osawa, Proc. Natl. Acad. Sci. U. S. A., 95 (1998) 4882.

[128] D. Voet, J.G. Voet, Biochemistry, John Wiley & Sons, Inc., Hoboken, 2004.

[129] M.P. Washburn, D. Wolters, J.R. Yates, 3rd, Nat. Biotechnol., 19 (2001) 242.

[130] J.D. West, L.J. Marnett, Chem. Res. Toxicol., 19 (2006) 173.

[131] W.C. Wiley, I.H. McLaren, Rev. Sci. Instrum., 26 (1955) 1150.

[132] H.L. Wong, D.C. Liebler, Chem. Res. Toxicol., 21 (2008) 796.

[133] J.C. Yang, G.A. Cortopassi, Free Radic. Biol. Med., 24 (1998) 624.

[134] J.R. Yates, C.I. Ruse, A. Nakorchevsky, Annu. Rev. Biomed. Eng., 11 (2009) 49.

[135] A.K. Yocum, T. Oe, A.L. Yergey, I.A. Blair, J. Mass Spectrom., 40 (2005) 754.

[136] B.S. Yoo, F.E. Regnier, Electrophoresis, 25 (2004) 1334.

[137] X. Zhu, V.E. Anderson, L.M. Sayre, Rapid Commun. Mass Spectrom., 23 (2009) 2113.

[138] X. Zhu, L.M. Sayre, Chem. Res. Toxicol., 20 (2007) 165.

[139] R.A. Zubarev, Curr. Opin. Biotechnol., 15 (2004) 12.

Appendix A

A New Role for an Old Probe: Affinity Labeling of Oxylipid Protein Conjugates by N'-Aminooxymethylcarbonylhydrazino D-biotin

Juan Chavez, Jianyong Wu, Bingnan Han, Woon-Gye Chung and Claudia S. Maier*

Department of Chemistry, Oregon State University, Corvallis, OR 97331

Analytical Chemistry

American Chemical Society

1155 Sixteenth Street N.W., Washington, DC, 20036

J. Chavez, J. Wu, B. Han, W.G. Chung, C.S. Maier, Anal Chem, 78 (2006) 6847

Abstract

Free radicals, electrophiles and endogenous reactive intermediates are generated during normal physiological processes, and are capable of modifying DNA, lipids and proteins. However, elevated levels of oxidative modifications of proteins by reactive species are implicated in the etiology and pathology of oxidative stress-mediated diseases, neurodegeneration and aging. A mass spectrometry-based approach is reported that aids to the identification and characterization of carbonyl modified proteins. The method uses N'-aminooxymethylcarbonylhydrazino-D-biotin, a biotinylated hydroxylamine derivative, that forms an oxime derivative with the aldehyde/keto group found in oxidatively modified proteins. In this paper, the method is demonstrated for one class of carbonyl-modified proteins, namely oxylipid peptide and protein conjugates formed by Michael addition-type conjugation reactions of α,β-unsaturated aldehydic lipid peroxidation products with nucleophilic peptide side chains. This new application of an “old” probe, which has been used for the detection of abasic sites in DNA strands, introduces a biotin moiety into the oxylipid peptide conjugate. The biotin-modified oxylipid peptide conjugates is then amenable to enrichment using avidin affinity capture. The described method represents an attractive alternative to hydrazine-based derivatization methods for oxidized peptides and proteins because the reduction step necessary for the transformation of the hydrazone bond to the chemically more stable hydrazine

bond can be omitted. Tandem mass spectrometry of the labeled oxylipid peptide conjugates indicates that the biotin moiety is at least partially retained on the fragment ion during the collisionally induced dissociation experiments, a prerequisite for the use of automated database searching of uninterpreted tandem mass spectra. The reported approach is outlined for the detection, identification and characterization of oxylipid peptide conjugates but the labeling chemistry may also be applicable to other carbonyl-modified proteins.

Introduction

Free-radical injury is central to the etiology and pathology of inflammatory diseases and age-related disorders. The burden of reactive oxygen species (ROS) is counteracted by an intricate antioxidant system, which includes antioxidant enzymes, e.g. SOD, catalase and glutathione peroxidase, and non-enzymatic, low molecular weight antioxidants, perhaps most importantly glutathione and ascorbic acid. However, the extent of the imbalance of ROS production and antioxidant defenses determines the degree of oxidative stress [1]. Oxidative-stress mediated modifications occur on DNA, proteins, and lipids [1-5]. Oxidative modification of proteins proceeds according to variety of mechanisms, [2, 5-7] some of which lead to backbone peptide bond cleavage or to side chain modifications. The latter includes the introduction of carbonyl functionalities, i.e. aldehyde or keto groups, by direct oxidation of most residues or via conjugation reactions of reactive

secondary oxidation products that arise, for example, from lipid peroxidation processes [7].

Polyunsaturated fatty acids of membrane lipids are highly susceptible to peroxidation by oxygen radicals. Exposure of linoleic acid, the major ω-6 polyunsaturated fatty acid in mammalian tissues, to reactive oxygen species leads to the formation of lipid peroxidation (LPO) products. In Esterbauer's studies on the production of cytotoxic compounds in LPO processes, 4-hydroxy-2-nonenal (HNE) was described as a major LPO product [8, 9]. To date, HNE is the best studied LPO product with cytotoxic potential. LPO products that contain α,β-unsaturated aldehyde/keto functionalities are highly reactive electrophiles that react readily with nucleophilic sites in proteins, such as cysteine sulfhydryls, histidine imidazole moieties and with ε-amino groups of lysine residues, forming Michael addition-type conjugates and Schiff's base-derived products [4,10]. Oxylipid-protein conjugates have been implicated in the pathogenesis of inflammatory, [11] neurodegenerative and age-related diseases [12, 13]. Consequently, there is a high interest in analytical methodology that are capable of identifying and characterizing oxidative protein modifications.

Traditionally, the total amount of protein-bound carbonyls was determined colorimetrically [14]. Many protocols for detecting oxidative protein modifcations are based on 2,4-dinitrophenylhydrazine (DNPH) derivatization followed by UV spectroscopy [15] or immunochemical detection using an anti-dinitrophenyl

primary antibody [16,17]. Although these methods are capable of detecting oxidatively modified proteins with high sensitivity, they fail to provide information such as the identity of the modified proteins, the chemical nature and site of the modification. Mass spectrometry-based approaches are, at least in part, capable of overcoming some of these latter limitations. For instance, matrix-assisted laser desorption/ionization time-of-flight (MALDI-ToF) mass spectrometry was used for identifying HNE-modified lysine residues in tryptic digests of in vitro modified glucose-6-phosphate dehydrogenase [18]. Also, the characterization of HNE-modified peptides directly from unfractionated digests of model proteins after using DNPH as MALDI matrix has been reported [19]. In 1996, Bolgar and Gaskell reported the detection of HNE-modified His-residues of oxidized low density lipoprotein by electrospray ionization (ESI) tandem mass spectrometry (MS/MS) [20]. Since then, numerous in vitro studies have been reported using ESI-MS/MS for identifying the site of modifications by LPO products in proteins. For example, ESI-MS/MS was employed for detecting HNE modifications in hemoglobin, [21] subunit VIII of bovine heart cytochrome c oxidase, [22] glyceraldehyde-3-phosphate dehydrogenase, [23] the heat shock proteins hsp72 and hsp90, [24, 25] and protein disulfide isomerase [26]. Labeling of carbonyl groups formed by metal-catalyzed oxidation of amino acid side chains by biotin hydrazine for both gel-based and mass spectrometric detection have been reported recently [27-29].

As a new alternative to hydrazine-based reagents for MS-based characterization strategies of oxidative stress-induced protein modifications, this study reports the use of N'-aminooxymethylcarbonylhydrazino D-biotin, a biotinylated hydroxylamine derivative which reacts with aldehyde/keto groups found in oxidatively modified proteins under formation of an oxime derivative which is amenable to tandem mass spectral analysis [30]. This aldehyde-reactive probe (ARP) is commonly used for the detection of DNA modifications that resulted in the formation of an aldehyde group from the oxidative damage on the abasic (AP) sites of DNA strands [31, 32]. The hydroxylamine moiety of ARP forms a stable C=N bond with the aldehyde functionality of the Michael-type oxylipid conjugate (Scheme 1). Thus, the reduction step which is necessary for the stabilization of the hydrazone bond formed during the derivatization of the protein carbonyl with hydrazide-based reagents becomes obsolete. The derivatization of oxidized proteins by ARP enables the use of avidin affinity selection protocols for enrichment of ARP-labeled peptides with oxidative modification. To demonstrate the applicability of the ARP approach for the characterization of oxidatively modified proteins we focus in this paper on one group of carbonylated proteins, namely Michael addition-type oxylipid conjugates.

Specifically, we describe the derivatization of HNE-modified peptide conjugates by ARP, and the selective affinity enrichment and MS-based detection of ARP-labeled peptides from tryptic digests of HNE-conjugated thioredoxin (TRX).

ARP-labeled oxylipid peptide conjugates were studied by tandem mass spectrometry. Successful database searching of uninterpreted mass spectra of ARP-labeled HNE-conjugated peptides was also performed demonstrating the potential of ARP as a new adjunct to the analysis of protein carbonyls.

Exeperimental section

Materials

Thioredoxin and sequencing grade-modified trypsin were from Promega Corporation (Madison, WI). HNE (10 mg/mL in ethanol) was obtained from Cayman Chemical (Ann Arbor, MI). Aldehyde Reactive Probe (ARP, N-aminooxymethylcarbonylhydrazino D-biotin) was purchased from Dojindo Laboratories (Kumamoto, Japan). UltraLink immobilized monomeric avidin was obtained from Pierce (Rockford, IL).

Methods.

Synthesis, modification with HNE and labeling with ARP of the peptide Ac-SVVDLTCR-amide.

The peptide Ac-Ser-Val-Val-Asp-Leu-Thr-Cys-Arg-amide(Ac-SVVDLTCR-amide) was synthesized using a PS3 automated solid phase peptide synthesizer (Protein Technologies, Inc., Tucson, AZ). 9-Fluoroenylmethoxy-carbonyl (Fmoc) derivatives of the amino acids were from SynPep Co. (Dublin, CA). The first

residue, i.e. the C-terminal residue of the final peptide product bound to the Fmoc-Arg(pbf)-Rink Amide-MBHA resin was purchased from AnaSpec Inc. (San Jose, CA).

One mg of the synthetic peptide in 1mL 10 mM phosphate buffer, pH 7.4 was reacted with 13 µL HNE (10 mg/mL) at room temperature for two hours. The HNE-adducted peptide was purified by HPLC on a C_{18} column (Vydac, 4.6 x 250 mm, 5 µm), lyophilized, and its mass confirmed by MALDI-MS. HNE-adducted peptide (100 g) was reacted with 200 µL 10 mM ARP in 10 mM sodium phosphate buffer, pH 7.4, for one hour at room temperature. The ARP-labeled HNE-peptide conjugate was isolated by HPLC as described above and lyophilized.

HNE modification and ARP-Labeling of *E. coli* Thioredoxin.

Adduction of thioredoxin (TRX) with HNE was accomplished by dissolving 1 mg (82 nMole) TRX in 1 mL 10 mM sodium phosphate, pH 7.4, to which a 10-fold molar excess (13 µL) of HNE (10 mg/ml) was added. The reaction mixture was then incubated at 37 ^{o}C for 2 hr. The TRX-HNE adduct was purified from unreacted HNE by reverse-phase HPLC using a C_4 column (Vydac, 10 x 250 mm, 5 µm). The isolated product was lyophilized and analyzed by MALDI-MS. Affinity labeling of TRX-HNE was carried out by the addition 250 µL of 10 mM ARP to the TRX-HNE reconstituted in 750 µL 10 mM sodium phosphate, pH 7.4.

The reaction mixture was incubated at 37 ^{o}C for 3.5 hr. Unreacted ARP was removed using the same HPLC method as described above. After lyophilization, ARP-labeled HNE-modified TRX adduct was digested using trypsin at a ratio of 1:50 at 37 ^{o}C for 18 hr.

Affinity chromatography.

Ultralink monomeric avidin (100 µl) was packed into the tip of a glass pasteur pipette plugged with glass wool. The column was equilibrated to room temperature and washed with five column volumes of PBS buffer. The irreversible binding sites were blocked by washing the column with three column volumes of 2 mM D-biotin. Excess biotin was removed from the reversible binding sites by washing the column with five column volumes of 0.1 M glycine, pH 2.8. The column was re-equilibrated by rinsing with five columns of PBS buffer. One hundred microliters of TRX-HNE-ARP tryptic digest was loaded onto the column and incubated for one hour. Non-labeled peptides were eluted from the column by rinsing with 10 column volumes of PBS buffer and collected in five 200 µL fractions. The HNE-ARP labeled peptides were eluted using 10 column volumes of 0.3 % formic acid and were also collected in five 200 µL fractions. The fractions were analyzed by MALDI-MS/MS and ESI-MS/MS.

Oxidation of a Trp-containing peptide and ARP treatment

The model peptide QAKWRLQTL (from AnaSpec Inc., San Jose, CA) was treated with H_2O_2 overnight and reaction was stopped by adding catalase. ARP (20 molar excess, 10 mM sodium phosphate buffer, pH 7.4) was added to the oxidized peptide. The reaction mixture was incubated at 37 oC for 1 hr.

Identification of carbonylated proteins in mitochondria.

Rat cardiac mitochondria were isolated by differential centrifugation and stored at -80oC [33]. The mitochondria were ruptured by several freeze thaw cycles. Protein concentration was determined by the Pierce-Coomassie protein assay. Membrane and soluble proteins were reacted with 5mM ARP for 2 hr at 37^{o}C. Excess ARP was removed by buffer exchange using Amicon Microcon centrifugal filters (10kDa MWCO). Proteins were digested with a 1:50 ratio of trypsin at 37 ^{o}C overnight. The resulting tryptic peptides were filtered through Amicon Microcon centrifugal filters (10kDa MWCO) to remove trypsin and membrane fragments. The peptide solutions were passed through a monomeric avidin cartridge (Applied Biosystems) following the manufacturer's instructions to enrich ARP-labeled peptides. The fraction containing the ARP-labeled peptides was analyzed by nano-LC MALDI-TOF/TOF mass spectrometry. The MS/MS spectra were interpreted both manually and in an automated fashion with Mascot software.

Mass Spectrometry.

MALDI-MS/MS analysis was performed on an ABI 4700 Proteomics Analyzer with TOF/TOF optics equipped with a 200-Hz frequency-tripled Nd:YAG laser operating at a wavelength of 355 nm (Applied Biosystems, Inc., Framingham, MA). Protein mass spectra were acquired in the linear mode, whereas all peptide mass spectra were obtained in the reflector mode. For both operational modes the accelerating voltage was set to 20 kV. For MS/MS experiments, the collision energy, which is defined by the potential difference between the source acceleration voltage (8 kV) and the floating collision cell (7 kV), was set at 1 kV. The precursor ion was selected by operating the timed gate window with 3-10 Da. Gas pressure (air) in the collision cell was set to 6 x 10^{-7} Torr. Fragment ions were accelerated by 15 kV into the reflector. Data were acquired in a mass range of m/z 700-4000 with external calibration using AB's 4700 calibration mixture consisting of the following peptides (in brackets the monoisotopic mass of the singly protonated ion is given in Da): des-Arg^1-bradykinin (904.4681), angiotensin I (1296.6853), Glu^1-fibrinopeptide B (1570.6774) and ACTH 18-39 (2465.1989).

ESI-MS/MS was performed using a quadrupole orthogonal time-of-flight mass spectrometer (Q-ToF Ultima Global, Micromass/Waters, Manchester, UK) coupled to a nanoAcquity Ultra Performance LC (Waters, Milford, MA). Peptide mixtures were trapped and washed on a nanoAcquity column (Symmetry C_{18}, 5 μm, 180 μm x 20 mm) for 3 min using 2 % acetonitrile containing 0.1 % formic

acid at 4 µL/min. Peptide fractionation was accomplished using an in-house packed 12 cm x 75 µm Jupiter C_5 or C_{18} (5 µm; Phenomenex Inc., Torrance, CA) picofrit column (New Objectives, Woburn, MA). Peptides were eluted using a binary gradient system consisting of solvent A, 0.1 % formic acid and solvent B, acetonitrile containing 0.1 % formic acid.

The electrospray ion source was operated in the positive ion mode with a spray voltage of 3.5 kV. The data-dependent MS/MS mode was used with a 0.6 s survey scan and 2.4 s MS/MS scans on the three most abundant ion signals in the MS survey scan, with previously selected m/z values being excluded for 60 s. The collision energy for MS/MS (25 to 65 eV) was dynamically selected based on the charge state of the ion selected by the quadrupole analyzer (q1). Mass spectra were calibrated using fragment ions of Glu^1-fibrinopeptide B (MH^+ 1570.6774 Da, monoisotopic mass). In addition, to compensate for temperature drifts, lock mass correction was used every 30 s for 1 scan using the doubly charged ion of Glu^1-fibrinopepide B ($[M+2H]^{2+}$ 785,8426 Da, monoisotopic mass).

Mascot software (Matrix Science, London, UK) was used to aid in the interpretation of tandem mass spectra. Searches were performed using the SwissProt database with Met oxidation (147.04 Da, monoisotopic mass), ARP-HNE labeled Cys, His, and Lys (monoisotopic masses 572.2 Da, 606.2 Da, and 597.2 Da, respectively) as variable peptide modifications. Trypsin/P was selected as the digesting enzyme allowing for the possibility of one missed

cleavage site. Mass tolerances were set to ± 100 ppm for the precursor ion and ± 0.1 Da for the fragment ions. The principal fragment ions were labeled according to the nomenclature of Biemann [34].

Results and discussion

Labeling of a HNE-modified Cys-containing peptide with N'-Aminooxymethyl-carbonylhydrazino-D-biotin and tandem mass spectrometric characterization.

To evaluate the potential of N'-aminooxymethylcarbonylhydrazino D-biotin as a biotin-labeled aldehyde reactive reagent, we used as a model system the synthetic peptide Ac-SVVDLTCR-amide. Cysteine sulfhydryl side chains are considered as likely targets for the electrophile HNE due to their nucleophilic properties.[10] After reaction with HNE in phosphate buffer (pH 7.4) for 2 hours, the HNE-conjugated peptide was purified by reverse-phase HPLC and lyophilized. Mass analysis of the HNE-peptide-conjugate indicated a mass shift by 156 Da compared to the unmodified peptide confirming that the Michael-type conjugate was obtained. The oxylipid peptide conjugate was subsequently reacted with ARP at room temperature for 1 hr. The reaction product was isolated chromatographically. Successful derivatization of the aldehyde functionality by ARP was confirmed by tandem mass spectrometry.

Tandem mass spectrometric analysis of the ARP-labeled HNE-Cys containing model peptide, Ac-SVVDLTCR-amide (Pep-HNE-ARP) was achieved by using

high energy collision dissociation on a MALDI tandem time-of-flight mass spectrometer with TOF/TOF optics (Figure 1). The tandem mass spectrum exhibited an almost complete b_n-ion series (b_2 to b_6). The first C-terminal ion, the y_1 ion, was seen at m/z 174.1. More importantly, we observed the C-terminal fragment ions, y_2* to y_5* which retained the ARP-HNE moiety. This ion series was accompanied by series of ions that indicate neutral loss of the ARP-HNE moiety from the respective y_n* ions (i.e. m/z = 469.3 Th) and these ions are annotated y_4, y_3 and y_2 in Figure 1. The presence of an Asp-residue in this peptide causes the relative predominance of the y_4* fragment ion. The enhanced cleavage probability of the peptide amide bond C-terminal to the Asp-residue in this peptide is particularly pronounced due to the presence of the C-terminal Arg-residue sequestering the proton [16, 35, 36]. Collectively, the observed peptide fragment ions confirm that the cysteine residue is modified by a HNE-ARP moiety. Neutral loss of the HNE-ARP moiety from the precursor ion MH^+ 1402.8 is also evident resulting in the ion at m/z 933.4. The fragment ions F1 and F2 indicate side-chain fragmentation of the ARP-HNE moiety to some degree. Noteworthy, the observation of fragment ions that retained the HNE-ARP moiety are a prerequisite for peptide identification based on the use of uninterpreted tandem mass spectra acquired under high energy collision experimental conditions in conjugation with automated database searching.

Specificity of ARP towards carbonylated protein modifications.

The oxidation of tryptophan leads to the formation of N-formylkynurenine by dioxygenation and ring breakage. We tested if the –NH-CHO moiety in the N-formylkynurenine residue shows reactivity towards ARP. The model peptide QAKWRLQTL (MH^+ 1143.7; Figure 1A in the supplementary material) was treated with H_2O_2 overnight and reaction was stopped by adding catalase. The mass spectrum of the reaction products showed the expected peptide ions that indicated oxidation of the Trp residue at m/z 1159.7 (+16 Th), m/z 1175.7 (+32 Th) and m/z 1147.7 (+4 Th) (for structures corresponding to those mass shifts see Figure 1A in the supplementary material). ARP (20 molar excess) was added to the oxidized peptide mixture. Mass spectral analysis of the reaction mixture after treatment with ARP indicated that the –NH-CHO moiety in N-formylkynurenine is unreactive towards ARP (Figure 1C in the supporting information) due to its tautomeric stabilization (–NH-CHO and –N=CH(OH)). Similarly, no ARP reaction product was observed for the decarboxylation product of N-formylkynurenine (structure 3 in Figure 1A in the supporting information). These results demonstrate that ARP has specificity in its reactivity towards different forms of protein carbonyl groups.

ARP labeling and mass spectrometry of a Michael-type oxylipid protein conjugate.

In proteins, products of lipid peroxidation, such as the α,β-unsaturated aldehyde HNE, are able to modify nucleophilic amino acid residues. In particular, Cys and His residues form readily Michael-type conjugates [10]. In addition, Schiff's base formation with the ε-amino group of Lys is also observed and this route leads potentially to formation of 2-pentylpyrrole [37]. For studying the applicability of ARP for the efficient labeling of Michael-type oxylipid moieties in proteins we used *E.coli* thioredoxin (TRX) as a simple model protein. TRX is composed of 108 amino acid residues, of which 10 are Lys residues. TRX possesses only one His residue located at position 6. In the oxidized protein, the two cysteine residues, Cys-32 and Cys-35, are disulfide-linked and, thus, not available for HNE modification. Using oxidized TRX in our ARP labeling studies enabled us to focus on the derivatization and characterization of oxylipid-His conjugates and, accordingly, to complement our Cys-containing peptide model studies.

Adducts of oxidized thioredoxin (TRX) to HNE were obtained by dissolving 1 mg (82 nMole) thioredoxin in 1 mL 10 mM sodium phosphate buffer (pH 7.4) to which a 10-fold molar excess of HNE was added. The reaction mixture was incubated for 2 hr at 37 ^{o}C. The stoichiometry of HNE conjugation was checked by MALDI-MS (Figure 2A). The mass spectral peak at m/z 11,674.9 represents the unmodified TRX and the ion peak at m/z 11,832.8 corresponds to the addition

of one HNE molecule (m/z 157.9 Th). The mass spectral analysis also indicated that, although a 10-fold molar excess of HNE to TRX was used in the modification reaction, a large amount of the TRX remained unmodified. After confirming the presence of the HNE adduct by MALDI-MS analysis the HNE-conjugated thioredoxin (TRX-HNE) was reacted with ARP. In the mass spectrum displayed in Figure 2B it can be seen that the TRX-HNE peak at m/z 11,832.8 is replaced by a peak at m/z 12,145.3 resulting from the ARP-labeled oxylipid protein conjugate, TRX-HNE-ARP.

A potential problem of approaches that are designed to label the aldehyde functionality of HNE-peptide or -protein conjugates is the fact that the HNE conjugate can undergo an intramolecular cyclization reaction in which the hydroxyl group at position C-4 reacts with C-1 of the aldehyde group to form a hemiacetal product [9]. Because the hemiacetal no longer contains an aldehyde-functional group, it is unreactive toward aldehyde-specific reagents and, therefore, would not be detected using ARP. However, the cyclization equilibrium is controlled by the pH value. The result from the MALDI-MS analysis shows that nearly all of the TRX-HNE adduct has been converted to TRX-HNE-ARP which suggests that the condensation reaction of the aldehyde functionality with ARP is very efficient under the conditions used, namely 10 mM sodium phosphate, pH 7.4.

Tandem mass spectrometric characterization of the ARP-labeled HNE-modified tryptic peptide T2.

After confirming that the oxylipid-protein conjugate was successfully labeled by ARP, the unreacted ARP was removed by HPLC. This was followed by digestion of the sample with trypsin and avidin affinity chromatography to enrich the ARP-labeled peptides of TRX. The enrichment was performed on the tryptic peptide mixture rather than the protein so that only the ARP-labeled peptides would be enriched. The ARP-labeled peptides were isolated from the crude tryptic digest using an immobilized monomeric avidin column. Avidin is naturally a tetrameric protein with a very high binding affinity for biotin necessitating very harsh elution conditions for retrieving biotin-labeled sample. Therefore, monomeric avidin was used which binds to biotinylated compounds reversibly and allows for milder elution conditions. The non-labeled peptides were eluted by washing with PBS buffer. Subsequently, the ARP-labeled peptides were eluted using 0.3 % formic acid instead of 2 mM biotin in PBS (as described in the manufacturer's instruction) in order to facilitate good compatibility with mass spectrometric analyses. Figure 3 shows the MALDI-MS spectra of the tryptic digest of TRX-HNE-ARP (Figure 3A) as well as the affinity-enriched peptide fraction (Figure 3B). Selective enrichment of the peptide with MH^+ 2201.2 is evident implying that this is an ARP-labeled peptide (Figure 3B). MALDI-MS/MS was performed on the peptide ion at m/z 2201.2 to confirm ARP

labeling and identify the site of modification (Figure 4).

High energy collision induced dissociation tandem mass spectrometry on the MALDI ToF/ToF instrument yielded a fragment ion spectrum which identified the ARP-labeled peptide as the tryptic peptide T2, encompassing the residue 4 to 18 (Figure 4). This peptide contains only one nucleophilic site, namely His-6. Indeed, the m/z difference of 606.3 Th between the y_{12} and y_{13} fragment ions confirmed the presence of a His-HNE-ARP residue in position 6 (Figure 4). The b_n-ions (b_3 to b_7, b_{10}, b_{12} and b_{13}) were consistently shifted by 469.3 Th to higher m/z values compared to the m/z-values that would be expected for an unmodified peptide with corresponding sequence. The fragment ion at m/z 1731.8 indicates the neutral loss of the ARP-HNE moiety from the precursor ion MH^+ 2201.2. Worth noting is the ARP-HNE-modified His immonium ion prominently visible at m/z 579.4. The intensive immonium ion formation from HNE-modified His residue has been also described previously by Bolgar and Gaskell [20] and Fenaille et al.[19].

We also studied the low energy collision induced dissociation behavior of the ARP-labeled HNE-modified T2 peptide using a quadrupole time-of flight instrument equipped with an electrospray ionization source. The triply-charged molecular ion of the ARP-labeled HNE-modified peptide T2, i.e. the $[M+3H]^{3+}$ ion at m/z 734.4, was selected as precursor ion (Figure 5). Almost complete y_n and b_n fragment ion series were observed. The m/z difference between the b_2 ion (at

m/z 227) and the b_3 ion (at m/z 833) locates the HNE-ARP moiety to the His residue. Accordingly, the b_4 to b_{12} ions were consistently shifted by 469 Th to higher m/z values. The modification of the His residue by an ARP-HNE moiety is also confirmed by the observation of the doubly charged y_{13} ion at m/z 988 and an intense His immonium ion at m/z 579.4. Ions that indicate extensive loss and/or side chain fragmentation of the ARP-HNE moiety were not observed in the tandem mass spectra acquired under the low energy CID conditions which are common to qTOF-type instruments.

In order to test the usefulness of the ARP labeling procedure for proteomic-type applications, we searched the uninterpreted tandem mass spectra from both the TOF/TOF and the q-TOF instrument against the SwissProt database using the Mascot software. The HNE-ARP moiety was implemented as variable modifications on Cys, His and Lys residues. The tandem mass spectrum of the ARP-labeled T2 peptide acquired on the MALDI-MS/MS instrument obtained an ion score of 68. Data-dependant analysis on the qToF instrument yielded tandem mass spectra for the doubly as well as the triply charged ion of the ARP-labeled T2 peptide; these spectra obtained excellent scores of 78 (data not shown) and 110 (Figure 5), respectively.

Identification of carbonylated proteins in mitochondria.

The ARP labeling approach is currently used in our laboratory for the detection

and identification of oxidatively modified proteins in mitochondria isolated from rat hearts. We repeatedly found several proteins modified by lipid peroxidation products. For example, the long chain-specific acyl-CoA dehydrogenase, (ACADL_RAT) was identified as an *in vivo* target of oxidative modification by lipid peroxidation products. The tandem mass spectrum of the ARP-labeled HNE-conjugated peptide (MH^+ 2415,09) is depicted in Figure 6. The observed y_n fragment ions (y_1, y_3-y_6, y_9, y_{11}, and y_{12}) identify the peptide as the partial sequence 166-185 of ACADL_RAT. The fragment ion at m/z 2099.3, annotated as F_2, is generated by side chain cleavage at the oxime bond (-O-N=CH-) whereby the oxylipid moiety is retained at the peptide. In agreement with our previous observations (see Figures 1 and 4) the fragment ion at m/z 1946.2 arises from neutral loss of the ARP-HNE moiety (Δm = 468.9 Th). Because the identified peptide encompasses only a single nucleophilic residue, i.e.Cys-166, the tandem mass spectral data support the notion that Cys-166 is an *in vivo* target site for HNE conjugation. Noteworthy, the same peptide was also found to be modified by 4-oxo-2-nonenal (data not shown). We will communicate these findings in combination with other biochemical studies in greater detail shortly.

Conclusion

In the above described study, N'-aminooxymethylcarbonylhydrazino D-biotin (also known as ARP) is introduced as a new reagent for the efficient labeling of

carbonyl groups in proteins and peptides. ARP is a hydroxyl amine-functionalized biotin-containing probe which efficiently reacts with aldehyde/keto groups, thereby forming an oxime-type (C=N) bond which is sufficiently stable in tandem mass spectrometric fragmentation studies to allow potentially the localization of the site of modification. The labeling procedure is a one-step reaction and proceeds readily under near physiological conditions in phosphate buffer at pH 7.4 at ambient temperature. A potentially important new application for this "old" probe, which was hitherto used for the detection of abasic sites in DNA, is the exciting field of proteins as targets of oxidative modifications, for example, by lipid peroxidation products. The described methodology allows the affinity-enrichment of biotinylated oxylipid peptide conjugates and enables their identification and characterization by mass spectrometry. However, it should be noted that oxidative modifications to proteins occur via many different pathways.[2, 4] The chemical diversity of oxidative protein modifications makes it at best very difficult to use automated searching of uninterpreted tandem mass spectra as the sole mean of mass spectral data interpretation.

The proof-of-concept study described in this paper introduces ARP as a potentially useful and alternative probe to hydrazine-based reagents for the detection and characterization of carbonylated proteins. Studies are currently ongoing that use the described ARP labeling approach for the detection and identification of oxidatively modified proteins in cardiac mitochondria.

Acknowledgements

Many thanks are due to Duane T. Mooney for his assistance during the early periods of this project. This work was supported by grants from the NIH/NIA (AG025372) and Oregon's Agricultural Research Foundation. The mass spectrometry core facility of the Environmental Health Sciences Center at Oregon State University is supported in part by a grant from NIEHS (ES00210).

References

[1] T. Finkel, N.J. Holbrook, Nature, 408 (2000) 239.

[2] E.R. Stadtman, Ann. N. Y. Acad. Sci., 928 (2001) 22.

[3] J.D. West, L.J. Marnett, Chem. Res. Toxicol., 19 (2006) 173.

[4] L.J. Marnett, J.N. Riggins, J.D. West, J. Clin. Invest., 111 (2003) 583.

[5] R.L. Levine, E.R. Stadtman, Exp. Gerontol., 36 (2001) 1495.

[6] R.T. Dean, S. Fu, R. Stocker, M.J. Davies, Biochem. J., 324 (Pt 1) (1997) 1.

[7] R.L. Levine, Free Radic. Biol. Med., 32 (2002) 790.

[8] A. Benedetti, M. Comporti, H. Esterbauer, Biochim. Biophys. Acta, 620 (1980) 281.

[9] H. Esterbauer, R.J. Schaur, H. Zollner, Free Radic. Biol. Med., 11 (1991) 81.

[10] J.A. Doorn, D.R. Petersen, Chem. Res. Toxicol., 15 (2002) 1445.

[11] M.M. Anderson, S.L. Hazen, F.F. Hsu, J.W. Heinecke, J. Clin. Invest., 99 (1997) 424.

[12] L.M. Sayre, M.A. Smith, G. Perry, Curr. Med. Chem., 8 (2001) 721.

[13] J.K. Andersen, Nat. Med., 10 Suppl (2004) S18.

[14] H. Ohkawa, N. Ohishi, K. Yagi, Anal. Biochem., 95 (1979) 351.

[15] R.L. Levine, D. Garland, C.N. Oliver, A. Amici, I. Climent, A.G. Lenz, B.W. Ahn, S. Shaltiel, E.R. Stadtman, Methods Enzymol., 186 (1990) 464.

[16] T. Reinheckel, S. Korn, S. Mohring, W. Augustin, W. Halangk, L. Schild, Arch. Biochem. Biophys., 376 (2000) 59.

[17] M.A. Korolainen, G. Goldsteins, I. Alafuzoff, J. Koistinaho, T. Pirttila, Electrophoresis, 23 (2002) 3428.

[18] J.M. Grace, T.L. MacDonald, R.J. Roberts, M. Kinter, Free Radic. Res., 25 (1996) 23.

[19] F. Fenaille, P. Mottier, R.J. Turesky, S. Ali, P.A. Guy, J. Chromatogr. A, 921 (2001) 237.

[20] M.S. Bolgar, S.J. Gaskell, Anal. Chem., 68 (1996) 2325.

[21] B.A. Bruenner, A.D. Jones, J.B. German, Chem. Res. Toxicol., 8 (1995) 552.

[22] A. Musatov, C.A. Carroll, Y.C. Liu, G.I. Henderson, S.T. Weintraub, N.C. Robinson, Biochemistry, 41 (2002) 8212.

[23] A. Furuhata, T. Ishii, S. Kumazawa, T. Yamada, T. Nakayama, K. Uchida, J. Biol. Chem., 278 (2003) 48658.

[24] D.L. Carbone, J.A. Doorn, Z. Kiebler, B.R. Ickes, D.R. Petersen, J. Pharmacol. Exp. Ther., 315 (2005) 8.

[25] D.L. Carbone, J.A. Doorn, Z. Kiebler, B.P. Sampey, D.R. Petersen, Chem. Res. Toxicol., 17 (2004) 1459.

[26] D.L. Carbone, J.A. Doorn, Z. Kiebler, D.R. Petersen, Chem. Res. Toxicol., 18 (2005) 1324.

[27] B.S. Yoo, F.E. Regnier, Electrophoresis, 25 (2004) 1334.

[28] H. Mirzaei, F. Regnier, Anal. Chem., 77 (2005) 2386.

[29] B.A. Soreghan, F. Yang, S.N. Thomas, J. Hsu, A.J. Yang, Pharm. Res., 20 (2003) 1713.

[30] H. Ide, K. Akamatsu, Y. Kimura, K. Michiue, K. Makino, A. Asaeda, Y. Takamori, K. Kubo, Biochemistry, 32 (1993) 8276.

[31] K. Kubo, H. Ide, S.S. Wallace, Y.W. Kow, Biochemistry, 31 (1992) 3703.

[32] H. Atamna, I. Cheung, B.N. Ames, Proc. Natl. Acad. Sci. U. S. A., 97 (2000) 686.

[33] J.W. Palmer, B. Tandler, C.L. Hoppel, J. Biol. Chem., 252 (1977) 8731.

[34] K. Biemann, Biomed. Environ. Mass Spectrom., 16 (1988) 99.

[35] K.A. Herrmann, V.H. Wysocki, E.R. Vorpagel, J. Am. Soc. Mass Spectrom., 16 (2005) 1067.

[36] V.H. Wysocki, G. Tsaprailis, L.L. Smith, L.A. Breci, J. Mass Spectrom., 35 (2000) 1399.

[37] R.G. Salomon, K. Kaur, E. Podrez, H.F. Hoff, A.V. Krushinsky, L.M. Sayre, Chem. Res. Toxicol., 13 (2000) 557.

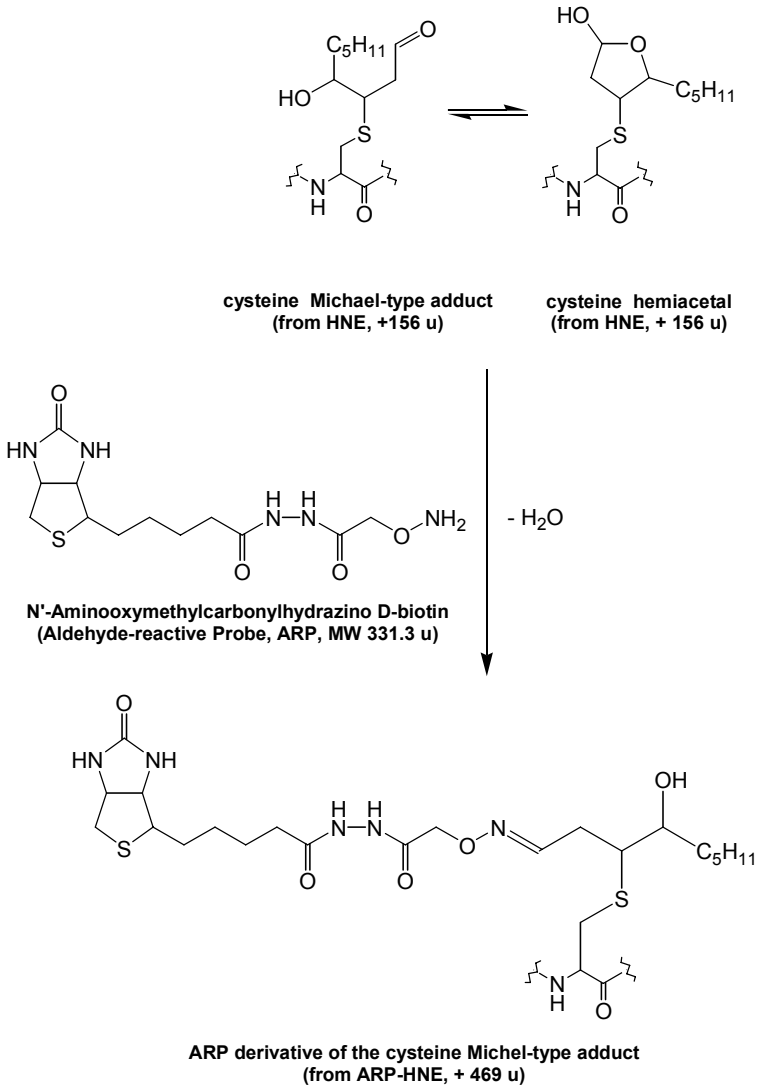

Scheme 1. Structure and reaction of N'-Aminooxymethylcarbonylhydrazineo D-biotin (Aldehyde-reactive probe, ARP) for labeling oxylipid–peptide conjugates, e.g. a HNE-modified cysteine-containing peptide.

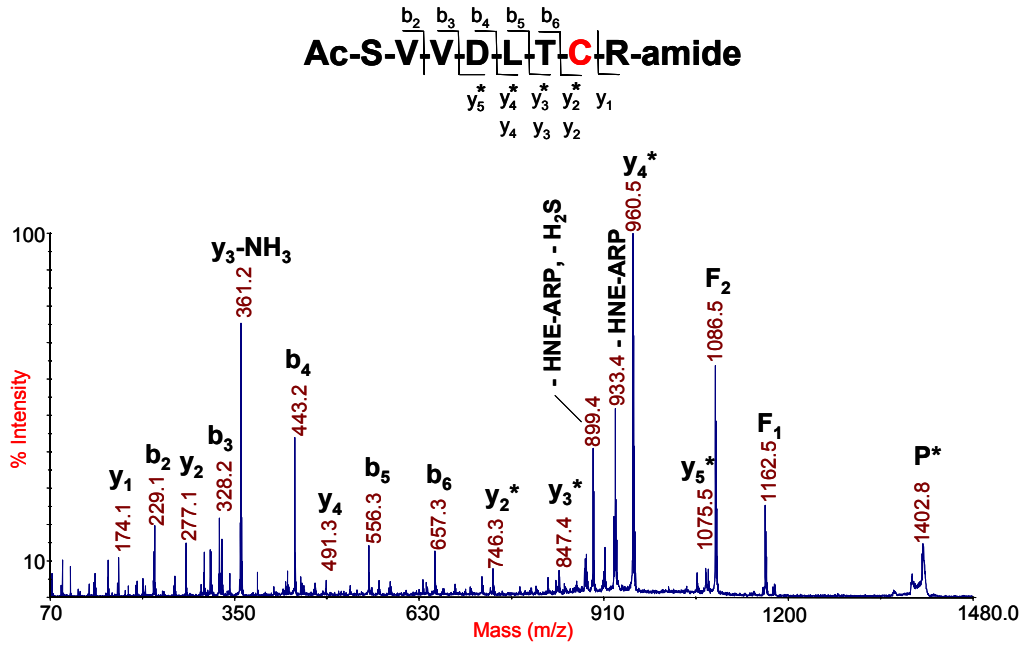

Figure 1. Tandem mass spectrum of the ARP-labeled HNE-peptide conjugate Ac-SVVDLTCR-amide. Michael-type conjugation of the model peptide was observed on the Cys-residue. Note, unequivocal localization of the ARP-HNE moiety to the Cys-residue is obtained by the y_n-fragment ions annotated with an asterisk *.

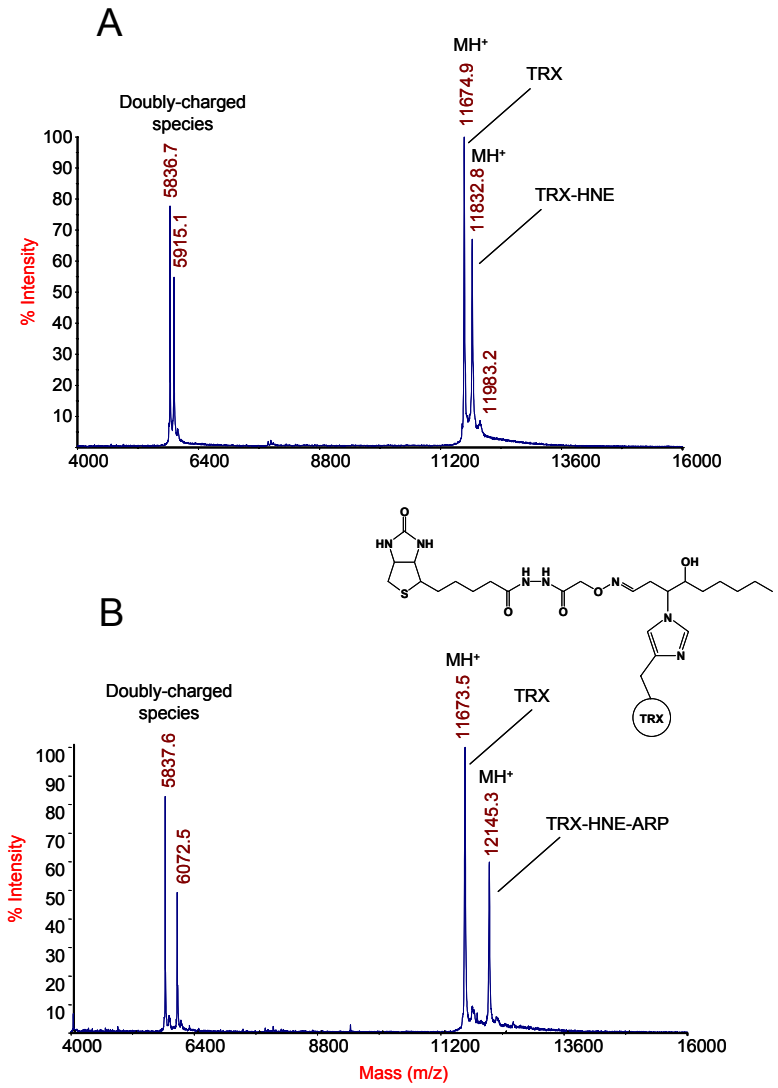

Figure 2. MALDI-MS spectra *E.coli* thioredoxin (TRX) after HNE-modification (A) and ARP-labeling (B). (A), the difference of ~158 Th between the mass peak at m/z 11,675 and m/z 11,833 indicates monoadduction by HNE *via* Michael-type addition. The low abundant ion at m/z 11,983 may indicate modification of TRX by a second HNE moiety but *via* Schiff's base formation (m/z 150 Th). (B), the difference of ~472 Th between the mass peak at m/z 11,674 and m/z 12,145 provides evidence that ARP labeling of the HNE moiety under formation of an oxime derivative was successful and highly efficient.

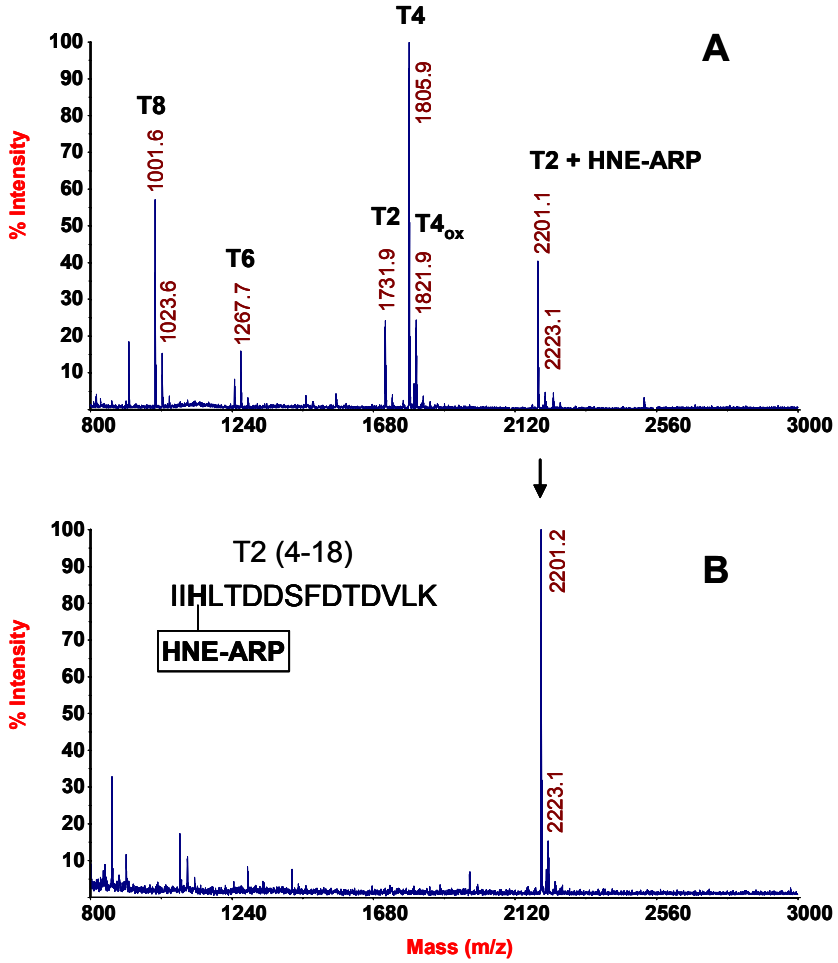

Figure 3. Affinity chromatographic enrichment of the ARP-labeled HNE-peptide conjugate. (A), MALDI mass spectrum of the unfractionated tryptic digest of HNE-modified thioredoxin and (B), the avidin affinity-enriched fraction containing the ARP-labeled HNE-conjugate of peptide T2.

The following non-labeled tryptic peptides were observed: T2, IIHLTDDSFDTDVLK (1731.9 Da), T4, MIAPILDEIADEYQGK (1806.1 Da), T6, LNIDQNPGTAPK (1267.4 Da) and T8 GIPTLLLFK (1001.3 Da).

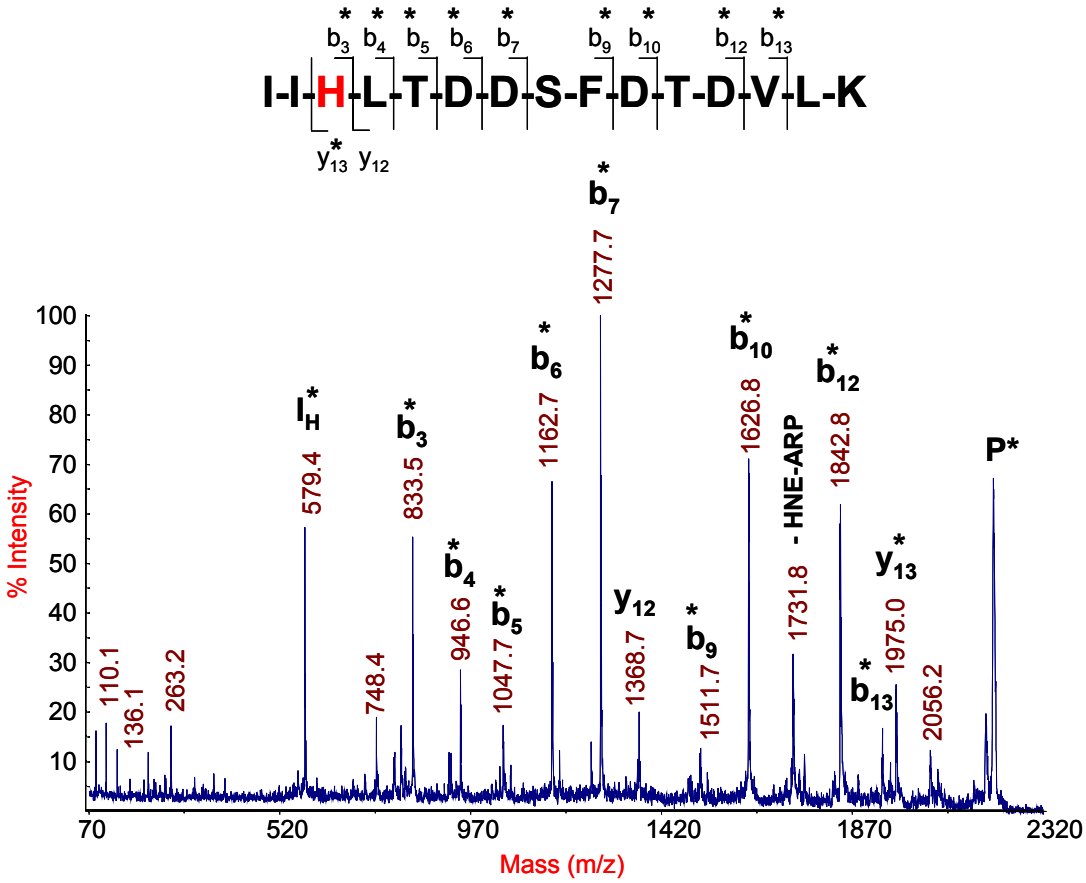

Figure 4. MALDI tandem mass spectrometric identification of the ARP-labeled tryptic peptide T2. Fragment ions marked with an asterisk * retained the ARP-HNE moiety during high energy collision induced fragmentation. The ion at m/z 579.4 corresponds to the immonium ion of the ARP-labeled HNE-conjugated histidine residue. The prominent ion at 1731.8 indicates neutral loss of the ARP-HNE moiety. This spectrum obtained a Mascot score of 68.

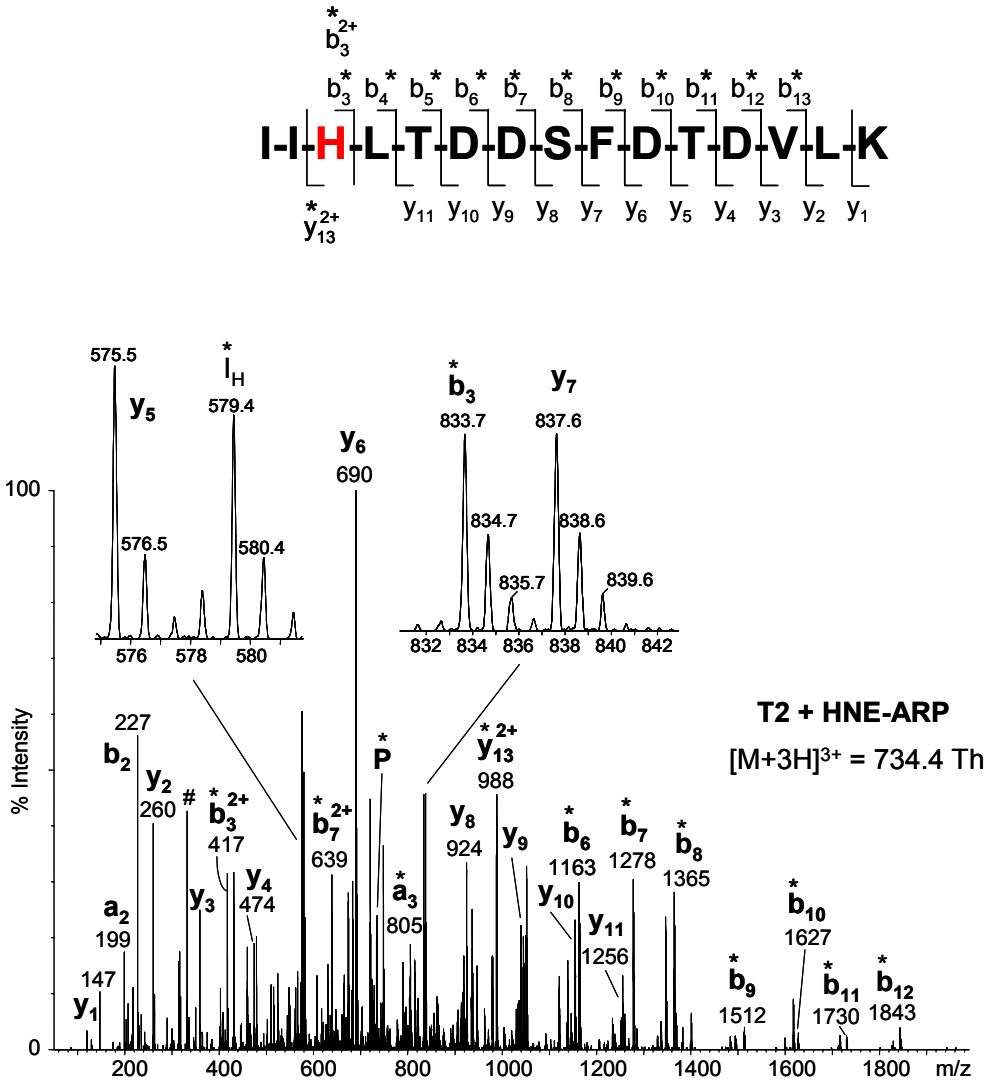

Figure 5. ESI tandem mass spectrum of the ARP-labeled tryptic peptide T2. The triply charged ion at m/z 734.4 was selected for low energy collision induced fragmentation. Product ions marked with an asterisk * retained the ARP-HNE moiety. The ion at m/z 579.4 corresponds to the immonium ion of the ARP-labeled HNE-conjugated histidine residue. The ion marked with # may represent an internal fragment ion, i.e. [TDD]. This spectrum obtained a Mascot score of 110.

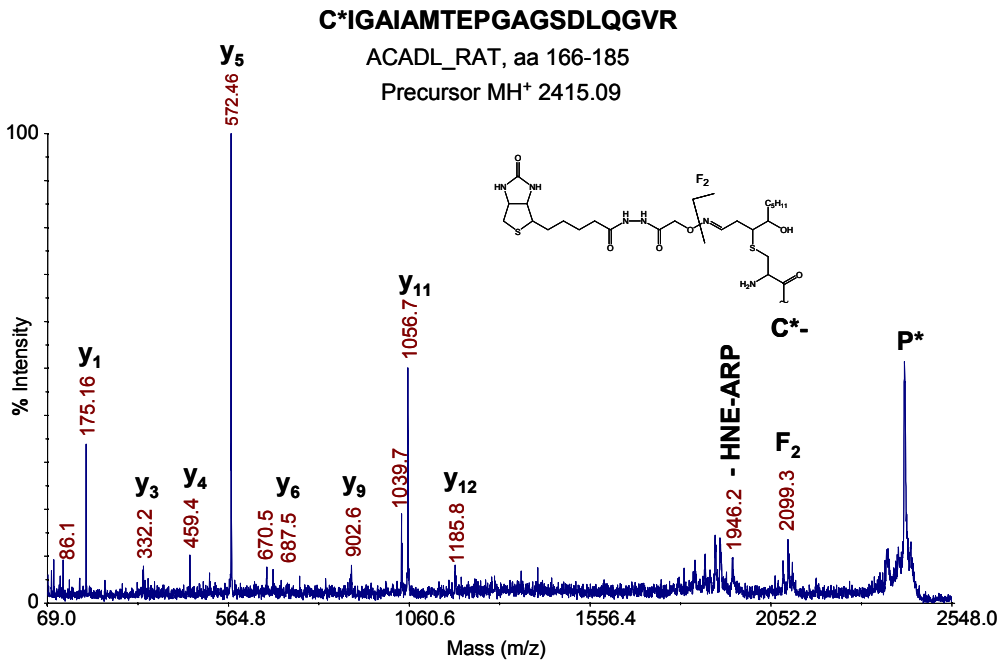

Figure 6. MALDI tandem mass spectrum of the ARP-labeled *in vivo* HNE-modified peptide from the long chain-specific acyl-CoA dehydrogenase (ACADL_RAT, aa 166-185) found in rat heart mitochondria. The fragment ion F_2 at m/z 2099.3 indicates side chain fragmentation at the oxime bond whereby the oxylipid moiety remains bound to the peptide. The ion at m/z 1946.2 indicates neutral loss of the ARP-HNE moiety. This spectrum obtained a Mascot score of 31.

Appendix B

Characterization of 2-alkenal Modified Mitochondrial Proteins by Affinity Labeling and Mass Spectrometry

Juan Chavez‡, Jianyong Wu‡, William Bisson, Claudia Maier‡*

‡Department of Chemistry, Oregon State University, Corvallis, Oregon 97331

***To whom correspondence should be addressed. Tel: 541-737-9533. Fax: 541-737-2062.**

E-mail: claudia.maier@oregonstate.edu

ABSTRACT

The modification of proteins by lipid peroxidation products is thought to be an underlying molecular factor in the pathogenesis of many degenerative diseases and age related disorders. Here we report on the identification of protein targets of electophilic 2-alkenals which are formed as a byproduct of naturally occurring oxidative stress. We employ the use of N'-aminooxymethylcarbonylhydrazino-D-biotin as an aldehyde reactive probe (ARP) to label and enrich carbonyl-modified peptides and proteins. The enriched ARP labeled peptides are then detected and sequenced using LC-MS/MS analysis. Employing this method for the analysis of proteins isolated from rat cardiac mitochondria, 39 unique sites on 27 proteins were identified as being modified by a variety of 2-alkenal products including acrolein, β -hydroxyacrolein, crotonaldehyde, 4-hydroxy-2-hexenal, 4-hydroxy-2-nonenal and 4-oxo-2-nonenal. These sites represent susceptible targets for oxidative modification and many of the sites are known to be important in the catalytic function of key mitochondrial enzymes.

Introduction

Since the 1950's when Harman's "free radical theory of aging" was introduced there have been a considerable number of studies focused on understanding the molecular mechanisms of oxidative stress and it's impact on living systems [1, 2].

It is widely accepted that oxidative stress plays a role in an increasing number of human health disorders and the aging process [3-9]. Within the rapidly advancing field of proteomics, several efforts have been devoted to identifying changes to the proteome in relation to oxidative stress.

Mitochondria are central to studies of oxidative stress, as they are known to be generators of reactive oxygen species (ROS) within the cell and play a pivotal role in cell death [7, 8, 10, 11]. There are a number of ROS producing sites within the mitochondria including complex 1 and complex 3 of the mitochondrial electron transport chain [12, 13]. Being that the ROS are generated in close proximity to the mitochondrial membrane, which is rich in polyunsaturated fatty acids, a whole host of reactive lipid peroxidation products are formed. These lipid peroxidation products are relatively long lived compared to the free radical ROS which led to their formation, allowing them to diffuse further from their site of production to potentially react with proteins and other biomolecules throughout the cell. Among the most abundant and studied of these are the highly electrophilic α,β-unsaturated aldehydes such as 4-hydroxy-2-nonenal (HNE), 4-oxo-2-nonenal (ONE), 4-hydroxy-2-hexenal (HHE), and acrolein [14].

A number of techniques exist for measuring the oxidative modification to proteins and other biomolecules. Among the most widely used of these techniques are assays based on the use of either 2,4–dinitrophenylhydrazine (DNPH) or thiobarbituric acid (TBARS) derivatization. While these methods are able to

provide researchers with a general overview of levels of oxidative stress induced modifications, they fail to provide specific information such as the identity of the modified proteins, and the site and chemical nature of the modification. In addition to the traditional colorimetric and immunochemical based methods of analysis, mass spectrometry has emerged as a powerful technique for studying the oxidative modification to biomolecules in ageing and disease related research [15]. Towards the goal of identifying the sites of oxidative modification in proteins, a variety of methods involving chemical derivatization followed by mass spectrometric detection have been developed. A variety of interesting chemistries have been employed to label and detect oxidatively modified sites in proteins including; hydrazide functionalized probes, Girard's P reagent, and Click chemistry to name a few [16-18]. One limitation of the many hydrazine-based reagents for labeling protein carbonyls is the pH-dependant reversibility of the hydrazone bond and the need for a reduction step to form a stable hydrazine adduct. We recently demonstrated an alternative approach to the hydrazine based chemistry, using N'-aminooxymethycarbonylhydrazino-D-biotin, a hydroxylamine functionalized biotin derivative, which forms stable oxime bonds with protein aldehydes, thus negating the need for a reduction step.

Several recent studies have been devoted to identifying the protein targets and sites of these lipid-derived electrophiles, in particular targets of HNE [19-21]. Numerous in vitro studies have demonstrated that α,β-unsaturated aldehydes,

being electrophilic in nature, covalently modify proteins at nucleophilic sites, in particular cysteine, histidine and lysine. Cysteine, with its thiol functional group being the most nucleophilic side chain, and being important to the structure and function of many enzymes has garnered many studies set out to identify target cysteine residues in proteins [22-24]. While there has been much success in identifying protein targets from in vitro studies, there is a void of results when it comes to the identification of oxidative modifications that occur in vivo. This information is truly of great importance and interest towards increasing our understanding of the effects of lipid derived aldehydes on the proteome, and is the focus of the current study.

Here we expand upon our previously described technique of using N'-aminooxymethylcarbonylhydrazino-D-biotin as an aldehyde reactive probe (ARP) which allows for a labeling, affinity enrichment and mass spectrometry based approach to identify the sites of carbonyl-modification to proteins occuring naturally within the mitochondria. ARP is a hydroxylamine functionalized biotin derivative, which is reactive toward carbonyl-modified proteins, and allows for affinity enrichment and mass spectrometric detection of the site and chemical nature of the modification. In our current study we have found this method to be successful in identifying a number of protein targets with susceptible nucleophilic sites, which turn out to be modified by a surprising variety of electrophilic 2-alkenal products. We are able to conclusively identify both the site and nature

of the modification, thus advancing the study of protein-oxylipid conjugates to a new level of detail.

Materials and Methods

Chemical Reagents

N'-aminooxymethylcarbonyl hydrazino-D-biotin (Aldehyde Reactive Probe, ARP) was purchased from Dojindo Molecular Technologies Inc. (Rockville, MD). Ultralink Monomeric Avidin, Zeba Spin Desalting columns, SuperSignal West Pico Chemiluminescent substrate were purchased from Thermo Scientific (Rockford, IL). Neutravidin-HRP was purchased from Pierce. Sequencing grade modified trypsin was purchased from Promega (Madison, WI). 12% Tris-HCl Ready Gels were purchased from Bio-Rad. Immobilon-P PVDF membranes were purchased from Millipore.

Preparation of rat cardiac mitochondria*:*

The Institutional Animal Care and Use Committee (IACUC) at Oregon State University approved the experimental protocol for the use of animals in this study. Male Fisher 344 rats, obtained from the National Institute of Aging (Bethesda, MD), were housed in individual plastic cages covered with Hepa filters and allowed free access to food and water. Rats were anethetized with diethyl ether and a midlateral incision was made in the chest to remove the heart.

Subsarcolemmal mitochondria were isolated from the rat hearts by differential centrifugation according to the procedures of Palmer with minor modifications by Suh et al. and stored at -80^{o}C until needed [25, 26]. Mitochondrial samples containing approximately 1mg total protein were washed twice with 0^{o}C 10mM NaH_2PO_4 pH 7.4. The mitochondria were then resuspended in 200 µl of 10mM NaH_2PO_4 pH 7.4. The mitochondria were ruptured by four rounds of freeze/thaw cycles which involved rapid freezing with liquid N_2 followed by thawing in a cold water bath with 10 minutes of sonication. Soluble and membrane proteins were separated by centrifugation at 14,000g for 15min. Pierce Coomassie Plus protein assay was used to determine the protein concentration.

ARP labeling of Mitochondrial Proteins.

ARP labeling of mitochondrial proteins was accomplished by simultaneously adjusting the protein concentration to ~1 µg/µl and the ARP concentration to 5mM in 10mM NaH_2PO_4 buffer pH 7.4. The mixture was then allowed to react for up to one hour at room temperature. Excess ARP was removed using Zeba desalting spin columns (Pierce) with a molecular weight cut off of around 7kDa. Protein samples were digested with a 1:50 w/w ratio of modified trypsin in 100mM NH_4HCO_3 pH 8.3 for 6-18 hours at 37^{o}C.

SDS-PAGE and Western Blot

One dimension SDS-PAGE was accomplished by loading 20 g of mitochondrial protein per well of Bio-Rad 12% tris-HCl readymade gels and running them at a constant 130 V for 60 minutes. For visualization of the protein bands the gels were incubated with Biosafe Coomassie dye for 1 hr. Western blotting was accomplished by transferring the proteins from the gel to a PVDF membrane by applying a constant current of 150 mA for 2 hours. The blot was then blocked with 5% milk in TBS buffer with 0.1% tween-20 and then washed extensively before being incubated with 40 ng/mL of HRP-NeutrAvidin for one hour. After several additional wash steps the gel was exposed to the PicoWest chemiluminescent substrate for 10 minutes and developed using Kodak BioMax X-Ray film.

Affinity Enrichment of ARP labeled peptides

100-300 µl of Ultralink monomeric avidin was packed into Handee Mini Spin Columns, which accommodate solvent addition with a Luer Lok syringe. The column was washed with 1.5ml of 10mM NaH_2PO_4, pH 7.4. Irreversible binding sites, consisting of tetrameric avidin, were blocked by washing with three column volumes of 2mM D-biotin. To remove excess D-biotin the column was washed with five column volumes of 2M Glycine-HCl pH 2.8. The column was then re-equilibrated by washing with 2mL of 2x phosphate buffered saline (PBS,

20mM NaH_2PO_4 300mM NaCl). The mitochondrial peptide sample was then slowly added to the affinity column and the flow thru collected. To remove non-labeled and non-specifically bound peptides the column was washed with 1mL 2 x PBS followed by 1mL of 10mM NaH_2PO_4 and finally 1.5mL of 50mM NH_4HCO_3 20%CH_3OH. The column was then rinsed with 1mL of MilliQ H_2O before eluting the ARP labeled peptides with 0.4% formic acid 30% acetonitrile. Collected fractions were then concentrated using vacuum centrifugation and stored at -20^{o}C before mass spectrometric analysis.

LC-MS/MS Analysis

The resulting ARP enriched peptides were analyzed by LC-MS/MS using a quadrupole orthogonal time-of-flight mass spectrometer (Q-TOF Ultima Global, Micromass/ Waters, Manchester, UK) mass spectrometer equipped with a NanoAcquity UPLC system. Peptides were fractionated by reverse phase chromatography on a 100 m i.d x 200mm long BEH column (Waters, Milford, MA) using a linear gradient of a binary solvent system consisting of solvent A (2% acetonitrile/ 0.1% formic acid) and solvent B (acetonitrile containing 0.1% formic acid). The electrospray source was operated in the positive mode with a spray voltage of 3.5kV. The mass spectrometer was operated in data dependant MS/MS mode, performing 0.6 second MS scans followed by 2.4 second MS/MS scans, on the three most abundant precursor ions in the MS scan with a 60 second

dynamic exclusion of previously selected ions. The MS/MS collision energy (25-65 eV) was dynamically selected based on the charge state of the precursor ion selected by the quadrupole analyzer. Mass spectra were calibrated using fragment ions of Glu^1-fibrinopeptide B (MH^+ 1570.6774 Da, monoisotopic mass). Additionally lock spray mass correction was performed on the doubly charged ion of Glu^1-fibrinopeptide ($[M+2H]^{2+}$ 785.8426 Th) every 30 seconds during the MS/MS run.

Peptide samples were also analyzed by LC-MALDI-MS/MS by performing off-line reversed-phase fractionation on a Dionex/LC Packings Ultimate nanoLC system coupled to a Probot target spotter. Peptides were fractionated over a 75 μm i.d x 150mm C18 PepMap 100 column (LC-Packings) using a binary gradient consisting of solvent A (5% acetonitrile/ 0.1% trifluoroacetic acid (TFA)) and solvent B (80% acetonitrile/ 0.1% TFA). A Probot was used to mix the eluting peptides with a-cyano-4-hydroxycinnamic acid (2mg/mL in 50% acetonitrile containing 0.1% TFA) and spot the mixture to a 144 spot stainless steel MALDI target plate. MALDI-MS/MS analysis was performed on an ABI 4700 proteomics analyzer with TOF/TOF optics equipped with a 200-Hz frequency-tripled Nd:YAG laser operating at a wavelength of 355 nm (Applied Biosystems, Inc., Framingham, MA). Operating in a data dependent reflectron mode, full MS scans was obtained for the range m/z 700-4000 followed by MS/MS scans on the 10 most abundant ion signals in the MS scan. Collision

induced dissociation was performed in at a collision energy of 1 keV in a collision cell with a gas pressure of 6 x 10^{-7} Torr. Mass spectra were calibrated externally using the ABI 4700 calibration mixture consisting of the following peptides des-Arg^1-bradykinin ([M+H]$^+$ 904.4681 Da), angiotensin I ([M+H]$^+$ 1296.6853 Da), Glu^1-fibrinopeptide B ([M+H]$^+$ 1570.6774 Da), and ACTH 18-39 ([M+H]$^+$ 2465.1989 Da).

MS/MS data analysis and identification of ARP-labeled peptides

Tandem mass spectrometric data generated on the Q-TOF were processed into peak list files using ProteinLynx Global Server v2.3 (PLGS Waters, Manchester, UK). Both the MS survey and MS/MS scans were calibrated using the lock mass of m/z 785.8426 with a lock spray tolerance of 0.1Da. MS/MS spectra were smoothed using the Savitzky-Golay algorithm performing 2 iterations over a smoothing window of 3 channels. The survey scan was deisotoped and centroided using a fast algorithm performing 30 iterations. MS and MS/MS spectra were centroided with a minimum peak width of 4 channels centroiding the top 80% with a TOF resolution set at 10,000 and a NP multiplier of 0.7. MALDI-MS/MS data were processed into peak list files using the Peaks to Mascot tool in 4000 Series Explorer V3.0 (Applied BIosystems). Default settings were used except for the peak density for MS/MS spectra was set to a max of 10

peaks per 200 Da, the minimum S/N was set to 10 with a minimum peak area of 500 and a max peak/precursor set to 40.

Peak list files of the tandem mass spectrometric data were analyzed with the aid of Mascot v2.1 (Matrix Science, London, UK) and Peaks Studio v4.5 (Bioinformatic Solutions Inc., Waterloo, ON Canada) protein database search engines. The Swiss Prot database v50 (270778 sequences, 99412397 residues) and the following parameters: taxonomy rodentia (20991 sequences), ± 0.2 Da mass tolerances for the precursor and fragment ions, possibility of 3 missed proteolytic cleavage sites, with trypsin/P or semitrypsin selected as the digesting enzyme, and ARP-HHE (CHK), ARP-HNE (CHK), ARP-Acrolein (CHK), ARP-ONE (CHK), ARP-MDA (KR), ARP-β-hydroxyacrolein, ARP-crotonaldehyde and methionine oxidation (M) selected as variable modifications at the residues specified in parenthesis. Identification of ARP labeled 2-alkenal modified peptides took place in multiple stages. First high scoring peptides, those peptides with Mascot scores above the identity threshold (>50) and/or Peaks scores above 0.90, were considered as putative identifications. Secondly intermediate scoring peptides, those with Mascot scores >20 and/or Peaks scores >0.50 and low scoring peptides, those with Mascot scores <20 and/or Peaks scores <0.50 were subjected to rigorous manual inspection before being considered as putative identifications. Manual analysis included assigning a continuity of b- and y- type ion series, comparison to homologous peptides with high scores, as well as inspection for the presence of

fragment ions not recognized by either Peaks or Mascot, that are specific for the ARP tag, fragment ions at m/z 227.09 (ARP F1), and m/z 332.14 (ARP), as well as fragment ions resulting from the neutral loss of all, or part of the ARP-2-alkenal moiety. The observed neutral loss ions include: (i) loss of 316.1 Da, designated F_2, resulting from the fragmentation of the N-O bond within the structure of ARP generating the neutral loss of an ARP fragment, (ii) loss of 331.14 Da resulting from fragmentation of the oxime bond and loss of the entire ARP moiety, (iii) loss of the entire ARP-2-alkenal modification by retro-Michael addition, and (iv) fragmentation of the C-S bond in the side chain of Cys, resulting in loss of the ARP-2-alkenal-SH neutral species. All tandem mass spectra from putatively identified ARP labeled 2-alkenal modified peptides are included in the supplemental materials with fragment ion annotation.

Calculation of B-factor and Solvent Accessible Area (SAA).

The 3D coordinates of porcine heart mitochondrial type II malate dehydrogenase (MDH) was retrieved from the crystal structures available in the Protein Data Bank (Pdb) 1MLD.[27] The B-factor and SAA values for all cysteine residues of MDH protein in the tetramer conformation were calculated using the program Molsoft ICM v3.5-1p. The mean B-factor values were derived from the atomic crystallographic data for each cysteine residue in each of the four monomers of the tetramer complex of MDH. The reported B-Factor values for each cysteine

residue are the average of the four monomers. The solvent accessible areas were calculated using a faster modification of the Shrake and Rupley alogorithm accounting for the presence of hydrogen atoms in the protein structure and using a water probe radius of 1.4 Å [28]. SAA values were calculated as the average of a span of three residues, including ±1 residue from the cysteine for each of the monomers of the tetrameric complex of MDH. The reported SAA values for each cysteine are the average of the four monomers.

Functional Pathway Network Analysis

The carbonyl-modified proteins identified by LC-MS/MS analysis were evaluated for their functional biological pathways using the Kyoto Encyclopeda of Genes and Genomes (KEGG) database. Cytoscape (v. 2.6.2) was used to construct a visual representation of the network connections between the modified proteins and their functional pathways.

Results.

Global Analysis of ARP Labeling of Carbonyl-Modified Mitochondrial Proteins

Mitochondria are well known sources of ROS and oxidative modification of mitochondrial proteins is associated with many human health disorders as well as the aging process [29, 30]. To identify mitochondrial protein targets of

electrophilic, 2-alkenal, lipid peroxidation products, we employed a chemical labeling and affinity enrichment technique using ARP. The relatively low abundance of carbonylated proteins under physiological conditions requires the use of an affinity enrichment approach. The hydroxylamine functionality of ARP reacts, through a condensation mechanism, with the carbonyl group on the oxidized protein to form a stable oxime product, adding a mass of 313.1 Da to the carbonylated protein. This is a particular advantage of the ARP based approach over similar affinity labeling methods such as those employing hydrazide functionalized probes such as DNPH and biotin hydrazide, which require reduction of the hydrazone bond to form a stable adduct. The biotin moiety present in the ARP tag allows for the use of avidin affinity enrichment of low-level modified peptides, which can then be characterized using LC-MS/MS analysis. Rat cardiac mitochondria were used for this study based on related studies indicating that oxidative modification to proteins may play a role in mitochondrial decay observed in aging and age related diseases [31].

In order to demonstrate the utility of ARP labeling for the detection of oxidatively modified proteins in rat cardiac mitochondria, we applied a previously demonstrated method to produce an “ARP-blot” [32]. Mitochondrial protein samples were reacted with 5mM ARP and then were separated by 1D-SDS-PAGE followed by Western blotting on a PVDF membrane. HRP conjugated NeutrAvidin was used with PicoWest chemiluminescent reagents (Pierce) to

visualize the ARP reactive bands (figure 1). Several ARP reactive protein bands are visible in the Western blot from the mitochondrial sample that was reacted with ARP. The control sample, to which no ARP was added, shows relatively no signal. Although not conclusively identified, the single HRP-NeutrAvidin reactive protein band visible in the control is likely due to a naturally biotinylated protein such as one of the mitochondrial carboxylase enzymes.

Identification of ARP labeled carbonylated proteins by affinity enrichment and tandem mass spectrometry.

Oxidatively modified mitochondrial proteins were labeled with ARP according to the previously described procedure. ARP labeled mitochondrial proteins were tryptically digested and subjected to monomeric avidin affinity enrichment and LC-MS/MS analysis by ESI-Q-TOF and MALDI-TOF/TOF. The resulting MS/MS data were searched against the Swiss Prot database with the aid of Mascot and Peaks software. Database search parameters allowed for the possibility of the specified ARP labeled post-translational modifications listed in the methods section. In our approach we used the Mascot and Peaks search results as a guide for identifying the tandem mass spectra of modified peptides, which were then confirmed by rigorous manual analysis. Using this approach we identified a variety of oxidative modifications to peptides originating from several mitochondrial proteins, the results of which are summarized in table 1. The

annotated tandem mass spectra from each of the assigned ARP labeled peptides are available as supplemental figures S1-S78. In total we identified 39 unique sites of modification in 27 mitochondrial proteins. The types of modifications identified consisted of six different 2-alkenal products including; acrolein, β-hydroxyacrolein, crotonaldehyde, 4-hydroxy-2-hexenal, 4-hydroxy-2-nonenal, and 4-oxo-2-nonenal. Three of the modified peptides including; NALANPLYCPDYR from ubiquinol-cytochrome-c reductase core protein 2, ETECTYFSTPLLLGK from malate dehydrogenase, and CIGAIAMTEPGAGDLQGVR from long-chain specific acyl-CoA dehydrogenase, were identified with more than one type of modification to the same residue.

Several of the proteins identified in table 1 are components of the mitochondrial electron transport chain (ETC). Many of these protein subunits have been previously identified as being carbonylated or modified by HNE in gel-based studies, which employed Western blot detection using anti-DNP or anti-HNE antibodies. For example succinate dehydrogenase [ubiquinone] flavoprotein subunit, ATP synthase α-chain, ATP synthase β-chain, ATP synthase γ-chain, cytochrome c oxidase subunit VIb isoform 1, and NADH dehydrogenase [ubiquinone] flavoprotein 1 were identified with carbonylation and/or HNE modifications, however the sites and types of modifications were not conclusively identified [33, 34].

By comparing the results in table 1 with other reports in the literature of studies

aimed at identifying sites of oxidative modification to proteins by the exogenous addition of electrophiles, we can see that there is some overlap of the sites and proteins identified. This is particularly interesting in that it suggests that the modified residues identified in table 1 represent susceptible targets for adduction by lipid peroxidation products. For example in comparison with previous results from our group in which we utilized a novel synthetic probe (HICAT) to label and quantify mitochondrial protein targets of HNE, we identified eight of the same proteins and sites of modification, including; H 227 of ATP synthase -subunit, C 100 of ATP synthase D chain, C 141 of ATP synthase O subunit, C 256 of ADP/ATP translocase 1, C166 of long-chain specific acyl-CoA dehydrogenase, C 93 and C 285 of malate dehydrogenase, and C 191 of ubiquinol-cytochorme-c reductase complex core protein 2 [18]. In a recent study by Wong and Liebler in which they added two thiol-reactive electrophilic probes (IAB & BMCC) to mitochondrial samples from HEK293 cells, they were able to identify 1693 sites of adduction belonging two 809 proteins. By comparing their results with the modified protein sites identified in our study, we can see that there are seven cases of overlap between the modified residues identified. These sites include C385 of Acontiase, C256 of ADP/ATP translocase, C100 of ATP synthase D chain, C317 of Methylmalonate-semialdehyde dehydrogenase, C 936 of NAD(P) transhydrogenase, C191 of Ubiquinol-cytochrome C reductase complex core protein 2, and C231 of Voltage-dependant anion selective channel protein 1.

The fact that only seven common sites exist out of the 1693 residues identified by Wong & Liebler and the 39 residues identified in this study raises some interesting questions as to what actually represent biologically significant targets of oxidiative stress, and what is the best approach to identify them. Clearly invitro studies in which relatively high concentrations of electrophilic probes are added are capable of identifying a large number of potential target sites, however such artificial situations may not accurately reflect the most biologically relevant sites. There is also the question of the site specificity of various electrophiles based on their differing chemical structures and physicochemical properties. Our results include a few examples that indicate that despite the variation in size and chemical structure of these 2-alkenals, their common electrophilic properties allow them to modify the same nucleophilic sites on proteins. Perhaps the most striking of these examples is the case of the long chain specific acyl-CoA dehydrogenase, which was identified with modifications from an unprecedented, five different types of 2-alkenal lipid peroxidation products to Cys166. These modifications included acrolein, β-hydroxyacrolein, 4-hydroxy-2-hexenal, 4-hydroxy-2-nonenal, and 4-oxo-2-nonenal. Figure 4 displays the MALDI-TOF/TOF generated tandem mass spectra of the tryptic peptide CIGAIAMTEPGAGSDLQGVR spanning residues 166 to 185 illustrating the diversity of modifications identified on the N-terminal cysteine.

Several of the sites identidified in this study are known to be very important to the

function of the specific proteins. For example the tryptic peptide including residue C166 from the long chain specific acyl-CoA dehydrogenase contains several residues which make up part of a FAD binding site, and adduction of this site by LPO's would very likely interfere with the proteins ability to bind FAD and therefore inhibit it's ability to catalyze the first step in the -oxidation of fatty acids.

Another example is cysteine 385 of aconitase, which was identified with an ARP-acrolein modification. Aconitase has been shown to be inhibited by acrolein in a concentration dependent manner [35]. Aconitase is found in the mitochondrial matrix and is involved in the second step of the citric acid cycle, catalyzing the reversible isomerization of citrate and isocitrate with cis-aconitate as a reaction intermediate. We identified the tryptic peptide VGLIGSCTNSSYEDMGR to be modified on C385 by ARP-acrolein. This same peptide was also identified in a separate study performed in our group in which (4-iodobutyl)triphenylphosphonium (IBTP) was used as a thiol reactive probe [24]. Taken together this evidence supports the notion that the susceptibility of cysteine 385 to modification by electrophilic species could account for the sensitivity and corresponding loss of activity of aconitase frequently observed under conditions of oxidative stress [36]. Cysteine 385 is known to be part of a 4Fe-4S iron sulfur cluster which is required for the catalytic activity. A specific Fe(II) atom, called Fe_a, is thought to coordinate the OH group of the substrate so

as to facilitate it's elimination. Unlike many iron sulfur clusters this iron-sulfur cluster is not associated with a redox process. Instead it has been postulated that the electronic properties of the 4Fe-4S cluster permit Fe_a to expand its coordination shell from the four ligands observed in the x-ray structure of the free enzyme (three S^{2-} and one OH^-) to the six octahedrally arranged ligands observed in the enzyme substrate complex. The modification of C385 by a lipid peroxidation product would undoubtedly inhibit the function of this enzyme, as irreversible oxidative disruption of the 4Fe-4S cluster is known to cause a loss of enzymatic activity [37, 38].

The peptide spanning residues 317 to 330 from methylmalonate-semialdehyde dehydrogenase was identified by both ESI-Q-TOF and MALDI-TOF/TOF analysis as containing a ARP-acrolein modification to Cys317. This is particularly significant in that Cys317 is the nucleophilic acitive site of this enzyme, which catalyzes the irreversible oxidative decarboxylation of malonsemialdehyde and methylmalonate semialdehyde to acetyl-CoA and propionyl-CoA respectively. Obviously such a modification would inhibit the function of this enzyme. The ESI-Q-TOF generated MS/MS is shown in figure 2. Note the presence of fragment ions at 227.09 m/z and 332.14 m/z, which are generated by the fragmentation of the ARP tag and are useful as diagnostic peaks to assist in the identification of ARP labeled peptides.

The fact that proteins contain sites susceptible to modification by lipid

peroxidation products raises the question of what this means in terms of the folded structure of the protein molecules. Why are certain residues targeted over others? Clearly one would think that in order to be modified, a residue would need to be located on or near the surface of the protein, and be reasonably exposed to the surrounding solvent. A residues susceptibility to modification would also undoubtedly depend on the side chains pKa value and the chemical microenvironment in which it is located. We attempted to address this question for the case of mitochondrial malate dehydrogenase (MDH), which was found modified by iipid peroxidation products on five cysteine residues (Cys 89, 93, 212, 275, 285). Structural analysis was performed on the crystal structure of porcine heart (MDH) using the protein modeling software Molsoft ICM V3.5-1p. Normalized B-Factor values, which serve as a measure of local flexibility of the protein structure over a given region, were obtained for all eight cysteine residues in a monomer of MDH in the tetramer conformation. The solvent accessible areas (SAA) for each of the eight cysteines, which provide a measure of how exposed each residue is to the surrounding solvent, were also calculated using a water probe radius of 1.4 Å. Four out of the five cysteine residues we identified as modified correspond with the cysteine residues with the largest B-Factor values. Cys 285, which has the largest B-Factor and second largest SAA of all of cysteines in MDH, was identified being modified by ARP-acrolein and ARP-HHE. The MALDI-TOF/TOF generated tandem mass spectra of the ARP-acrolein and

ARP-HHE modified peptides spanning residues 282-296 are shown below in figure 3 along with the ribbon structure of MDH illustrating the position of Cys 285 and a table with the corresponding average B-Factor and SAA values for all cysteine residues in a MDH tetramer. Thus for the case of malate dehydrogenase it seems that B-factor and SAA values correspond with the susceptibility of residues towards oxidative modification.

Functional Network Analysis of 2-alkenal Modified Proteins

In order to get an understanding of the potential impact of 2-alkenal modification to mitochondrial proteins on a systems level we performed a network analysis of the functional pathways of our identified proteins. The KEGG database was queried to obtain the functional pathway information and used Cytoscape to visualize the connections between the proteins and their pathways. The network of modified proteins is depicted in figure 5. The network analysis shows that many of the proteins identified in this study are involved in the functional pathways of degenerative diseases including Alzheimer's disease, Huntington's disease, and Parkinson's disease, all in which oxidative stress induced modification to proteins has been implicated to play an important role. Many of the identified proteins are also involved in calcium signaling, which is involved in mitochondrial regulation of cell death.

Discussion:

To the best of our knowledge this work represents the most exhaustive analysis of native oxidative modifications to mitochondrial proteins by 2-alkenal lipid derived compounds, through the use of affinity enrichment and mass spectrometry. In total we identified 27 proteins containing 39 unique nucleophilic sites that were modified by six varieties of 2-alkenals. The majority of modified proteins identified (40%) were members of the respiratory chain. This is to be expected as the electron transport enzymes are both a major source of ROS within the mitochondria and in close proximity to a high concentration of poly unsaturated fatty acids present in the inner mitochondrial membrane. TCA cycle proteins comprised the second most abundant category of identified modified proteins at 19%. A pie chart displaying the percentages of all identified proteins and modified sites is shown in figure 6A. Eighty five percent of the 2-alkenal Michael type additions characterized were present on cysteine residues, while 12% of the modification sites were to histidine with 3% occurring on lysine (figure 6B). This is also not surprising as cysteine is well known to be the most nucleophilic of the three residues. The proteins and modified sites identified in this study represent targets within the mitochondrial proteome that are susceptible to oxidative damage by electrophilic lipid peroxidation products. A few of the sites identified in this study match with those identified by other studies employing invitro addition of HNE or other electrophilic probes, followed by

affinity enrichment and mass spectrometry. However there are a number of sites, which are exclusive to either this study, or the in vitro studies. In order to get a better understanding of the role that oxidative modifications play in biological processes, we feel it is important to characterize the naturally occurring modifications.

Acrolein modification of Mitochondrial Proteins

The Michael type addition of acrolein to nuleophilic sites in proteins is by far the most common modification we identified in this experiment, occurring on 26 out of the 27 carbonylated proteins and comprising a total of 84% of the 2-alkenal modifications identified (figure 6C). Acrolein is known to be the most reactive of the α,β-unsaturated aldehydes and is common environmental toxin which can be formed from combustion of organic matter or formed biologically through the metabolism of allyl compounds and lipid peroxidation of polyunsaturated fatty acids [14, 39]. The toxicity of acrolein has been shown to be approximately one to three orders of magnitude greater than formaldehyde, acetaldehyde, and HNE [40]. Exposure to acrolein induces conditions of oxidative stress by depleting protective nucleophiles such as glutathione (GSH) and ascorbic acid [41, 42]. Recent studies have shown concentrations of acrolein as low as 1 μM can induce oxidative stress damage resulting in functional impairment of mitochondria [35]. Acroleins higher reactivity towards protein

nucleophiles could in part explain why we have it detected more frequently than other α,β-unsaturated aldehydes. Uchida et al. reported the formation of N^E-(3-formyl-3,4-dehydropiperidino) lysine (FDP-lysine) as a major reaction product between acrolein and Lys residues. However although the structure of FDP-lysine contains a free aldehyde group, which would be reactive with ARP, we were not able to identify any of these types of adducts in our experiments [39]. Being that FDP lysine requires two molar equivalents of acrolein per nucleophilic residue to form it is likely that FDP-lysine modifications only form under invitro conditions containing relatively high concentrations of acrolein and are unlikely to occur under normal physiological conditions. It is important to note that most anti-acrolein antibodies used for the immunochemical detection of acrolein-protein adducts are specific for FDP-lysine derivatives, so their sensitivity towards acrolein Micheal type adducts of cysteine residues, such as those primarily identified in this study, remains unknown. It is possible that the ARP approach and the immunological approach are sensitive to two different populations of acrolein adducts. Recent studies have shown acrolein to be a mitochondrial toxin inhibiting electron transport and increasing overall oxidative stress damage in brain and liver mitochondria [35, 40]. Several important mitochondrial enzymes including aconitase, ADP/ATP translocase complex I, complex II, pyruvate dehydrogenase and alpha ketogluterate dehydrogenase have been shown to be inhibited by acrolein [35, 40]. Out of those six enzymes we

were able to identify the sites of acrolein modifications to aconitase, ADP/ATP translocase, complex I, and complex II in our experiments.

Other Lipid peroxidation products.

In addition to acrolein we also identified a few cases of other lipid peroxidation products adducted to mitochondrial proteins. These other products include 4-hyroxy-2-hexenal, 4-hydroxy-2-nonenal, 4-oxo-2-nonenal, crotonaldehyde, beta-hyroxyacrolein. 4-hydroxy-2-nonenal and 4-oxo-2-nonenal arise primarily from the lipid peroxidation of the ω-6 fatty acids, linoleic and arachadonic acids, while 4-Hydroxy-2-hexenal on the other hand, is an end product of the peroxidation of ω-3 fatty acids, including α-linolenic, eicosapaenoic, and docosahexanoic acids. Combined these other 2-alkenal products comprised only 16% of the modifications identified (figure 6. C). It is quite surprising that this wide variety of LPO's were all identified as adducting to the same residue sites.

To assess the structural implications of why certain residues are susceptible to modification we performed structural analysis of malate dehydrogenase by integrating our mass spectrometry data identifying sites of modification with the known x-ray crystal structure for MDH. This proved useful in that the sites of acrolein and HHE adduction correspond to the cysteine residues with high B-factors and solvent accessible areas. Further studies will be necessary to see if this correlation extends to other protein systems and if B-factor and SAA values

may be useful in predicting susceptible sites of modification by lipid derived electrophiles.

Evaluation and method validation of the ARP approach (Possible pitfalls & limitations with ARP approach)

With the rapidly increasing number of new analytical proteomics techniques it is of critical importance to perform validation of the analytical method to ensure the results are scientifically sound. Du to the extreme sample complexity, biological variability and absence of reference standards this becomes a daunting task. We assessed the robustness of the ARP labeling and enrichment method on several levels in an attempt to validate our analytical approach. We tested the reproducibility of our method by repeating our analysis several times using new sample preparations from different animals and analyzing the samples on multiple instruments. We found that 20 of the ARP labeled oxylipid modified peptides belonging to 15 proteins were reproducibly identifiable in repeated sample preparations. The overwhelming presence of acrolein modified peptides towards other oxylipids raised the question as to whether or not our method was in some way biased towards acrolein modifications vs. HNE, ONE and other LPO adducts. To test this hypothesis we added HNE in-vitro into the mitochondria then followed the same affinity enrichment and mass spectrometric analysis described above. In this case we identified an overwhelming abundance of HNE modified

peptides compared with other modifications. These results demonstrate that our method is not discriminating against HNE modified peptides, as when HNE is added, we enrich and detect HNE adducted peptides. Instead we suggest the abundance of acrolein modifications is likely due to a relatively high concentration of acrolein compared to other LPO's in the mitochondria as well as acrolein's higher reactivity towards protein nucleophilic sites.

Additionally many of the modified proteins identified are known to be of relatively high abundance in the mitochondria. With such a large dynamic range of protein concentrations present in the mitochondria, it is extremely difficult to sample the proteins of lower abundance. This problem becomes exaggerated by the fact that LPO modified proteins are already of very low abundance compared to their non-modified variants. It's possible that this problem could be overcome by employing a variety of additional fractionaltion techniques, however this would also require a larger amount of starting material to be sure to have enough of the lowest abundance modified proteins.

It's important to consider the possibility that oxidative modifications can occur during the processing of the sample. We believe to have minimized contributions by these artificially generated oxidative modifications by careful treatment of the sample and by using as gentle of conditions as possible. However even if such modifications do occur as artifacts of sample preparation the proteins and amino acid residue sites that were modified still represent

susceptible targets to oxidative damage and are therefore still relevant. The results shown here are important to increasing our understanding of these types of modifications to proteins and the biological implications such modifications may have. The present study is a discovery effort with the goal of identifying the sites and types of endogenously occurring, 2-alkenal modifications to mitochondrial proteins. Now that we have characterized a number of these adducts, future experiments are needed to determine what impact these modifications have on the proteins structure and function as well as the function of the mitochondria and cell as a whole. Ongoing experiments in our laboratory include performing quantitative analysis of acrolein, modified peptides in the mitochondria to better understand how the levels of these modifications change with ageing. Additionally in preliminary unpublished results from our laboratory we have identified several of the same cysteine containing peptide sequences as being modified by glutathione.

Acknowledgements

This work was supported by grants from the NIH/NIA (AG025372). The mass spectrometry core facility of the Environmental Health Sciences Center at Oregon State University is supported in part by a grant from NIEHS (ES00210).

References

[1] D. Harman, J. Gerontol., 11 (1956) 298.

[2] D. Harman, Proc. Natl. Acad. Sci. U. S. A., 78 (1981) 7124.

[3] B.S. Berlett, E.R. Stadtman, J. Biol. Chem., 272 (1997) 20313.

[4] E.R. Stadtman, Ann. N. Y. Acad. Sci., 928 (2001) 22.

[5] B.W. Gibson, Int. J. Biochem. Cell Biol., 37 (2005) 927.

[6] M.K. Dennehy, K.A. Richards, G.R. Wernke, Y. Shyr, D.C. Liebler, Chem. Res. Toxicol., 19 (2006) 20.

[7] J. Sastre, F.V. Pallardo, J. Vina, IUBMB Life, 49 (2000) 427.

[8] N.J. Linford, S.E. Schriner, P.S. Rabinovitch, Cancer Res., 66 (2006) 2497.

[9] E. Cadenas, K.J. Davies, Free Radic. Biol. Med., 29 (2000) 222.

[10] S. Orrenius, V. Gogvadze, B. Zhivotovsky, Annu. Rev. Pharmacol. Toxicol., 47 (2007) 143.

[11] M. Ott, V. Gogvadze, S. Orrenius, B. Zhivotovsky, Apoptosis, 12 (2007) 913.

[12] A.Y. Andreyev, Y.E. Kushnareva, A.A. Starkov, Biochemistry (Mosc), 70 (2005) 200.

[13] Y. O'Malley, B.D. Fink, N.C. Ross, T.E. Prisinzano, W.I. Sivitz, J. Biol. Chem., 281 (2006) 39766.

[14] H. Esterbauer, R.J. Schaur, H. Zollner, Free Radic. Biol. Med., 11 (1991) 81.

[15] C. Schoneich, Mass Spectrom. Rev., 24 (2005) 701.

[16] A. Vila, K.A. Tallman, A.T. Jacobs, D.C. Liebler, N.A. Porter, L.J. Marnett, Chem. Res. Toxicol., 21 (2008) 432.

[17] H. Mirzaei, F. Regnier, J. Chromatogr. A, 1134 (2006) 122.

[18] B. Han, J.F. Stevens, C.S. Maier, Anal. Chem., 79 (2007) 3342.

[19] S.G. Codreanu, B. Zhang, S.M. Sobecki, D.D. Billheimer, D.C. Liebler, Mol. Cell Proteomics, 8 (2009) 670.

[20] P.A. Grimsrud, M.J. Picklo, Sr., T.J. Griffin, D.A. Bernlohr, Mol. Cell Proteomics, 6 (2007) 624.

[21] D.L. Meany, H. Xie, L.V. Thompson, E.A. Arriaga, T.J. Griffin, Proteomics, 7 (2007) 1150.

[22] H.L. Wong, D.C. Liebler, Chem. Res. Toxicol., 21 (2008) 796.

[23] A. Landar, J.Y. Oh, N.M. Giles, A. Isom, M. Kirk, S. Barnes, V.M. Darley-Usmar, Free Radic. Biol. Med., 40 (2006) 459.

[24] K. Marley, D.T. Mooney, G. Clark-Scannell, T.T. Tong, J. Watson, T.M. Hagen, J.F. Stevens, C.S. Maier, J. Proteome Res., 4 (2005) 1403.

[25] J.W. Palmer, B. Tandler, C.L. Hoppel, J. Biol. Chem., 252 (1977) 8731.

[26] B. Paizs, S. Suhai, Mass Spectrom. Rev., 24 (2005) 508.

[27] W.B. Gleason, Z. Fu, J. Birktoft, L. Banaszak, Biochemistry, 33 (1994) 2078.

[28] A. Shrake, J.A. Rupley, J. Mol. Biol., 79 (1973) 351.

[29] E.R. Stadtman, Free Radic. Res., 40 (2006) 1250.

[30] D.C. Wallace, Science, 283 (1999) 1482.

[31] T.M. Hagen, R. Moreau, J.H. Suh, F. Visioli, Ann. N. Y. Acad. Sci., 959 (2002) 491.

[32] W.G. Chung, C.L. Miranda, C.S. Maier, Electrophoresis, 29 (2008) 1317.

[33] K.B. Choksi, W.H. Boylston, J.P. Rabek, W.R. Widger, J. Papaconstantinou, Biochim. Biophys. Acta, 1688 (2004) 95.

[34] S. Judge, Y.M. Jang, A. Smith, T. Hagen, C. Leeuwenburgh, FASEB J., 19 (2005) 419.

[35] J. Luo, R. Shi, Neurochem. Int., 46 (2005) 243.

[36] A.L. Bulteau, M. Ikeda-Saito, L.I. Szweda, Biochemistry, 42 (2003) 14846.

[37] A.L. Bulteau, K.C. Lundberg, M. Ikeda-Saito, G. Isaya, L.I. Szweda, Proc. Natl. Acad. Sci. U S A., 102 (2005) 5987.

[38] L.V. Matasova, T.N. Popova, Biochemistry (Mosc), 73 (2008) 957.

[39] K. Uchida, M. Kanematsu, Y. Morimitsu, T. Osawa, N. Noguchi, E. Niki, J. Biol. Chem., 273 (1998) 16058.

[40] L. Sun, C. Luo, J. Long, D. Wei, J. Liu, Mitochondrion, 6 (2006) 136.

[41] N.D. Horton, B.M. Mamiya, J.P. Kehrer, Toxicology, 122 (1997) 111.

[42] J.F. Stevens, C.S. Maier, Mol. Nutr. Food Res., 52 (2008) 7.

Table 1. Summary of the mitochondrial proteins modified by lipid peroxidation derived 2-alkenals and subsequently labeled with ARP and identified by tandem mass spectrometry. The MS/MS identified peptide sequences containing the ARP label and 2-alkenal modification from each of the corresponding carbonylated proteins is shown. The amino acid residue and chemical nature of the modification are indicated for each case. Biological and functional assignments were made on the basis of information from the NCBI (http://www.ncbi.nlm.nih.gov/Pubmed) and the UniProt Knowledgebase (http://www.uniprot.org) websites.

Table 1. ARP-labeled 2-alkenal Modified Peptides Identified from Rat Cardiac Mitochondrial Proteins[‡]

Biological Function	SwissProt ID	UniProt Accession	Protein Name	Peptide Sequence	Modified Residue	Modifications
Respiratory Chain	AT5F1_RAT	P19511	ATP synthase B chain	C*IGDLK[a,b]	C239	ARP-acrolein
	ATP5H_RAT	P31399	ATP synthase D chain	NC*AQFVTGSQAR[a,b,c]	C100	ARP-acrolein
	ATPA_RAT	P15999	ATP synthase subunit alpha	GC*SMGEYFR[a,b,c,d]	C294	ARP-acrolein
				SGC*SMGEYFR[a,b,c,d]	C294	ARP-acrolein
				YSGC*SMGEYFR[a,b,d]	C294	ARP-acrolein
				LAPYSGC*SMGEYFR[a,c]	C294	ARP-acrolein
	ATPB_RAT	P10719	ATP synthase subunit beta	H*GGYSVFAGVGER[a,b,c,d]	H227	ARP-crotonaldehyde
	ATPG_RAT	P35435	ATP synthase gamma chain	GLC*GAIHSSVAK[a,b,c]	C78	ARP-acrolein
				H*SDQFLVSFK[a,b]	H120	ARP-acrolein
	ATPO_RAT	Q06647	ATP synthase O subunit	GEVPC*TVTTAFPLDEAVLSELK[a,b,c]	C141	ARP-acrolein
	CX6B1_MOUSE[‡] (EDM07730)	P56391	Cytochrome c oxidase subunit VIb isoform 1	GGDVSVC*EWYR[a,c]	C54	ARP-acrolein
	NDUV1_MOUSE[‡] (AAH83709)	Q91YT0	NADH dehydrogenase [ubiquinone] flavoprotein 1	QIEGHTIC*ALGDGAAWPVQGLIR[a]	C425	ARP-acrolein
	QCR1_RAT	Q68FY0	Ubiquinol-cytochrome-c reductase complex core protein 1	NALISHLDGTTPVC*EDIGR[a,b,c]	C410	ARP-acrolein
				YFYDQC*PAVAGYGPIEQLSDYNR[a]	C453	ARP-acrolein
	QCR2_RAT	P32551	Ubiquinol-cytochrome-c reductase complex core protein 2	NALANPLYC*PDYR[a,b,c]	C191	ARP-acrolein, ARP-HNE
				NPLYC*PDYR[a,d]	C191	ARP-acrolein
	DHSA_RAT	Q920L2	Succinate dehydrogenase [ubiquinone] flavoprotein subunit	GH*SLLHTLYGR[a,b]	H190	ARP-acrolein

Table 1. (Continued)

Transport	Q6IRH6_RAT	Q6IRH6	Slc25a3 protein	AVEEQYSC*EYGSGR[a,b]	C52	ARP-acrolein
	ADT1_RAT	Q05962	ADP/ATP translocase 1	GADIMYTGTVDC*WR[a,b,c]	C256	M(ox), ARP-acrolein
				TGTVDC*WR[a,c,d]	C256	ARP-acrolein
				EFNGLGDC*LTK[a,c]	C159	ARP-acrolein
				YFAGNLASGGAAGATSLC*[a,c,d]	C128	ARP-acrolein
				C*FVYPLDFAR[a,b,c]	C128	ARP-acrolein
				DIMYTGTVDC*WR[b]	C256	ARP-acrolein
				KGADIMYTGTVDC*WR[b]	C256	ARP-acrolein
	ADT2_RAT	Q09073	ADP/ATP translocase 2	VSFAK*DFLAGGVAAAISK[a,c]	K10	ARP-HNE
				TGTLDC*WR[a,d]	C257	ARP-acrolein
	VDAC1_RAT	Q9Z2L0	Voltage-dependent anion-selective channel protein 1	YQVDPDAC*FSAK[a,b,c]	C232	ARP-acrolein
	VDAC3_RAT	Q9R1Z0	Voltage-dependent anion-selective channel protein 3	VC*NYGLIFTQK[a]	C65	ARP-acrolein
TCA Cycle	ACON_RAT	Q9ER34	Aconitate hydratase	VGLIGSC*TNSSYEDMGR[a,b]	C385	ARP-acrolein
				VAVPSTIHC*DHLIEAQLGGEK[a]	C126	ARP-acrolein
	IDHP_RAT	P56574	Isocitrate dehydrogenase [NADP]	C*ATITPDEAR[b]	C184	ARP-acrolein
				DLAGC*IHGLSNVK[a]	C418	ARP-acrolein
	MDHM_RAT	P04636	Malate dehydrogenase	ETEC*TYFSTPLLLGK[a,b,c]	C285	ARP-acrolein, ARP-HHE
				TEC*TYFSTPLLLGK[a,b,d]	C285	ARP-acrolein
				EGVIEC*SFVQSK[a]	C275	ARP-acrolein
				GYLGPEQLPDC*LK[a]	C89	ARP-acrolein
				TIIPLISQC*TPK[a]	C212	ARP-acrolein
				GC*DVVVIPAFVPR[a]	C93	ARP-acrolein
	ODPA_RAT	P26284	Pyruvate dehydrogenase E1 component alpha subunit	VDGMDILC*VR[b]	C261	ARP-acrolein
				H*GFTFTR[a]	H121	ARP-crotonaldehyde
	ODPB_RAT	P49432	Pyruvate dehydrogenase E1 component subunit beta	EGIEC*EVINLR[a]	C263	ARP-acrolein
Oxidoreductase	ETFD_RAT	Q6UPE1	Electron transfer flavoprotein-ubiquinone oxidoreductase	AAQIGHTLSGAC*LDPAAFK[a,b]	C117	ARP-acrolein
	MMSA_RAT	Q02253	Methylmalonate-semialdehyde dehydrogenase	C*MALSTAVLVGEAK[a,b]	C317	ARP-acrolein
	NNTM_MOUSE[d] (AAH91271)	Q61941	NAD(P) transhydrogenase	EANSIVITPGYGLC*AAK[a,b,c]	C936	ARP-acrolein

Table 1. (Continued)

Chaperone	CH60_RAT	P63039	60 kDa heat shock protein	C*EFQDAYVLLSEK[a]	C237	ARP-acrolein
Lipid Metabolism	ACADL_RAT	P15650	Long-chain specific acyl-CoA dehydrogenase	C*IGAIAMTEPGAGSDLQGVR[a,b,c]	C166	ARP-Acrolein, ARP-βHA, ARP-HHE, ARP-HNE, ARP-ONE
Kinase	KCRB_RAT	P07335	Creatine Kinase B Type	LGYILTC*PSNLGTGLR[a,c]	C283	ARP-acrolein
				ILTC*PSNLGTGLR[a,d]	C283	ARP-acrolein

An * marks the ARP-labeled 2-alkenal modified residue. ‡ Rat version not present in Swiss Prot database, gene bank accession numbers for rat proteins containing the equivalent peptide sequences provided. All MS/MS spectra were visually inspected and fragment ions annotated manually and are available in the supplemental material. [a]= peptide identified by ESI-Q-TOF [b]= peptide identified by MALDI-TOF/TOF [c]= peptide identified in repeated biological sample preparations [d]= identified peptide sequence is semi-tryptic

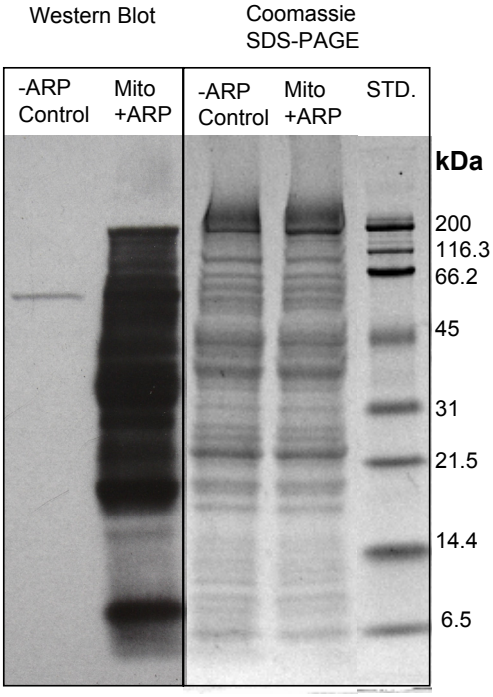

Figure 1. SDS-PAGE and Western blot of mitochondrial proteins from rat hearts. The difference in signal between –ARP control and the +ARP mitochondrial samples demonstrates the presence of a large number or ARP reactive proteins, as well as the selectivity of NeutrAvidin-HRP for the ARP labeled proteins.

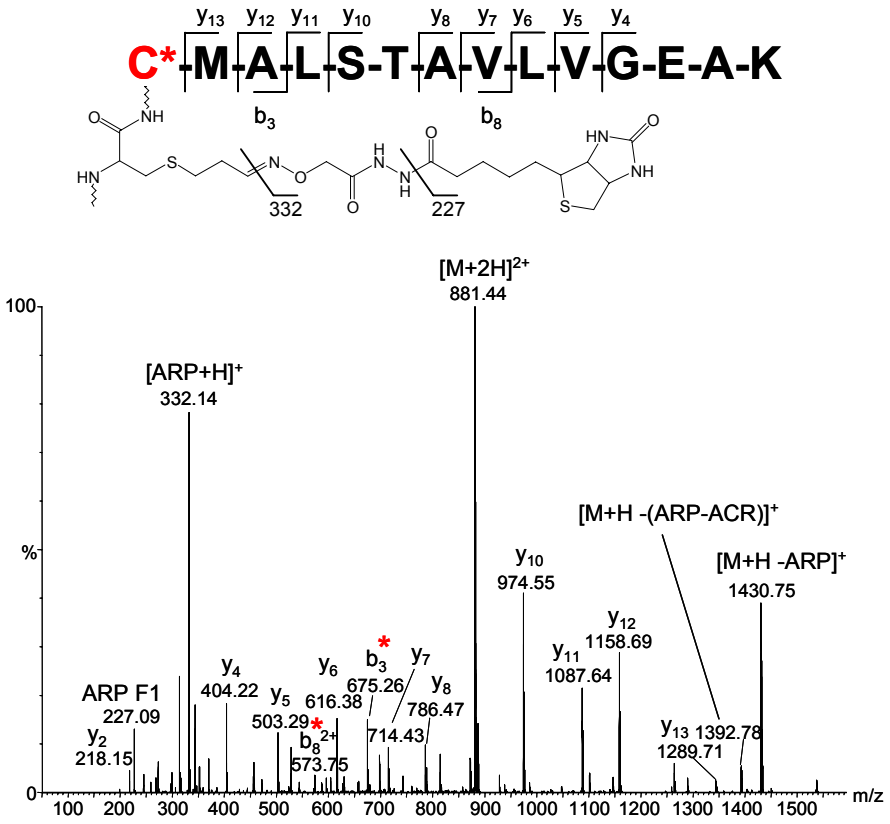

Figure 2. ESI-Q-TOF generated MS/MS of the peptide CMALSTAVLVGEAK, spanning residues 317-330 of methylmalonate-semialdehyde dehydrogenase containing an ARP-acrolein modification at C317. C317 also happens to be the nucleophilic active site for this enzyme. This spectrum also contains the fragment ions at 332.22 m/z and 227.15 m/z, which are generated from the ARP tag and are diagnostic of ARP labeling.

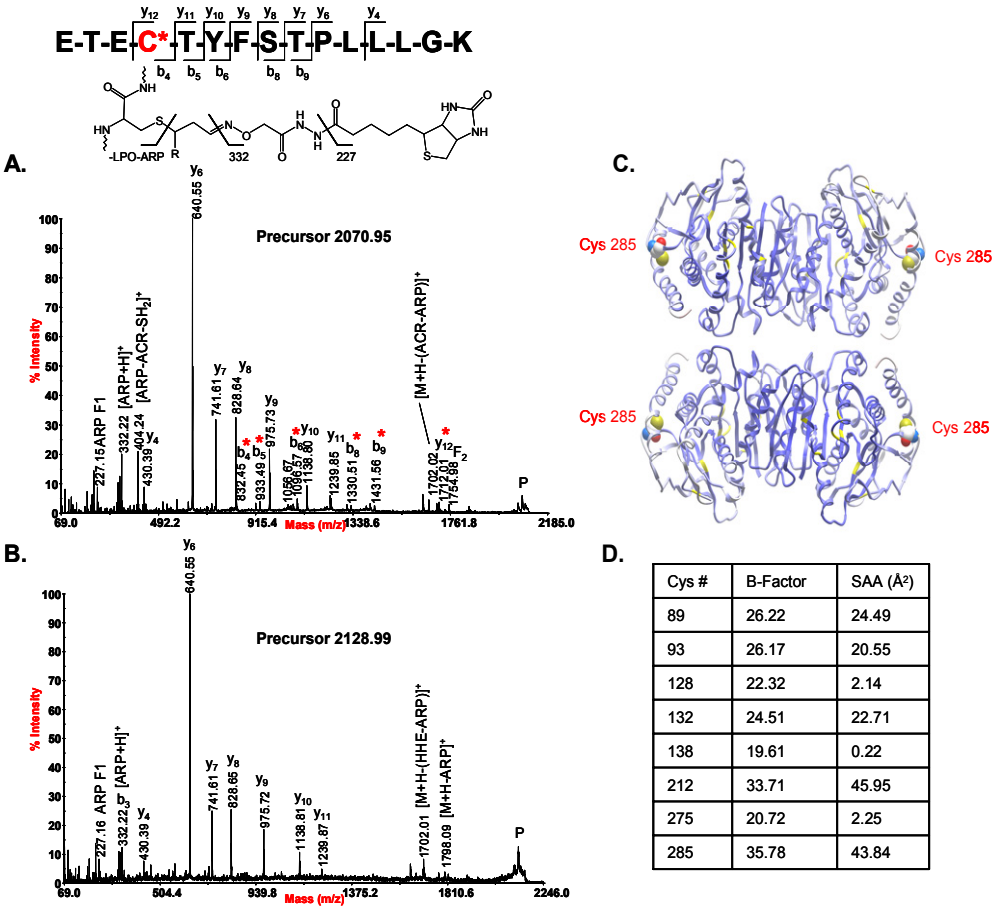

Cys #	B-Factor	SAA (Å²)
89	26.22	24.49
93	26.17	20.55
128	22.32	2.14
132	24.51	22.71
138	19.61	0.22
212	33.71	45.95
275	20.72	2.25
285	35.78	43.84

Figure 3. A.MALDI-TOF/TOF generated tandem mass spectrum of the peptide spanning residues 282-296 from malate dehydrogenase which was found with the ARP-acrolein and ARP-HHE modifications on Cys 285. Cys 285 is the most solvent accessible Cys residue according to solvent accessibility analysis. **B.** Tandem mass spectrum of the ARP-HHE modified version of the same peptide. **C.** Porcine heart MDH tetramer (PDB:1MLD) with the protein backbone displayed as ribbon (cysteine amino acids colored in yellow) and colored by B-Factor (ICM v3.6-1d, Molsoft). The residue Cys285 is displayed as cpk and colored by atom type with the carbon atoms in white. **D.** Table listing the average B-Factor and solvent accessible area values data of all Cys residues of MDH protein in tetramer conformation

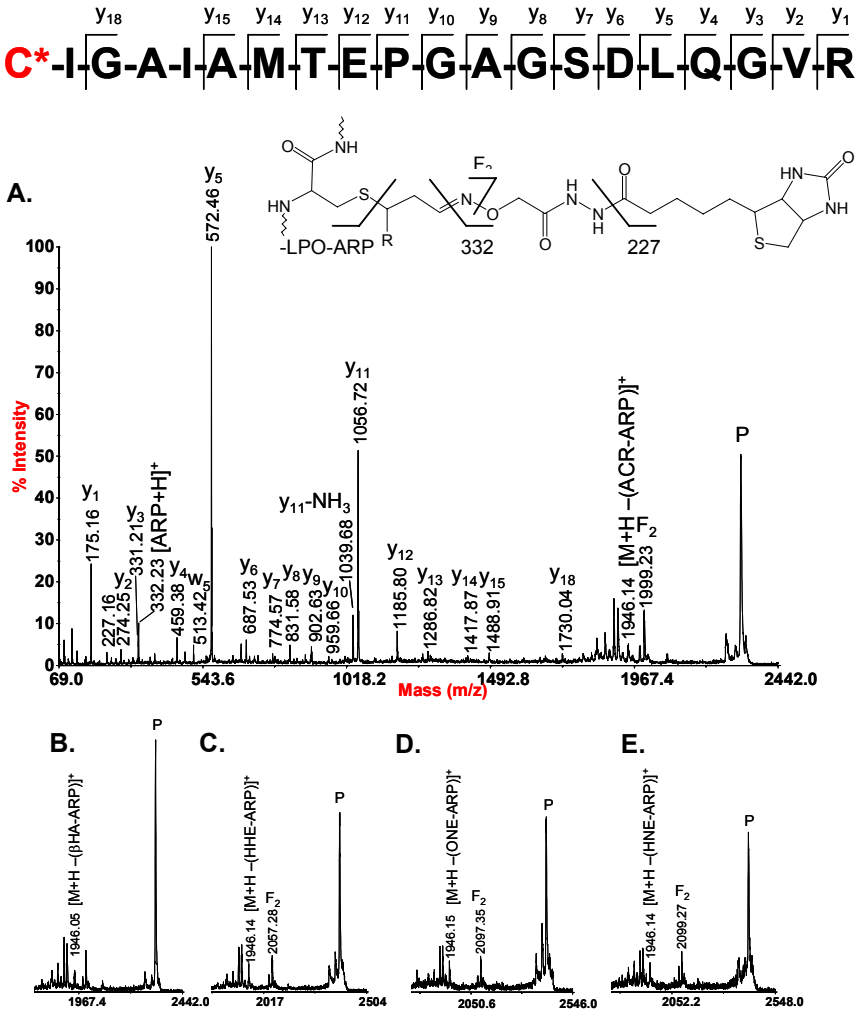

Figure 4. Tandem mass spectra from the peptide spanning residues 166 to 185 from the long chain specific acyl-CoA dehydrogenase which was found to be modified on Cys 166 by a surprising variey of lipid peroxidation products and subsequently labeled with ARP. **A.** Full tandem mass spectrum of the ARP-acrolein modified version of the peptide. **B.,C.,D., and E.** display the high m/z region of the tandem mass spectra for the ARP- -hydroxyacrolein modified, ARP-HHE modified, ARP-ONE modified, and ARP-HNE modified versions of the peptide respectively.

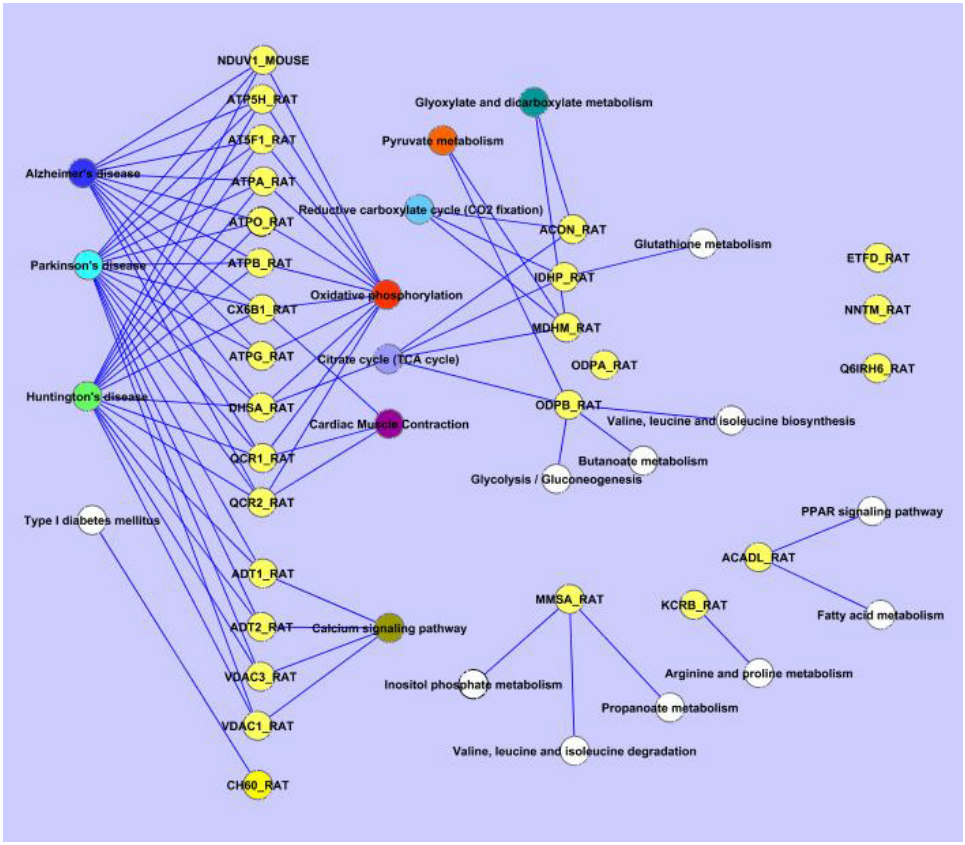

Figure 5. Biological pathway analysis from the network of carbonylated proteins generated with funcation data from the KEGG database. Carbonylated proteins are colored as yellow nodes and the functional pathways are displayed as colored nodes. White colored nodes represent pathways for which only one protein was identified.

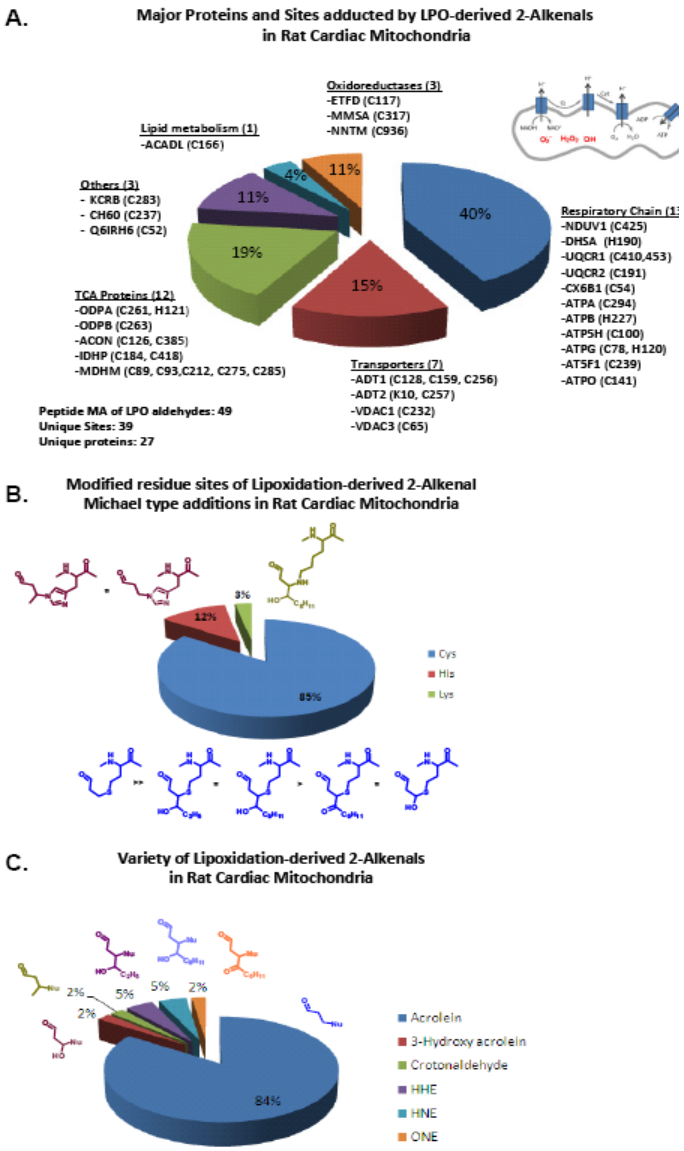

Figure 6. **A.** Pie chart displaying the mitochondrial proteins and amino acid residue sites identified with modifications by lipid peroxidation derived 2-alkenals. **B.** Pie chart illustrating the percentage breakdown of the types of residues identified with Micheal-type additions of lipid peroxidation derived 2-alkenals. **C.** Pie chart indicating the percentages of the different types of lipid peroxidation derived 2-alkenals identified in this study.